NOTE TO USERS

Page(s) not included in the original manuscript and are unavailable from the author or university. The manuscript was scanned as received.

92

This reproduction is the best copy available.

UMI®

uOttawa

L'Université canadienne
Canada's university

FACULTÉ DES ÉTUDES SUPÉRIEURES ET POSTOCTORALES

uOttawa

L'Université canadienne
Canada's university

FACULTY OF GRADUATE AND POSDOCTORAL STUDIES

Rogdrigo Ivan Serna-Guerrero
AUTEUR DE LA THÈSE / AUTHOR OF THESIS

M.A.Sc. (Chemical Engineering)
GRADE / DEGREE

Department of Chemical Engineering
FACULTÉ, ÉCOLE, DÉPARTEMENT / FACULTY, SCHOOL, DEPARTMENT

Adsorption of Volatile Organic Compounds on Pore Expanded Mesoporous Materials and MCM-41

TITRE DE LA THÈSE / TITLE OF THESIS

Abdelhamid Sayari
DIRECTEUR (DIRECTRICE) DE LA THÈSE / THESIS SUPERVISOR

CO-DIRECTEUR (CO-DIRECTRICE) DE LA THÈSE / THESIS CO-SUPERVISOR

EXAMINATEURS (EXAMINATRICES) DE LA THÈSE / THESIS EXAMINERS

Boguslaw Kruczek

Jules Thibault

Gary W. Slater
LE DOYEN DE LA FACULTÉ DES ÉTUDES SUPÉRIEURES ET POSTDOCTORALES /
DEAN OF THE FACULTY OF GRADUATE AND POSTDOCORAL STUDIES

Adsorption of Volatile Organic Compounds on Pore Expanded Mesoporous Materials and MCM-41 Silica

by

Rodrigo Ivan Serna-Guerrero

A thesis submitted in partial fulfillment
of the requirements for the degree of

Master of Applied Science

In the

DEPARTMENT OF CHEMICAL ENGINEERING
UNIVERSITY OF OTTAWA

Your file Votre référence
ISBN: 0-494-14949-3
Our file Notre référence
ISBN: 0-494-14949-3

Abstract

The increasingly stringent environmental regulations worldwide demand the use of efficient methods for air purification. This work is a contribution toward developing efficient adsorbents for volatile organic compounds (VOCs). Three different varieties of ordered mesoporous silicas were evaluated: an ordered MCM-41 mesoporous silica prepared in the presence of a surfactant, a MCM-41 whose pores have been expanded by a post-synthesis hydrothermal treatment in the presence of an organic expander (referred to as MCM-EC), and a pore-expanded hybrid mesoporous silica produced by the selective extraction of its pore expander agent (denominated MCM-EE). With the intention to analyze their performance as adsorbents, the heat of adsorption ($-\Delta H_a$) and adsorption capacity (q) were determined experimentally for five typical VOCs: dichloromethane, chloroform, benzene, toluene and cyclohexane.

To determine $-\Delta H_a$ for each adsorbent, a dynamic method known as pulse chromatography was used. The hybrid surfactant-containing silica (MCM-EE) exhibited the highest heat of adsorption for dichloromethane and chloroform with values of $-\Delta H_a$ of 57 and 66 kJ/mol, respectively. The pore-expanded silica MCM-EC had the highest $-\Delta H_a$ for benzene, toluene and cyclohexane with values of 72, 83, and 56 kJ/mol.

The adsorption capacity was measured using breakthrough curves of the adsorbents in the presence of three types of streams: (i) a single VOC in a dry environment, (ii) a single VOC in a stream containing moisture and (iii) a mixture of two VOCs. For single components under dry conditions, the volumetric capacities obtained were in the order MCM-41>MCM-EC>MCM-EE for aromatic compounds and

cyclohexane. For halogenated compounds, the order obtained was MCM-41>MCM-EE>MCM-EC. In humid streams, MCM-EE showed the best efficiency for dichloromethane with a capacity equal to 89% of the capacity in a dry stream. For the case of benzene, MCM-41 exhibited the best efficiency, adsorbing 87% of the amount adsorbed under dry conditions. For cyclohexane in the presence of moisture, the three adsorbents presented a very similar efficiency with 68% for MCM-EC and MCM-41 and 66% for MCM-EE. As for the two-component systems, in the mixture comprised of benzene and dichloromethane, MCM-41 presented a better selectivity for the former and MCM-EE for the latter. In the second mixture, consisting of benzene and toluene, MCM-EE presented a much higher selectivity towards benzene, while MCM-41 was significantly more selective towards toluene.

Résume

Les règlements environnementaux de plus en plus rigoureux dans le monde entier exigent l'utilisation de méthodes efficaces pour la purification de l'air. Ce travail est une contribution pour le développement d'adsorbants efficaces pour les composés organiques volatils (VOCs). Trois variétés différentes de silices mésoporouses ordonnées avec des caractéristiques prometteuses ont été évaluées: une silice mesoporous ordonnée MCM-41 préparée en présence d'un surfactant, un MCM-41 dont les pores ont été élargis par un traitement hydrothermique post-synthèse en présence d'un agent organique (désigné sous le nom de MCM-EC), et une silice mésoporouse hybride avec des pores élargis produite par l'extraction sélective de l'agent organique (nommé MCM-EE). Pour évaluer l'efficacité de ces adsorbants, les chaleurs d'adsorption ($-\Delta H_a$) et les capacités d'adsorption (q) ont été déterminées expérimentalement pour cinq VOC typiques: dichlorométhane, chloroforme, benzène, toluène et cyclohexane.

Pour déterminer $-\Delta H_a$ pour chaque adsorbant, une méthode dynamique connue sous le nom de chromatographie pulsée a été employée. La silice hybride contenant le surfactant (MCM-EE) a montré la chaleur d'adsorption la plus élevée pour le dichlorométhane et le chloroforme avec des valeurs du $-\Delta H_a$ de 57 et 66 kJ/mol, respectivement. La silice MCM-EC a pores élargis a montré des chaleurs d'adsorption pour le benzène, le toluène et le cyclohexane avec des valeurs de 72, 83, et 56 kJ/mol.

La capacité d'adsorption a été mesurée en utilisant les courbes de saturation des adsorbants en présence de trois types de courants gazeux: (i) un seul VOC dans un environnement sec, (ii) un seul VOC dans un courant humide et (iii) un mélange de deux

VOC. Pour les composés purs dans des conditions sèches, les capacités volumétriques obtenues étaient dans l'ordre MCM-41>MCM-EC>MCM-EE pour les composés aromatiques et le cyclohexane. Pour les composés halogénés, l'ordre obtenu était MCM-41>MCM-EE>MCM-EC. Dans un environnement humide, MCM-EE a montré la meilleure efficacité pour le dichlorométhane avec une capacité d'adsorption de 89% comparée avec le courant sec. Pour le cas du benzène, MCM-41 a montré la meilleure efficacité, adsorbant 87% de la quantité adsorbée dans des conditions sèches. Pour le cyclohexane en présence d'humidité, les trois adsorbants ont présenté des efficacités semblables avec 68% pour MCM-EC et MCM-41 et 66% pour MCM-EE. Pour les systèmes à deux composés, dans le mélange comprenant le benzène et le dichlorométhane, MCM-41 a présenté une meilleure sélectivité pour le premier et le MCM-EE pour le dernier. Dans le deuxième mélange, composé de benzène et de toluène, MCM-EE a présenté une sélectivité beaucoup plus élevée envers le benzène tandis que MCM-41 était sensiblement plus de sélectif envers le toluène.

Table of Contents

List of Tables

List of Figures

List of symbols

A	Arrhenius equation pre-exponential factor (mol g^{-1} kPa^{-1})
A_c	Cross-sectional area of the adsorption column (cm^2)
C_0	Concentration of the organic compound in the inlet stream (mol ml^{-1})
C_A	Concentration of the organic compound in the outlet stream (mol ml^{-1})
C_F	Correction factor of the KJS equation, equal to 0.3 nm
ΔH_a	Heat of adsorption (kJ mol^{-1})
F	Total flow rate (ml min^{-1})
F_A	Molar flow of adsorbate (mol min^{-1})
K	Dimensionless form of Henry's Law constant
K_p	Dimensional form of Henry's Law constant (mol g^{-1} kPa^{-1})
L	Length of the column (cm)
N_A	Maximum amount of adsorbed molecules (mmol)
P	Total pressure of the system (mmHg)
P_0	Reference pressure (mmHg)
P_{vap}	Vapor pressure of the adsorbate (mmHg)
q	Adsorbent capacity (mol g^{-1})
q'	Adsorbent volumetric capacity (mol ml^{-1})
R	Ideal gas universal constant (kJ mol^{-1} K^{-1})
r	pore size as a function of relative pressure (nm)
t	Elapsed time (s)
T	Absolute temperature (K)

T_c Temperature in the fixed bed column (°C)

T_s Temperature in the glass saturator (°C)

t_b Breakthrough time (s)

t_q Stoichiometric time (s)

t_s Saturation time (s)

T_s Temperature in the saturator (°C)

u Linear surface velocity of the fluid (cm s^{-1})

V Packed volume of the column (ml)

v Volumetric flow of gases (cm^3 s^{-1})

v^p Volume of nitrogen adsorbed during characterization (cm^3 g^{-1})

V_L Molar volume of the liquid adsorbate (cm^3 mol^{-1})

W Total mass of adsorbent in the column (g)

y_A Molar fraction of adsorbate in the gaseous mixture

Greek symbols

ε Interparticle spatial void, bed porosity

γ Surface tension (N m^{-1})

μ_D Mean dead time (s)

μ_1 First absolute moment of the curve, mean retention time (s)

ρ_b. Apparent density (g cm^{-3})

ρ_p Particle density of the adsorbent (g cm^{-3})

ρ_p Pellet density (g cm^{-3})

τ Statistical film thickness (nm)

Acknowledgements

I want to thank my supervisor, Professor Abdel Sayari for his truthful guidance during the development of the present work and for giving me the opportunity to join his research group.

My sincere gratitude to everyone at the Centre for Catalysis Research and Innovation at the University of Ottawa for offering me their friendship, support and knowledge. Particularly, I want to thank Peter Harlick for all his helpful comments to improve my work as engineer and researcher.

I dedicate this thesis to my parents Gabriel and Martha; words can not express how thankful I am for having you as guide and support. Though far, you will always be with me.

To Gabriela. Thanks for joining me in this adventure and encouraging me to follow my dreams. Your love gives me strength and happiness.

"What is now proved, was once only imagined"

-William Blake

I. Theoretical Background

1. Introduction

Air pollution is nowadays one of the most important concerns of governments, environmental organizations and industry alike. The 20th century was characterized not only by its overwhelming technological advances, but also for the massive industrialization all around the globe. While the benefits of industrial development are obvious, its negative effects on the quality of air became evident with the occurrence of tragic events around the world, like the smog episodes in London that claimed the life of dozens of people (J. C. Mycock et al., 1995; N. P. Cheremisinoff, 2000). This made clear that industry may represent a threat to the Earth's equilibrium if no actions are taken to minimize its impact.

Consequently, the end of the past century witnessed an increased concern by governments around the globe and the public in general, motivating the development of new standards and regulations to control the emission of pollutants to the environment. The United States of America for example, developed the Clean Air Act which was a pioneer document intended to regulate industrial emissions while setting parameters for long term improvement in air quality, and served as basis and example for other regulations worldwide (USEPA, 1990; J. C, Mycock et al., 1995; D. Redalieu, 1995). In Canada for example, the Canadian Environmental Protection Act includes regulations with similar purposes. In addition to these national regulations, some international

agreements have also been developed. The recently approved Kyoto protocol, for example, summarizes plans for prevention and control of pollutants responsible of the global warming (the so-called "greenhouse effect"). Likewise, the Montreal protocol proposes regulations for those contaminants capable of depleting the ozone layer (C. A. Koh et al., 2002). In this way, international cooperation has been acknowledged as vital, since emissions of air pollutants may affect wide areas, way beyond a single nation's borders (J. C. Mycock et al., 1995).

Within the last decade, environmental regulations have grown stricter, and it is expected that such tendency will continue for the next years. In order to meet such strict requirements, great efforts have been placed in the research and development of cleaner, environmentally friendly technologies (F. I. Khan and A. K. Goshal, 2000). It must be said that, even though the original incentive of companies to improve their environmental performance was to avoid sanctions and governmental fees (B. Garrod and P. Chadwick, 1996), this perspective has changed with the appearance of the so-called "green movements" and of "total quality" policies. At present, many companies understand the benefits of good environmental practices in terms of product quality, added value and trademark prestige (G. Theyel, 2000). As well, the claim of some authors that the adequate use of new technologies can generate profits while preserving the environment has served as incentive after an expected high investment to fulfill regulatory demands (C. N. Madu et al., 1995; R. Florida, 1996).

The research of new materials and technology to achieve high production efficiencies may prevent the release of any potentially hazardous compounds by preventing the generation of waste. While there is a wide range of technologies available

for such purpose (J. C. Mycock et al., 1995; F. I. Khan and A. K. Ghoshal, 2000), the current work is devoted to the use of adsorption as a purification technology for air streams. Adsorption separation is particularly suitable for air purification not only due to its potential high efficiency but also because it allows the separation of some valuable components that can be recycled and reused in the manufacturing process, hence enhancing its economic performance (J. C. Mycock et al., 1995; F. I. Khan and A. K. Ghoshal, 2000)

Volatile organic compounds (VOC) are a particularly important subject in the study of air pollution prevention and control, due to their extensive use in industry and their negative impact when released to the environment (F. I. Khan and A. K. Ghoshal, 2000). In the present work, the adsorptive properties of three varieties of ordered mesoporous silicas (A. Stein et al. 2000; A. Sayari and S. Hamoudi 2001) as adsorbents of some representative VOCs are determined experimentally. It is the intention of this research to analyze the adequacy of these novel materials as an alternative for the purification of industrial air streams by adsorption.

2. Air Pollution by Volatile Organic Compounds.

While air quality has been affected by human activities since the very beginning of mankind, the era of industrialization has caused a deeper impact than ever before (T. Godish, 2004). Among the wide variety of substances released to the environment, the main air pollutants are commonly classified in terms of their chemical nature into sulfur oxides (SO_x), nitrogen oxides (NO_x), carbon oxides (CO and CO_2), particulate matter (PM) and volatile organic compounds (VOC) (N. P. Cheremisinoff 2000; T. Godish, 2004). Even though all of these gases are of great environmental relevance, the latter one is a main concern for the chemical industry since industrial processes are currently the main contributors of hazardous VOCs released to the environment (N. de Nevers, 2000; P. Hunter and S. T. Oyama, 2000). The extensive use and production of VOCs represents large emissions, making its minimization an important environmental challenge.

Volatile organic compounds can be defined as any organic compound whose partial pressure at standard conditions is greater than 0.07 kPa and presents an atmospheric boiling point of up to 260 °C (N. de Nevers, 2000). A definition provided by the United States Environmental Protection Agency (USEPA) describes VOCs as any compound of carbon that participates in a photochemical reaction (P. Hunter and S. T. Oyama, 2000). The purpose of such definition is to exclude compounds with low reactivity like CO and CO_2 which may require a special classification, while including almost every compound with less than 12 carbon atoms in its structure. In this way, the definition includes an extensive number of hydrocarbons whose reactivity is likely to impact negatively to the environment thus being considered Hazardous Air Pollutants

(HAP) (USEPA, 1990; Environment Canada, 1999). Because of the wide variety of compounds included in the definition of VOC, various classifications have been proposed. Some authors classified them as hydrocarbons and compounds (P. Hunter and S. T. Oyama, 2000), where the former refers to all substances formed only by carbon and hydrogen atoms and the latter to those with other functional groups in their structure. In other publications, they have also been classified in terms of their functional groups as halogenated hydrocarbons, aromatic compounds, alcohols and ketones (J. Pires et al. 2001).

Since volatile organic compounds involve a wide variety of substances, their effects on the environment are diverse as well. While there is controversy on the effect of some specific organic compounds on the environment (P. Hunter and S. T. Oyama, 2000), it is generally accepted that these contaminants affect negatively the human and animal health, harm crops, vegetation and forests, and damage the structure of buildings (N. P. Cheremisinoff, 2000; N. de Nevers, 2000; P. Hunter, 2000; T. Godish, 2004). Furthermore, air pollutants can be easily transported into other physical medium, contaminating water streams and soil (N. P. Cheremisinoff, 2000; N. de Nevers, 2000; P. Hunter and S. T. Oyama, 2000; R. S. Bansode et al. 2003; T. Godish, 2004).

One of the main reasons why the emission of volatile organic compounds is of great concern is their reactivity with other substances in the atmosphere. It is known that powered by sunlight, VOCs react photochemically with nitrous oxides (NO_x) in the atmosphere producing smog with high contents of ozone (O_3) and other photochemical oxidants (N. P. Cheremisinoff, 2000; N. de Nevers, 2000; P. Hunter and S. T. Oyama, 2000). At a tropospheric level, O_3 is a poison, with a deleterious effect on human health,

attacking mainly the respiratory system (N. P. Cheremisinoff, 2000) and it is suspected that its concentration levels in the lower atmosphere have increased in recent years because of increased VOC emissions (M. C. Gomez et al., 2004). Ozone has a threshold for odor detection of 0.01-0.05 ppm for most individuals and causes headaches and throat dryness at concentrations of 0.1-1 ppm (P. Hunter and S. T. Oyama, 2000). At higher concentrations, ozone can cause asthmatic symptoms, throat irritations, hemorrhaging, pulmonary edema, and in extreme cases, death (P. Hunter and S. T. Oyama, 2000). Moreover, it affects all sorts of animal tissue, damages vegetation and is capable of killing trees and crops (N. P. Cheremisinoff, 2000). For these reasons, current ozone regulations are concerned both with the levels of ozone and ozone precursor hydrocarbons in the atmosphere (A. Latella et al., 2005).

On the other hand, ozone in the stratosphere forms a layer that provides a protective character from the ultraviolet (UV) solar radiation (N. P. Cheremisinoff, 2000; P. Hunter and S. T. Oyama, 2000; T. Godish, 2004). It has been proposed that some volatile organic compounds, mainly halogenated hydrocarbons, decompose at stratospheric levels and act as catalysts in the degradation of stratospheric ozone molecules into regular O_2 (P. Hunter and S. T. Oyama, 2000; T. Godish, 2004). It is worth mentioning that O_2 molecules do not provide any protection from solar radiations, and as a consequence, the protective character of the ozone layer is reduced. This generates high risk of skin cancer and other degenerative and mutagenic diseases in flora and fauna because UV radiation is capable of altering the genetic structure of living cells (T. Godish 2004).

Both halogenated hydrocarbons and tropospheric ozone are suspected responsibles of global warming (the so-called "greenhouse effect") (W. Lei et al. 2004), with an estimated contribution of 13 and 8% respectively to the total warming attributed to greenhouse gases (T. Godish, 2004).

While exposure to individual species of VOCs is not always considered a high risk, some particular substances are considered to have a nefarious effect on human health (C. A. Koh et al., 2002; T. Godish, 2004). The USEPA classification of Hazardous Air Pollutants includes more than 180 substances that are potential risks to human health or the environment, including a significant number of VOCs (USEPA, 1990; M. Lordgodei and M. S. Kim, 2004). In particular, many species of aromatic and polycyclic aromatic hydrocarbons (PAH) are considered health hazards for being recognized as mutagenic, carcinogenic and poisonous (USEPA, 1990; Environment Canada, 1999; T. Godish 2004).

Having exposed the impact of VOCs emission, it is important to mention that it represents a global problem, affecting cities all around the world (B. T. Jobson, et al. 2004; A. Latella, et al., 2005), in both urban (M. C. Gomez, et al. 2004; W. Lei et al. 2004; O. Baroja et al. 2005) and rural areas (H. Guo, et al. 2004). Since air pollutants are easily transported, they are not localized only in the surroundings of the industrial sites, but covering extensive areas (R. J. Brennan and R. H. Schiestl, 1998; N. P. Cheremisinoff, 2000). In a study conducted by the United States Geological Survey (USGS) (T. J. Lopes and D. A. Bender, 1998), the presence of various organic compounds was found in storm water samples in urban areas. The occurrence of such contaminants was directly associated to their existence in the atmosphere proving their

transport from industrial sites. A list of the major organic compounds reported in such study is presented in Table 2.1. As can be seen, the most commonly detected hydrocarbons were aromatics, gasoline additives and eight chlorinated compounds. Toluene was overall the most frequently detected, and trichloromethane (chloroform) was the most recurrent halogenated compound.

Table 2.1 VOCs detected in urban stormwater

Compound	Per cent detection in stormwater*	Ranking of detection in stormwater
Methylbenzene (toluene)	23	1
Total xylenes	18	2
Trichloromethane (chloroform)	13	3
1, 2, 4 Trimethylbenzene	12	4
Tetrachloromethane	8.0	5
Naphtalene	7.4	6
Methyl tert-butyl ether	6.9	7
Dichloromethane	5.9	8
Bromodichloro-methane	5.8	9
Ethylbenzene	5.0	10
Trichloroethane	4.7	11
Cis-1, 2-dichlorothene	4.6	12
1, 1, 1 trichloroethane	4.2	13
Benzene	3.9	14
Dibromochloro-methane	3.4	15

*Relative to the total number of stormwater samples analyzed

The production and use of VOCs are expected to continue because of their importance in many industrial processes, since they are widely used as solvents, thinners, degreasers, cleaners, lubricants and fuels (N. P. Cheremisinoff, 2000; N. de Nevers, 2000; P. Hunter and S. T. Oyama, 2000; F. I. Khan and A. K. Ghoshal 2000). Due to the chemical stability of some compounds, they are as well utilized as refrigerants and

propellers (T. Godish, 2004). One of the main problems of VOCs is that, due to their volatile nature, they mix very easily with air, producing losses wherever their use is intended. It is known that a considerable percentage of VOCs released are fugitive emissions caused during their transportation or use (N. de Nevers, 2000; F. I. Khan and A. K. Ghoshal, 2000). Some reports concerning the use of volatile organic compounds as solvents claim to have loses of up to 80 per cent of solvent by spontaneous volatilization during its use (B. A. Wofford et al. 1999). As can be seen, this represents not only a threat to the labor force's health, but also a considerable economic loss.

VOC emissions are not, however, associated only with their use. They are also undesired byproducts in oil refining processes (F de Santis, et al., 2004; B. T. Jobson et al., 2004; O. Baroja, et. al., 2005), wastewater treatment plants and landfills (J. G. Leahy, et al., 2004). Additionally, the incomplete combustion of fossil fuels produces a mixture of highly reactive organic compounds (R. J. Heinsohn and R. L. Kabel 1999). Combustion is one of the greatest contributors to the presence of VOCs in the atmosphere, generating almost 40% of the total amount of VOCs emitted (P. Hunter and S. T. Oyama, 2000; T. Godish, 2004).

One of the main reasons why the present study focuses on adsorption of organic compounds is that adsorption technologies may not only prevent their emission to the atmosphere, but also allow their recuperation for reuse (J. C. Mycock, et al. 1995). In this way, the processes overall efficiency is improved, with the consequent economical advantages. Additionally, VOC adsorption may be a good alternative to accomplish environmental standards in all sorts of air contaminating processes (P. Hunter and S. T. Oyama, 2000).

Table 2.2 Properties of selected volatile organic compounds

	Label	CAS Registry No.	log o/w*	Freeze point (K)	Boiling Point (K)	Molecular weight
Dichloromethane	DCM	75-09-2	1.25	178	313	85
Chloroform	CFM	67-66-3	1.97	210	334	119
Benzene	BZN	71-43-2	2.13	279	353	78
Toluene	TLN	108-88-3	2.69	178	384	92
Cyclohexane	CXN	110-82-7	3.44	280	354	84

*logarithm of the octanol/water partition coefficient

The objective of this work is to analyze some relevant organic compounds in terms of environmental impact and as representatives of some families of organic compounds included in the wide classification of VOCs. As explained early, the impact of aromatic and halogenated hydrocarbons are a main issue in the study of volatile organic compounds. Thus, two aromatic compounds (i. e. benzene and toluene) and two halogenated hydrocarbons (i. e. trichloromethane and dichloromethane) were selected for being substances regulated by the USEPA (USEPA , 1990), Environment Canada (Environment Canada, 1999) and other governments around the globe (P. E. Yu-Chin Chiang et al. 2001). Additionally, cyclohexane was chosen for being a cyclic, not aromatic hydrocarbon with high hydrophobicity, extensively used in industry as solvent (C. S. Moon, et al., 2001). Some relevant properties of the aforementioned substances are presented in Table 2.2. These compounds are as well the five more recurrent VOCs in the city of Ottawa, according to a recently published assessment report (J. Zhu, et al., 2005).

Another extremely important property of volatile organic compounds is their vapor pressure P_{vap}. This property can be directly related to the concentration of the organic compound in a vapor phase environment and is a function of temperature as expressed by Equation 1 (C. L. Yaws, 1999):

$$\log_{10} P_{vap} = A + \frac{B}{T} + C\log_{10} T + DT + E\,T^2 \qquad (1)$$

Where T is the absolute temperature in K, P_{vap} is the vapor pressure of the VOC expressed in mmHg and A, B, C, D and E are the regression coefficients characteristic for each organic compound, and are presented in Table 2.3. For practical purposes, a graphic representation of P_{vap} as a function of T can be found in Appendix C.

Table 2.3. Regression coefficients to determine vapor pressure of pure organic compounds according to Eq. 1 (C. L. Yaws, 1999).

	A	B	C	D	E
Dichloromethane	32.5609	-2.5166E+03	-8.8015E+00	1.2934E-10	3.3194E-06
Chloroform	56.6178	-3.2462E+03	-1.8700E+01	9.5150E-03	1.1553E-12
Benzene	31.7718	-2.73E+03	-8.44E+00	-5.35E-09	2.72E-06
Toluene	34.0775	-3.04E+03	-9.16E+00	1.03E-11	2.70E-06
Cyclohexane	48.5529	-3.09E+03	-1.55E+01	7.38E-03	6.36E-12

A more extensive description of the volatile organic compounds studied in the present work is presented next:

a) Aromatic Hydrocarbons.

Aromatic hydrocarbons are widely used as solvents, and fuel additives making them commonly present in ambient air (T. Godish, 2004). The group of aromatic compounds known as BTEX (i. e. Benzene, toluene, ethyl-benzene and xylene) is of particular concern for many reasons. These compounds are not only some of the most abundant VOCs in the environment (O. Baroja, et al., 2005), but they are also known to be highly reactive (W. Lei, et al., 2004). Long term exposure to them has been linked to cancer and other mutagenic diseases (L. G. Roberts, et al., 2003; B. T. Jobson, et al. 2004). The work by Moon et al. (2001) for example, reports the evaluation of more than 800 solvent-consuming workplaces. According to such study, the presence of toluene was the most abundant in the working environment. Benzene and cyclohexane were also considered among the most recurrent compounds detected.

Benzene is extensively used in industry as solvent (N. Brautbar and J. Williams, 2002) and as raw material in the production of other chemical compounds like cumene, styrene and maleic anhydride (A. C. Capleton and L. S. Levy, 2005). Exposure to benzene vapors is known to be a cause of mutagenic illness like leukemia (R. J. Heinsohn and R. L. Kabel 1999), and it is considered carcinogenic according to the Canadian Environmental Protection Act (CEPA) based on evidence provided by experiments in animals (Environment Canada 1993a).

Toluene is also considered a Priority Substance by the CEPA (Environment Canada, 1999c). It is extensively used as solvent for products as diverse as paints, varnishes, pesticide formulations, printing ink, adhesives, sealants and cleaning agents (Environment Canada 1993c; C. S. Moon, et al., 2001). It is also used for chemical

extractions and as reactant in the production of benzene principally, and other chemical products (Environment Canada 1993c). The highest emissions of toluene in Canada are consequence of its use as solvent (around 54 thousand tons per year), but it is also released to the environment as byproducts of petroleum refining processes, landfills and incomplete combustion of natural and fossil fuels (Environment Canada 1993c). At high concentrations, it is suspected to attack the neurological and respiratory systems in humans (J. G. Leahy, et al., 2004), and there is evidence on animal testing that chronic exposure has an adverse effect on kidney and lungs and produces central nervous system depression (Environment Canada 1993c; B. S. Nielsen, et al., 2003; J. H. C. M. Lammers, et al. 2005). Epidemiological studies suggest that toluene exposure can produce severe liver damage, especially in conjunction with other aromatics solvents (N. Brautbar and J. Williams, 2002).

b) Halogenated Hydrocarbons

Halogenated hydrocarbons are volatile and semivolatile substances containing at least one atom of chlorine, bromine or fluorine. They exhibit a long lifetime in the atmosphere (J. Mather, et al. 1998) for which it is an environmental priority to prevent their release to the atmosphere. Among a wide variety of uses in industry, they are commonly used as aerosol propellants, refrigerants, degreasing solvents and foaming agents (N. Brautbar and J. Williams, 2002; T. Godish, 2004). Other sources to the environment include the manufacturing of herbicides, pesticides, paint, and pulp and paper (A. Giaya and R. W. Thompson, 2000; J. W. Lee et al., 2005)

Dichloromethane, for example, is mainly used as paint remover, as blowing agent in foam production, as a component in aerosols, as degreasing solvent, and as extraction solvent for oleoresins and film processing (Environment Canada, 1993b; A. McCulloch, et al. 1999; N. Sonoyama et al., 2001). Its half life in the troposphere has been estimated between 100 days and one year, which allows its transport to the stratosphere, where it is more easily degraded by photochemical reactions. While there is no conclusive data presently, dichloromethane is a suspected carcinogen with hepatic and pulmonary effects mainly during chronic exposure (Environment Canada, 1993b; J. W. Lee et al., 2005).

Chloroform is used in the chemical industry as a solvent and as raw material in the production of fluoropolymers (Environment Canada, 2000). It is extensively used in the manufacturing of rubbers, ink, paint and electronic components (C. H. Lao, et al., 2003). Chloroform is a byproduct during water purification and paper bleaching by chlorination, being the greatest contributors of chloroform production and emissions in Canada (Environment Canada, 2000). Significant emissions are also produced by metal degreasing plants (C. H. Lao, et al., 2003). Other sources of chloroform include waste incinerators and waste composting facilities (Environment Canada, 2000). Because of its low capacity to absorb light, direct photolysis does not represent a significant degradation process, resulting in long lifetimes in the atmosphere of up to 600 days (J. Mather, et al. 1998; Environment Canada, 2000). Therefore, chloroform can be transported through long distances in the atmosphere before being degraded.

Research studies on acute exposure to chloroform in animals suggest damage in the liver and kidneys and potential severe nervous system depression causing death (Environment Canada, 2000). The chronic exposure to chloroform has an adverse effect

on the cardiovascular and respiratory system (A. C. Capleton and L. S. Levy, 2005), in addition to its carcinogenic (A. Adachi, et al. 2001; M. Ahmenda, et al., 2004) and mutagenic (R. J. Brennan and R. H. Schiestl, 1998) behavior.

3. Purification of Industrial Emissions by Adsorption

The imperative need to minimize pollutant emissions in industry has resulted in the development of a wide variety of separation and purification technologies (F. I. Khan and A. K. Ghoshal, 2000). Some of these technologies like thermal and catalytic combustion (M.-M. C. M. Alvim Ferraz, et. al., 1999) and biofilters (A. Aizupuru, 2003) offer viable routes to achieve clean industrial emissions with the transformation of contaminant molecules into innocuous or less harmful compounds (P. Hunter and S. T. Oyama, 2000; F. I. Khan and A. K. Ghoshal, 2000). However, for being processes based on the degradation of chemical species, such options may not be appropriate for streams with reusable substances, especially when they represent a considerable economical expense in the process. To recover valuable substances, the method used must perform a separation with no chemical transformation of the compound of interest.

During the last decades, adsorption separation has attracted particular attention as a purification process (W. J. Thomas and B. Chrittenden, 1998), due to the high efficiencies it can achieve and to the fact that, unlike other separation technologies, it can be operated within a wide range of concentrations (P. Hunter and S. T. Oyama, 2000). This flexibility makes it suitable for many applications, from the separation of streams with only a few ppm of contaminants (e. g. for air purification) (N. de Nevers, 2000; F. I. Khan and A. K. Ghoshal, 2000) up to high concentrations, as in the case of solvent recovery (J. C. Mycock, et al. 1995).

Adsorption refers to the process where molecules in a fluid stream are attracted and attached to a surface, generally solid in separation technologies (N. de Nevers, 2000; P. Hunter and S. T. Oyama, 2000). In adsorption, the component in the fluid phase that is being adsorbed is commonly referred to as "adsorbate" while the solid phase is known as the "adsorbent" (M. D. Ruthven, 1984). The adsorbed molecules are attached to the solid surface by low energy attraction forces (known as Van der Waals forces), similar to energies of condensation (M. D. Ruthven, 1984; J. C. Mycock, et al., 1995; P. Hunter and S. T. Oyama, 2000). Therefore, no structural transformation of the adsorbed molecules occurs.

Among the various parameters involved in adsorption processes, it is of a particular interest to determine the heat of adsorption ($-\Delta H_a$) in a system for various reasons. In the first place, $-\Delta H_a$ is a measurement of compatibility between the solid and the adsorbed species since it is related to the strength of the bond generated between them. It is also a measurement of the energy required to detach the adsorbed species during regeneration processes. Because adsorption involves low attraction energies, it is expected that the adsorbent-adsorbate interactions can be broken in a relatively easy way. A special case is the phenomenon known as chemical adsorption or "chemisorption", where the adsorbate molecules are attached to the solid surface by strong covalent forces (P. Hunter and S. T. Oyama, 2000). However, since the subsequent retrieval of the adsorbate in chemisorption is particularly difficult (J. C. Mycock, et al., 1995; P. Hunter and S. T. Oyama, 2000), its study is not within the scope of the present work.

It is known that the adsorption capacity of a solid is limited since there are a finite number of active sites where molecules can be adsorbed. The adsorption capacity refers

to the total amount of molecules that a particular solid can potentially adsorb and it depends on the physical and chemical characteristics of the adsorbent and on some process conditions like adsorbate concentration in the fluid phase and temperature (M. D. Ruthven, 1984; W. J. Thomas and B. Chrittenden, 1998). When adsorbents are exposed to a continuous flow of adsorbate, all the space available to accommodate adsorbed molecules is eventually occupied and the solid is said to be "saturated". Saturation is a state of thermodynamic equilibrium where the rates at which molecules are attached and detached from the solid surface are assumed to be equal; therefore molecules are no longer adsorbed from a macromolecular point of view. The number of adsorbed molecules required to reach a saturated state depend on the concentration of adsorbate in the fluid stream. In the cases where the adsorbent can be reused, it undergoes a regeneration step to remove the adsorbate from it after saturation is reached (M. D. Ruthven, 1984; W. J. Thomas and B. Chrittenden, 1998; P. Hunter and S. T. Oyama, 2000). The reverse process of adsorption is known as desorption and if performed properly it can recuperate the adsorbate in a very efficient manner while regenerating the adsorbent's capacity. The most popular methods used for desorption are the increment of temperature in the adsorption column (Temperature Swing Adsorption or TSA), the decrement of pressure (Pressure Swing Adsorption or PSA) and the flow of purge stream through the adsorption system (M. D. Ruthven, 1984; W. J. Thomas and B. Chrittenden, 1998). It is also a common practice to use combinations of these methods to enhance the regeneration efficiency; a good example is the regeneration process of activated carbon by steam injection (M. D. Ruthven, 1984; P. Hunter and S. T. Oyama, 2000). It is through desorption that recuperation of organic compounds takes place, since its outcome is most

likely a highly concentrated stream of adsorbate that can be easily treated whether for reuse or disposal.

Adsorption separation technologies are considered as good alternatives for the recuperation of fugitive emissions and are currently used by industries characterized by their extensive use of solvents and with products as diverse as synthetic fibers, pharmaceuticals, printing and coating just to mention a few (P. Hunter, S. T. Oyama, 2000). As can be seen, adsorption separation does not only provide a good efficiency for the accomplishment of environmental standards, it may also boost the economical performance of any plant by reutilizing solvents otherwise lost, making it an attractive investment. Adsorption can be a good example on how it is possible to improve both environmental and economic performance.

A crucial factor in any adsorption system is the adequate selection of the solid adsorbent employed. There are many materials that can be used as adsorbents, and the physical, chemical and structural characteristics of each one determine its performance as adsorbent for a certain substance in the fluid stream (M. D. Ruthven, 1984; J. C. Mycock, et al., 1995; W. J. Thomas and B. Chrittenden, 1998). In general, a good adsorbent presents high surface area and excellent mechanical stability. It is accepted as well, that adsorbents with polar characteristics will perform better for the adsorption of polar compounds, while non polar adsorbents are more compatible with hydrophobic adsorbates (M. Lordgooei and M. S. Kim, 2004). Ideally, an adsorbent for VOC removal should present the following characteristics: large accessible pore volume, no catalytic activity, a hydrophobic character, high thermal and hydrothermal stability, and must be easily regenerated (X. S. Zhao et al., 1998).

Silica, alumina and zeolites are some of the most commonly used materials in industry; nowadays, however, activated carbon is the most popular adsorbent used for separation of volatile organic compounds from air and water streams (J. C. Mycock et al., 1995; D. O. Cooney, 1999; J. H. Yun et al. 1999; F. Delage et al., 2000; J. Benkhedda et al. 2001; M. A. Lillo-Rodenas et al., 2002; R. R. Bansode et al. 2003). Activated Carbon is a highly porous material, with pores distributed mainly in the microporous range (i. e. from 1-20 Å) (M. P. Cal et al. 1996; M. Molina-Sabio et. al., 1996; Y. C. Chiang et al., 2001); it generally exhibits high surface area and a hydrophobic nature (M. P. Cal, et al., 1996; S. Qi et al., 2000). There are many varieties of activated carbon commercially available, for which a properly chosen type can offer a good efficiency (D. O. Cooney, 1999; Y. C. Chiang et al., 2001). Its main advantage is that it can be produced from cheap raw materials like coal, wood or nut shells (C. Moreno-Castilla, et al. 1995; D. O. Cooney, 1999; M. A. Lillo-Rodenas et al, 2002; R. R. Bansode et al., 2003; T. V. Anurova et al., 2004). However, its pore size is hard to control during activation, resulting usually in wide pore size distributions (C. Moreno-Castilla, et al. 1995; M. Molina-Sabio et al., 1996; P. A. Gauden et al., 2004). In operation, common problems include pore clogging and competitive adsorption of water in highly humid environments resulting in a diminished adsorption capacity (M. P. Cal et al. 1996; S. Qi et al., 2000; X. Hu et al., 2001; C. Ooka et al., 2004). Moreover, as a consequence of the inherent exothermic nature of adsorption, there are reports on the ignition of columns using activated carbon during operation, representing a very significant threat to an industrial plant's security (F. I. Khan and A. K. Ghoshal, 2000; X. Hu et al., 2001; P. Pre et al., 2002). Because of these disadvantages, other adsorbent materials are currently under

investigation to provide a feasible and more efficient alternative to those already available in the market.

4. Ordered Mesoporous Materials.

It was during 1992 when researchers of the Mobile Corporation synthesized the first family of ordered mesoporous silicas, which was denominated M41S (C. T. Kresge et al. 1992). This group of new materials exhibited two main characteristics that draw the attention of the scientific community worldwide. In the first place, the M41S silicas presented a highly ordered porous structure, something never seen before in a mesoporous material (J. S. Beck et al., 1992). Secondly, it was possible to adjust its pore size as required, while presenting a narrow pore size distribution (J. S. Beck et al., 1992; C. T. Kresge et al., 1992).

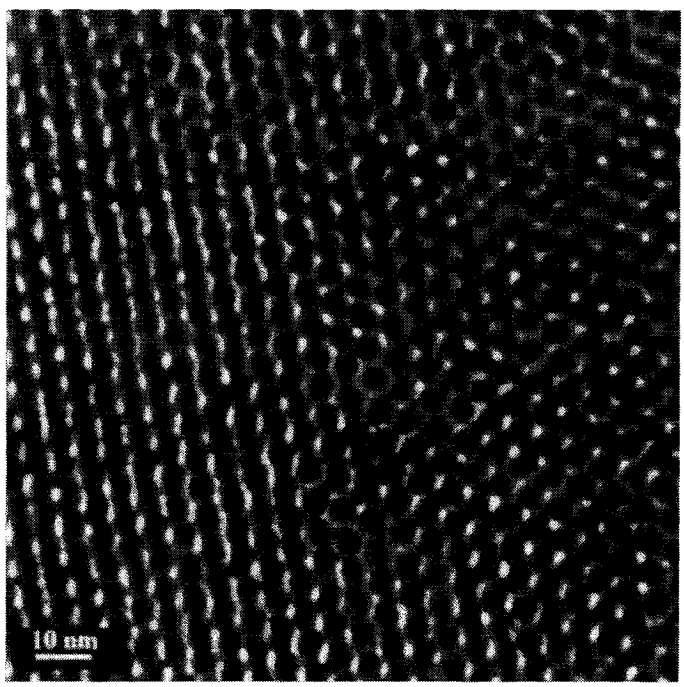

Figure 4.1. Typical transmission electron micrograph for MCM-41

Having such properties, it is no surprise that during the last years, extensive efforts have been placed with the aim of exploiting these materials and their characteristic properties. Many authoritative reviews on the preparation, characterization and potential applications of periodic mesoporous materials are currently available (A. Sayari, 1996; A. Sayari and P. Liu, 1997; X. S. Zhao et al., 1996; A. Corma, 1997; U. Ciesla and F. Schüth, 1999; J. Y. Ying et al., 1999; A. Stein et al., 2000; A. Sayari and S. Hamoudi, 2001; P. Selvam et al., 2001; X. He, 2002). A member of the M41S family, the MCM-41 type silica has the particular characteristic of presenting mesopores ordered in a two dimensional hexagonal array (J. S. Beck et al., 1992; C. T. Kresge et al., 1992). Figure 4.1 shows a typical electron transmission micrograph of MCM-41 published elsewhere (Sayari et al. 2000a), where such hexagonal (or honeycomb) structure is displayed. Due to its structural properties, it has been claimed as a material potentially adequate as catalyst support, catalyst, and adsorbent, since it presents high surface area and pore volume (M. Kruk and M. Jaroniec, 2001; M. M. L. Ribeiro Carrot et al., 2001) as well as good mechanical stability (J. Wu et. al., 2001).

The ordered structure of MCM-41 and the uniformity of its cylindrical pores have even made it useful to understand some characteristics of porous materials. Morishige et al. (2004) for example, used MCM-41 to demonstrate that, in materials with cylindrical pores, capillary condensation, rather than evaporation, occurs near thermodynamic equilibrium. It has also been employed as basis to prove the classic theories used to calculate pore sizes, helping with the development of new, more accurate ones. Using a series of highly ordered MCM-41 samples with different pore sizes, Kruk et al. (1997) found that there are certain inaccuracies on the determination of pore sizes by the highly

popular Kelvin equation, and that the Barret-Joyner-Halenda approach for the determination of pore size distribution based on the assumption of cylindrical pore shapes had to be proven experimentally. Therefore, based on experimental results obtained by the adsorption of nitrogen on such samples, a corrected form of the Kelvin equation (named "KJS model" after its authors) was proposed, and later proven to be highly precise:

$$r = \frac{2\,\gamma\,V_L}{R\,T\,\ln[(P_{vap}/P)]} + \tau + C_F \qquad (2)$$

where

r = Pore size as a function of relative pressure

V_L = Molar volume of the liquid adsorbate

γ = Surface tension

R = Universal gas constant

T = Absolute temperature

P = Pressure

τ = Statistical film thickness as a function of relative pressure

C_F = Correction factor equal to 0.3 nm

The highly ordered structure of MCM-41 is directly related to its formation mechanism. Indeed the synthesis of MCM-41 (and other periodic mesoporous materials discovered later) requires a well-defined supramolecular template around which the silica condenses to generate its distinctive ordered structure (J. S. Beck et al., 1992; C. T.

Kresge et al., 1992). The templates used are typically liquid crystals formed by surfactant or polymeric micelles in aqueous solutions. For a better understanding, Figure 4.2 shows a schematic representation of the mechanism for the synthesis of MCM-41 (C. T. Kresge et al., 1992; U. Ciesla and F. Schüth, 1999; P. Selvam et al., 2001). First, the surfactant molecules in solution generate cylindrical rod-like micelles. The next step consists of the ordering of the surfactant micelles in a hexagonal array around which the silica polymerizes. It is important to mention that there is still controversy about the mechanism of the crystal template formation (P. Selvam et al., 2001) (i. e. whether the micellar rods are ordered spontaneously or as a consequence of the interaction with silicate anions). After silica condensation, a periodic structure is generated which is dependent on the nature of the template employed (J. S. Beck et al., 1992). To obtain the pure siliceous material, the most straightforward approach to separate the organic template is by calcination of the as-synthesized silica (J. S. Beck et al., 1992; C. T. Kresge et al. 1992; M. M. L. Ribeiro Carrot et al., 2001; J. C. Vartuli et al., 2001; S. Z. Qiao, et al. 2004), but it can also be extracted using an organic solvent (P. T. Tanev and T. J. Pinnavaia, 1996) or by ionic exchange (N. Lang and A. Tuel, 2004).

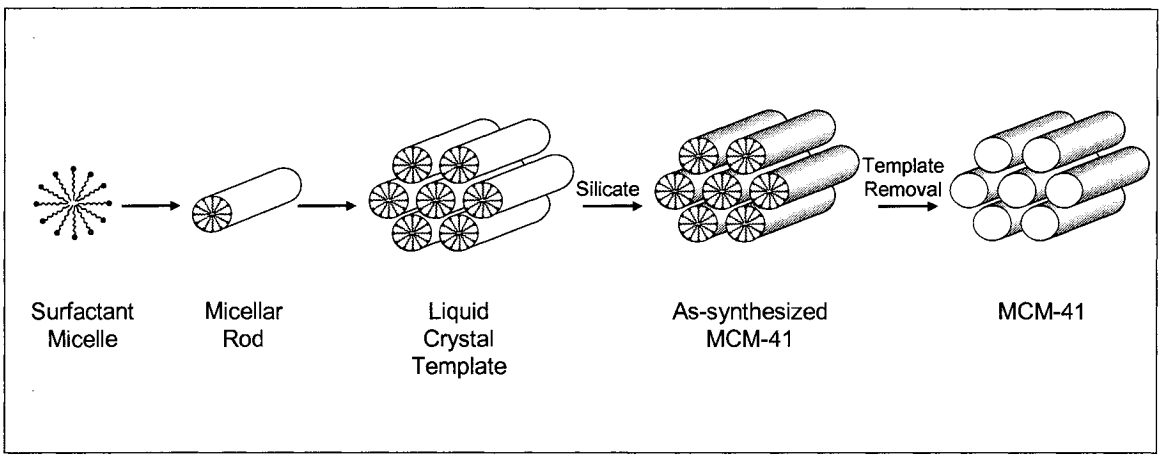

Figure 4.2. Synthesis route of MCM-41

The use of a liquid crystal template offers the possibility to manipulate the structural characteristics of the MCM-41. This is, in fact, one of the most attractive and widely exploited characteristics of the MCM-41 silica. Stated in the original work by Beck et al. (1992) and corroborated by other authors (M. Kruk et al., 1997; M. M. L. Ribeiro Carrot et al., 2001; J. C. Vartuli et al., 2001), it has been demonstrated that surfactant templates with different chain lengths produce structures with pore sizes and pore volumes that reflect the molecular size of the template. As expected, such variation affects directly the adsorption capacity and efficiency of the mesoporous material (J. C. Vartuli et al., 2001; S. Z. Qiao et al., 2004).

It is also known that other synthesis conditions influence the structural properties of MCM-41. The work of Sayari et al. (2002) analyzes the effect of temperature on the production of ordered mesoporous silicas using different alkyl-trimethylammonium bromides as templates. With the results thereby obtained, a recipe for the preparation of highly ordered MCM-41 was proposed, suggesting that larger pore sizes can be achieved at higher temperatures, but sacrificing uniformity in the pores.

The increase in pore size has been pursued with the manipulation of the surfactant template. Whether by direct synthesis or post-synthesis treatment with an expander additive, the range of pores in this mesostructure has been broadened to pores with diameters as large as 12 nm. Researchers like Corma et al. (1997) and Cheng et al. (1997) for example, have manipulated synthesis conditions such as temperature and gel composition to obtain large pore sizes by the expansion of the surfactant micelle (cetyl-trimethylammonium bromide).

To obtain a more significant increase, other authors have used additional molecules like amines (A. Sayari et al., 1999), alcohols (H. P. Lin et al., 1999), trimethylbenzene (J. S. Beck et al. 1992) and other organic compounds (N. K. Raman et al., 1996; S. K. Jana et al., 2004; M. Luechinger et al., 2005) as swelling agents. It is believed that these organic molecules are absorbed by the surfactant micelles increasing its size and with it, the pore size of the siliceous structure as represented schematically in Figure 4.3. The work by Jana et al. (2004) analyzes the properties of MCM-41 synthesized by adding methyl-substituted benzene, iso-propyl-substituted benzene and six different alkanes as swelling agents in the reactive mixture, obtaining a maximum pore size of around 9 nm. In all cases, an evident dependency of pore size on concentration of the swelling agent was found before reaching a maximum size attainable.

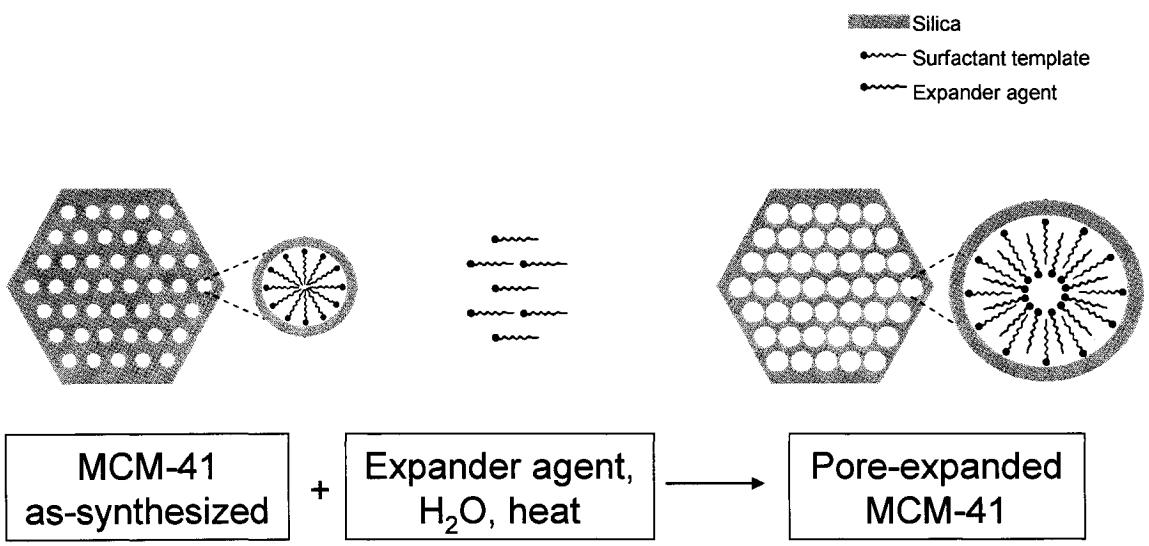

Figure 4.3. Schematic representation of the pore expansion process of MCM-41 by hydrothermal treatment

Another approach is the use of organic compounds as expander agents for post-synthesis hydrothermal restructuration of MCM-41 (A. Sayari et al., 1998; A. Sayari et al., 1999; M. Kruk et al., 2000). In this method, a non-calcined mesoporous material is treated in aqueous emulsions of the expander agent under static heating. In the work by Sayari et al. (1998) different amines were used as expanders producing materials with high pore volumes and narrow pore size distribution, and concluded that the best uniformity of pore structure is obtained in the presence of dimethyldecylamine. Similarly to the case of direct synthesis with swelling agents, the structural properties of the MCM-41 after hydrothermal regeneration are highly dependent on the concentration of the expander agent.

It must be mentioned, however, that pore expansion present certain limitations. It has been proposed (A. Sayari et al., 1997; A. Sayari et al., 1999) that the level of ordering and the shape of the pores can be deformed when the pore size is increased beyond a certain level. While good ordering can still be achieved with expanded mesopores, the quality of material seems to be diminished beyond a pore size of around 6.5 nm (A. Sayari et al., 1997). The study by Luechinger et al. suggest that the use of certain swelling agents for direct synthesis can alter the silica structure, producing a disordered or even lamellar structure (M. Luechinger et al., 2005). Care must be therefore taken in applications where the high ordering of MCM-41 is an extremely relevant issue.

Besides their adjustable pore size, another relevant characteristic of ordered mesoporous silicas is their hydrophobic nature, particularly in varieties with low content of alumina (X. S. Zhao et al., 2001; D. P. Serrano et al., 2004). Such feature makes it useful when working with organic compounds since they will be naturally attracted to a

non polar surface. Based on such assumption, some authors have proposed the use of MCM-41 as adsorbent of volatile organic compounds (V. R. Choudhary and K. Mantri, 2000; X. S. Zhao et al., 2001; D. P. Serrano et al. 2004). In the study presented by Zhao et al. (1998), a comparison between MCM-41, hydrophobic zeolites type Y, silicates and activated carbon as adsorbents of VOCs was presented. These results support the use of MCM-41, since it exhibited a considerably higher capacity at relative pressures of the adsorbate of P_{vap}/P= 0.1 in all cases, whether for aromatic (benzene), halogenated (carbon tetrachloride) or saturated (hexane) hydrocarbons.

Since the hydrophobic nature of an adsorbent is particularly suitable for the selective adsorption of organic compounds (hence minimizing the competitive adsorption of polar substances like water) the use of MCM-41 as-synthesized (i. e. before calcination) has also been proposed (R. Denoyel et al., 1998; H. Zhao et. al., 2000; K. Hanna et al., 2002). It is expected that the organophilic nature of the mesoporous material and thus its selectivity is enhanced by the organic nature of the template attached to the silica surface. This type of material is commonly known as hybrid silicas for containing both inorganic and organic species in its structure.

In a study devoted to the adsorption of chlorinated VOCs (trichloroethylene and tetrachloroethylene specifically), Zhao et al. (2000) reported a higher adsorption capacity by the as-synthesized MCM-41 compared with a sample after calcination. Such result suggested a better compatibility between the organic compounds studied and the surfactant filled mesopores as compared to a bare silica surface. Similarly, Denoyel et al. (1998) and Miyake et. al. (2002) proposed the use of as-synthesized MCM-41 for the adsorption of 3-chlorophenol and phenol respectively suggesting an increase in the

adsorption capacity because of the dissolution of organic compounds in the confined surfactant phase, a phenomenon denominated "adsolubilization".

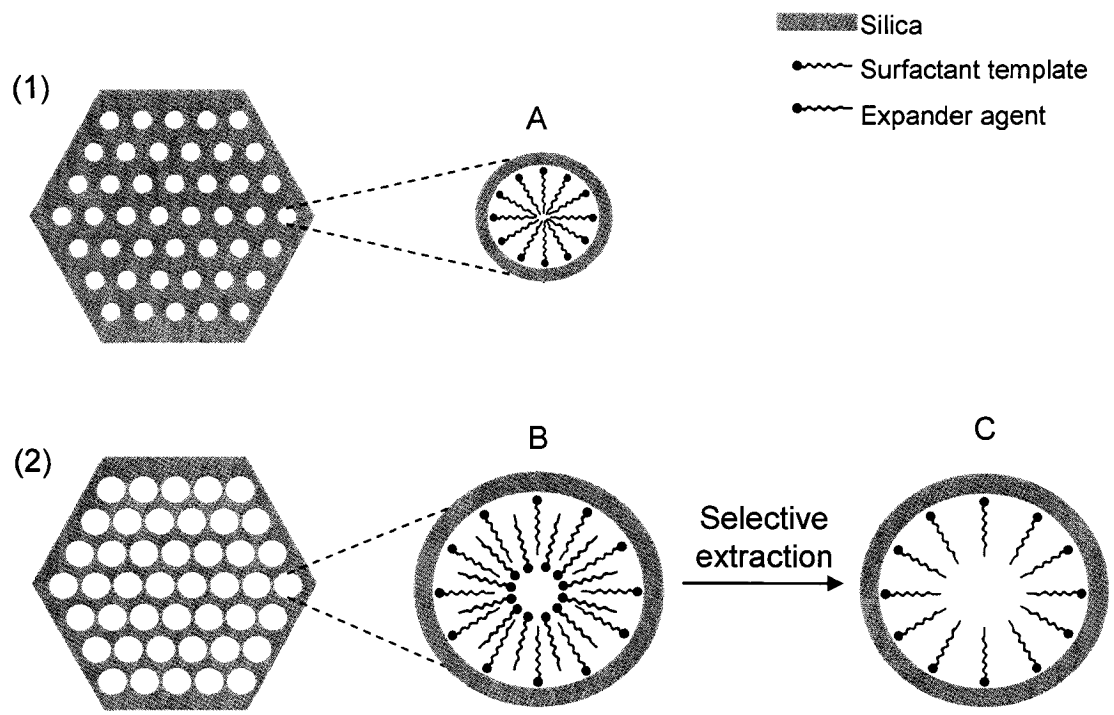

Figure 4.4. Schematic representation of the hybrid mesoporous silicas studied in the works of (1) Denoyel et al. (1998), Hanna et al. (2002) and Miyake et al. (2002) and (2) Kruk et al. (2002), current work

Furthermore, Hanna et al. (2002) studied the adsorption of dichlorophenol, chlorophenol, phenol and paratoluidine on as-synthesized MCM-41 and it was found that the adsorption capacity was not affected by the size of the surfactant molecule used as a template during synthesis. Such effect can be attributed to the fact that the pores are filled with surfactant, making inaccessible the volume inside the pores, as represented by

material "A" in Figure 4.4. In this way, the interaction with the adsorbate would not take place inside the pores, and the adsorption would be independent of the pore size. It is worth noting that the latter effect is not desired, since it is known that the surface area provided by the pores is a great contribution to the total surface area and hence, to the active sites for adsorption. It is therefore necessary to exploit the benefits offered by a surfactant layer using a material whose void spaces allow the access of the adsorbate into its pores.

To take advantage of the compatibility between hydrophobic solids and organic compounds, numerous authors have explored the use of hybrid materials like organoclays (S. Y. Lee et al., 2004; E. Klumpp et al., 2004, D. Yaron-Marcovich and S. Nir, Y. Chen, 2004; H. Zhao and K. L. Nagy, 2004) and silicas (K. B. Gurevich et al., 2002; L. Wei et al., 2004). With the structural characteristics of ordered mesoporous silicas, their use as supporting materials has become attractive and so, the incorporation of organic functional groups on its surface or within its structure is widely researched (A. Stein et. al., 2000; A. Sayari et al., 2001). Unfortunately, most of the routes proposed for the production of hybrid mesoporous silicas include complicated reactions and stringent synthesis conditions. The work of Kruk et al. (2002) however, proposes a way to produce hybrid mesoporous silica in a relatively simple manner. It is believed that before calcination, the pores of MCM-41 expanded by additive compounds are filled with two different compounds: the surfactant template and the expander agent, as represented by material "B" in Figure 4.4. If the latter is selectively extracted, it is possible to keep the organic template attached to the silica surface, forming a hybrid material (represented by "C" in Figure 4.3). It was proven that when MCM-41 is synthesized under basic conditions, the

layer of surfactant template is strongly attached to the inorganic walls. An important advantage offered by this material is that, with the extraction of the expander, enough free volume is left inside the pores to allow the entrance of the adsorbate fluid.

As can be seen, this type of material appears to be suitable for the purpose of the present work. In the first place, volatile organic compounds have a hydrophobic nature, being more likely adsorbed on a material with similar surface polarity. Secondly, it must be acknowledged that the organic compounds released industrially are mixed with atmospheric air, in which humidity is always present. By having an adsorbent with highly hydorphobic surface, the competitive adsorption of water regularly found (for example in activated carbon) is minimized.

Summarizing, the use of a hybrid MCM-41 synthesized with the method proposed by Kruk et al. (2002) is studied in the present work for the following reasons:

- It is synthesized in a simple manner, while regular procedures to incorporate organic groups into the silica structure may be complicated.
- It offers a tailored pore size to enhance the contact of organic compounds and the adsorption sites. Other studies using MCM-41 with surfactant filled pores hardly present any pore volume for not being previously expanded.

The study hereby presented has the objective to evaluate the efficiency of ordered mesoporous materials type MCM-41 as adsorbents for volatile organic compounds. With that aim, three adsorbents are analyzed, including a highly ordered MCM-41, a pore expanded variety and a hybrid surfactant-layered silica. It is expected that these materials offer in general some advantages over other adsorbents currently available at a commercial scale in terms of their compatibility with organic substances.

II. Experimental Section

5. Synthesis of Adsorbents

A schematic representation of the procedure followed for the production of the adsorbents is presented in Figure 5.1. MCM-41 silica was prepared using the procedure described previously by Sayari et al. (1998) and (2000b) for the synthesis of highly ordered MCM-41 as explained next. An amount of 578.6 g of trimethyl ammonium hydroxide (TMAOH) at 25% w/w purity was diluted in 5500 g of water under vigorous stirring in a stainless steel vessel. 820 g of cetyltrimethylammonium bromide (CTAB) were subsequently added, and stirred for 15 minutes. Afterwards, 328.4 g of Cabbot Cab-O-Sil fumed silica was added. In this manner, a mixture with a molar composition of 1.0 SiO_2:0.343 TMAOH:0.41 CTAB:57 H_2O was obtained. After stirring for 30 more minutes, the resulting gel was heated statically at 100 °C for 40 h. The obtained material was thoroughly washed with water, filtered and dried with air at ambient temperature. A sample of this product was calcined for 5 hours at 550 °C under flux of air and nitrogen to completely remove the template from its surface.

A sample of the as-synthesized MCM-41 (i.e., before calcination) obtained as described above was expanded by a post-synthesis hydrothermal treatment (A. Sayari et. al, 1998) using dimethyldecylamine (DMDA) as expander agent as follows. A suspension was formed by adding 437.5 g of DMDA in 5250 g of water under vigorous stirring. An amount of 350 g of as-synthesized MCM-41 was subsequently added and the mixture was left stirring for 15 min. The resulting suspension was heated in a stainless steel

reactor at a constant heating temperature of 120 °C for 72 h, time after which it was washed with water, filtered and dried with air.

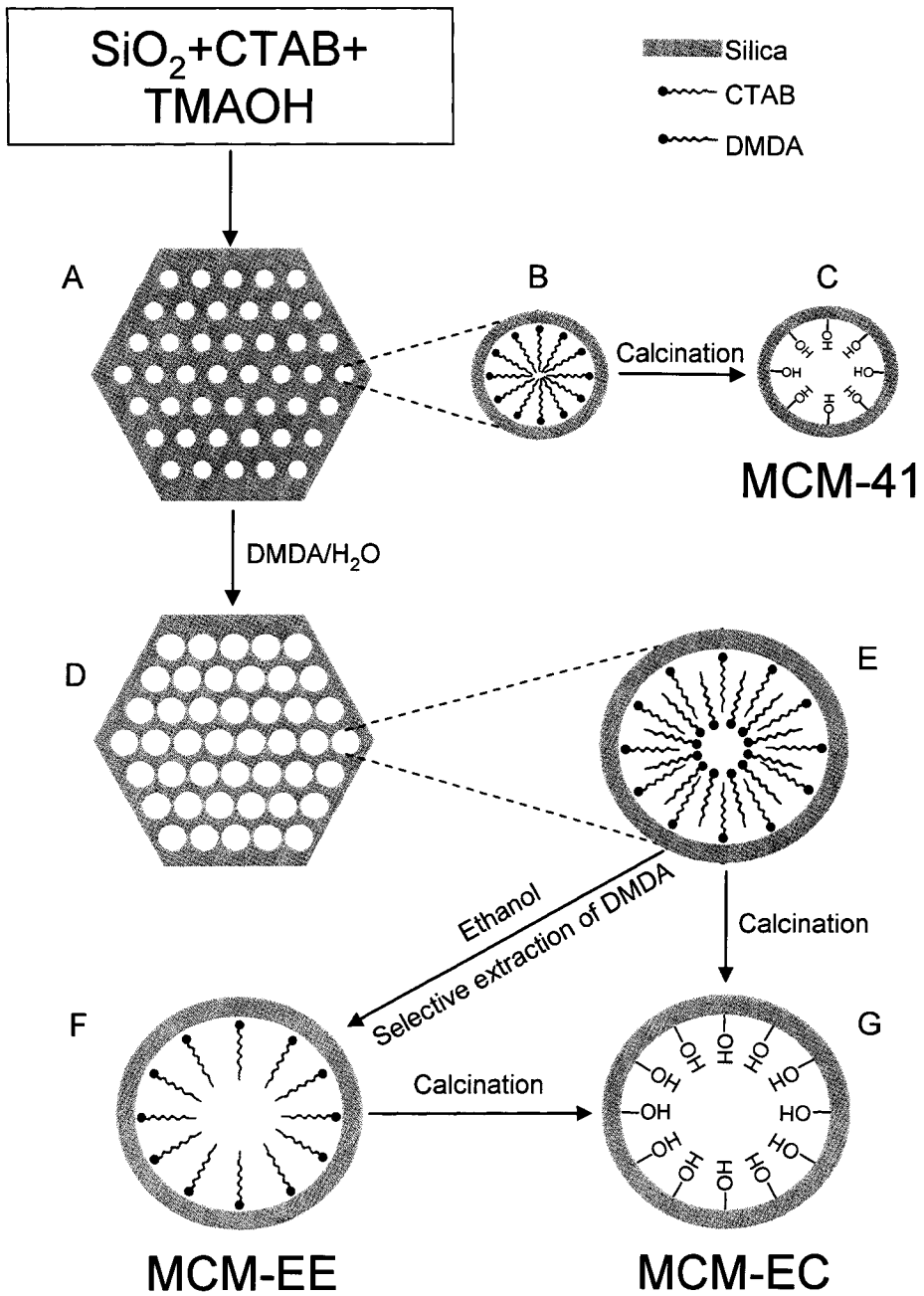

Figure 5.1 Schematic representation of the synthesis and post-synthesis modification of ordered mesoporous silicas

DMDA was selectively extracted following the procedure described by Sayari et al (2005), washing the material with 18.5 ml of ethanol per gram of as-synthesized MCM-41 and filtered. The solids obtained were washed a second time with 9.25 ml of ethanol per gram of as-synthesized MCM-41; the resulting solid product was denominated MCM-EE ("EE" stands for Expanded and selectively Extracted). A sample of the material obtained after expansion was calcined at 550 °C for 5 h to remove both expander and template surfactants and was labeled MCM-EC ("EC" stands for Expanded and Calcined).

In this manner, three different varieties of ordered mesoporous materials were obtained: a highly ordered mesoporous silica with a two dimensional hexagonal pore system (MCM-41), a mesoporous silica with enlarged pore size obtained by a hydrothermal treatment (MCM-EC), and a hybrid surfactant-layered mesoporous silica obtained via the selective extraction of the swelling agent DMDA (MCM-EE).

Since the powdered form of the adsorbents may produce significant pressure drops in a packed column, pellets were prepared by compressing the material with a hydraulic press under a maximum pressure of 450 kg/cm^2. This resulted in solid pieces of material capable of holding together without need of any binder. The solid pieces were grounded and sieved using nets with openings of 40 and 60 mesh size, to obtain a ratio of column diameter size to pellet average diameter size of approximately 11:1. A comparative analysis between the structural properties of the powder and pelletized adsorbents will be presented in Chapter 8.

6. Heat of Adsorption by Pulse Chromatography.

6.1 Mathematical Background

$-\Delta H_a$ and Henry's Law constant K_p were determined according to the method known as pulse chromatography. In this method, as described by Schneider and Smith (1968), a pulse of fixed volume and known concentration of adsorbate is send to a column packed with adsorbent. The concentration at the column outlet is continuously monitored, in order to generate profiles of concentration in the fluid phase with respect to time. A schematic representation of a typical profile of concentration vs. time obtained with pulse chromatography is presented in Figure 6.1.

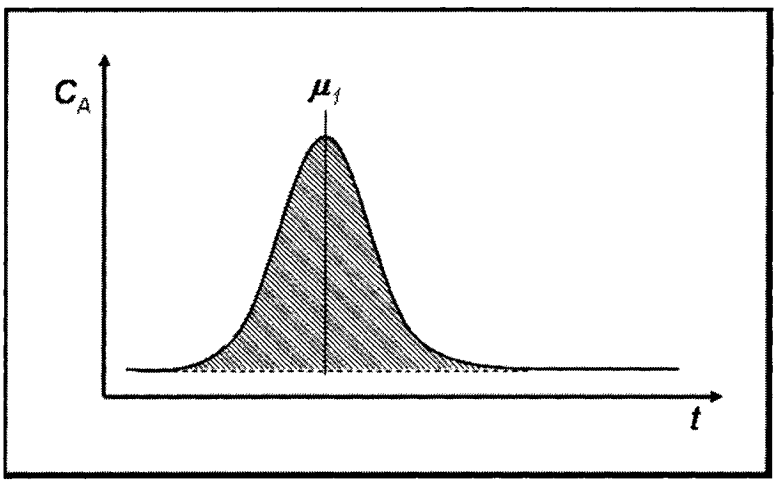

Figure 6.1. Typical profile of concentration vs. time obtained with pulse chromatography

The objective of the profile generated by pulse chromatography is to provide data to calculate an experimental estimate of the mean retention time of the adsorbate inside the column. A good approximation of this parameter can be obtained making use of the method of moments, where the first absolute moment μ_1 of concentration as a function of

time corresponds to the peak's center of gravity (represented by the point μ_1 in Figure 6.1), and is a measurement of the mean retention time of the adsorbate in a fixed bed column. The values of the first absolute moment can be estimated from the profiles determined experimentally according to Eq. (3) (P. Schneider and J. M. Smith, 1968; G. Dogu and J. M. Smith, 1976; D. M. Ruthven and R. Kumar, 1980; T. Kopac et al., 1996):

$$\mu_1 = \frac{\int (t - \mu_D)\, C_A \, dt}{\int C_A \, dt} \tag{3}$$

Where μ_1 is the first absolute moment of the curve, t is time, μ_D is the mean dead time which is a correction factor to account for the time used by a pulse of adsorbate to reach the detector in the absence of adsorption phenomena, and C_A is the concentration of the organic compound in the outlet stream as a function of time.

It must be said that the following assumptions are made by the pulse chromatographic method: (i) the amount adsorbed on the adsorbent surface is a linear function of the concentration in the fluid phase, (ii) the axial dispersion of the adsorbent in the column is negligible, and (iii) the interstitial velocity of the fluid phase is constant (P. Schneider and J. M. Smith, 1968; J. Nokerman et al., 2005). The first assumption, i.e. linearity of the mass transfer rate, is satisfied at low adsorbate concentrations, known as the Henry's law region. Since there is a continuous flow of carrier gas flowing through the packed column, the amount of adsorbate in the pulse is assumed to be infinitely diluted, thus working under conditions where the adsorbate concentration in the fluid phase is extremely low. In this way, the condition of linearity is expected to be

accomplished when a single pulse of adsorbate is used. It is also considered that the carrier gas does not affect the adsorption process.

Under the aforementioned assumptions, the mean retention time can be expressed as a function of the effective isotherm slope (i. e. Henry's Law constant), the fluid interstitial velocity and other characteristics of the packed column as expressed by Eq. (4) (M. D. Ruthven, 1984; P. J. E. Harlick and F. H. Tezel, 2003):

$$\mu_1 = \frac{L}{u}\left[1+\frac{(1-\varepsilon)}{\varepsilon}K\right] \tag{4}$$

Where K is a dimensionless form of Henry's Law constant, ε is the interparticle spatial void, also known as bed porosity (W. J. Thomas and B. Crittenden, 1998), L is the length of the column, and u is the linear interstitial velocity of the fluid. The interstitial velocity refers to the linear velocity of the fluid inside the column void space, and is calculated with:

$$u = \frac{v}{A_c\,\varepsilon} \tag{5}$$

Where v is the volumetric flow of gases and A_c is the cross-sectional area of the column. If K is estimated for adsorption at a set of different temperatures, a plot of K_p as a function of T^1 can be generated, where the slope of the function is proportional to $-\Delta H_a$, according to a linearized-Arrhenius type equation with the form (M. D. Ruthven, 1984; P. J. E. Harlick and F. H. Tezel, 2003; J. Nokerman et al., 2005):

$$\ln K_p = \ln A - \frac{\Delta H_a}{R\,T} \tag{6}$$

Where K_p is the dimensional form of Henry's Law constant, A is a pre-exponential factor, $-\Delta H_a$ is the heat of adsorption, R is the ideal gas universal constant, and T is the absolute temperature of adsorption. The dimensional form of Henry's law constant K_p can be obtained from its dimensionless form K, as follows:

$$K_p = \frac{K}{R\,T\,\rho_p}$$

Where ρ_p is the particle density of the adsorbent.

6.2 Experimental Setup

Before investigating the adsorption of each organic pollutant, a stainless steel column with inner diameter of 0.36 cm and length of 12.7 cm was packed with fresh pellets of adsorbent. The MCM-EE loaded was regenerated in an electric oven set at 50 °C under a 50 ml/min flow of UHP grade nitrogen, until the signal produced by the Flame Ionization Detector (FID) positioned downstream the column reached a stable baseline. The temperature used for regeneration was sufficiently low to avoid any thermal degradation of the organic surfactant within the material. In the case of MCM-41 and MCM-EC the temperature for regeneration was set to 100 °C. After regeneration, the oven temperature was adjusted to the set point required for experimental analysis.

The experimental setup used to determine $-\Delta H_a$ and K_p is presented schematically in Figure 6.2, and is described next. The setup counts with two MKS mass flow controllers, a VWR 10 liter capacity ethylene glycol/water bath with programmable temperature controller, and a Valco Inc. two-position six-ways valve with electric actuator. The temperature in the system was monitored using "K" type thermocouples, labeled as "TE" in Figure 6.2. As previously mentioned, the column used was made of stainless steel tubing with an inner diameter of 0.36 cm and length of 12.7 cm. An electric oven and flame ionization detector for adsorption temperature control and concentration monitoring respectively were taken from an SRI 8610 gas chromatograph. All the system was connected using 3.18 mm nominal diameter stainless steel tubing and stainless steel fittings supplied by Swagelok Inc. The mass flow and electronic actuator were remotely controlled with the use of a National Instruments SCB-68 data acquisition electronic interface, and a program developed in National Instruments LabView 7.1 software. The aforementioned electronic interface also allowed the recording of the FID and thermocouples response.

To run the equipment, a stream of inert carrier gas (i. e. nitrogen UHP grade) is supplied to the system where it is split in two lines. The first of these streams is used as carrier gas and flows into the fixed bed column after passing through a two position valve. The second stream is directed into a glass saturator containing approximately 50 ml of the organic compound of interest. With the aim of controlling the partial pressure of the organic compound, the saturator lies inside a bath of water and ethylene glycol with controllable temperature (T_s).

After the stream of nitrogen has been mixed with the organic compound in the saturator, it flows into a two position valve with a stainless steel loop; the inner volume of the loop is 0.025 ml. The valve is operated with an electric actuator which shifts between its positions: "Load" and "Inject". When in Load position, the stream of nitrogen saturated with VOC flows inside the loop, filling it with a mixture of nitrogen and organic vapors before being sent to a venting stream. The flow of nitrogen is regulated using mass flow controllers set at 50 ml/min for the pure nitrogen carrier stream and 10 ml/min for the stream entering the saturator.

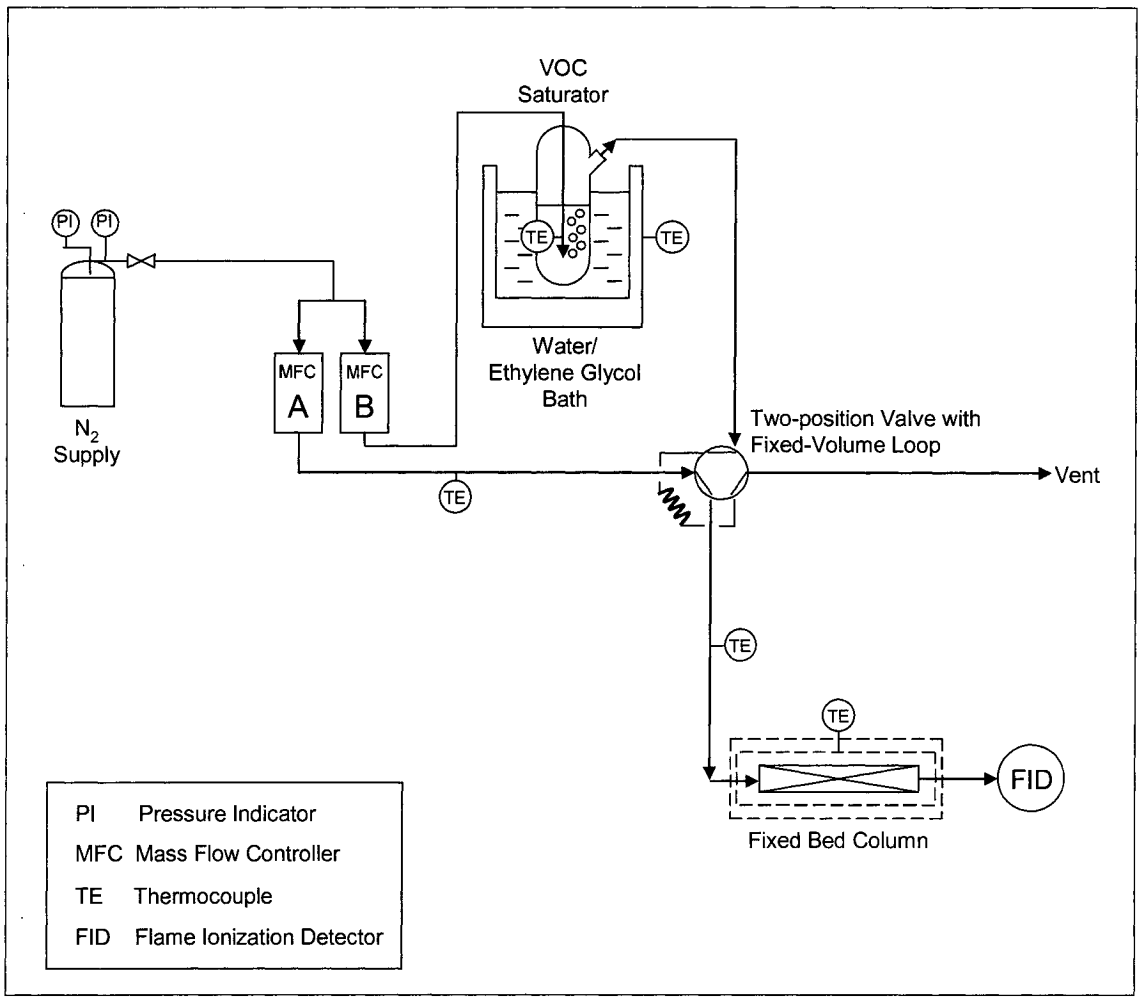

Figure 6.2. Experimental setup for the determination of $-\Delta H_a$ by the pulse chromatographic method.

When the valve is changed to the Inject position, the stream of pure nitrogen flows through the loop before entering the fixed bed column, carrying a pulse of VOC with it. In this position, the saturated stream flows directly into the venting stream. In this manner, only the VOC trapped in the loop during the Load position will be carried by the pure nitrogen carrier gas into the fixed bed column when the position of the valve is switched. The column outlet is monitored using an FID to obtain the profile of concentration versus time as required by the pulse chromatography method.

7. Adsorption Capacity Estimation by Breakthrough Curves

7.1 Mathematical Background

Another important aspect of this experimental work consists in the determination of adsorption capacity (q). This property represents the maximum amount of molecules that can be attached to the adsorbent surface under fixed temperature and pressure. The adsorption capacity is extremely relevant in industrial processes since it is directly related with the frequency for which regeneration of the adsorbent is required. The method selected to determine the adsorption capacity was the generation of a breakthrough curve under controlled conditions for three different environments. In the first one, the adsorption column was fed with a single volatile organic compound in a dry gas stream. The second environment involved the use of a mixed stream of VOC and water in order to analyze the effects of humidity in the process of adsorption. Finally, streams containing two different organic compounds were mixed and sent to the adsorption column with the aim of studying the effects of competitive adsorption and selectivity of the adsorbent. Selectivity in the present work should be understood as the preference of an adsorbent to adsorb particular chemical species present in a mixture.

For the estimation of q, the experimental system was designed to send a continuous flow of a mixture of nitrogen and the volatile organic compound of interest at a known concentration while the column outlet is monitored by a flame ionization detector (FID). It has been shown that the saturation of an adsorbent in a fixed bed column system takes place progressively downstream the flow of adsorbate (M. D.

Ruthven, 1984; W. J. Thomas and B. Crittenden, 1998; D. O. Cooney, 1999). Therefore, no traceable concentration of adsorbate is expected at the column outlet until most of the adsorbent has reached saturation. By plotting the adsorbate concentration versus time, a representative profile known as breakthrough curve is generated, representing the saturation profile of the adsorbent in the column (M. D. Ruthven, 1984; W. J. Thomas and B. Crittenden, 1998; D. O. Cooney 1999). A typical profile of a breakthrough curve is exhibited in Figure 7.1. The time marked as t_b corresponds to the moment when the concentration at the column exit starts to increase, and is commonly known as breakthrough time. It is of great interest in industry to know t_b, since it indicates the time before which the fixed bed can be operated without exceeding concentration standards downstream the column. On the other hand, t_s corresponds to the moment where concentrations at the column inlet and outlet are the same, representing a complete saturation of the adsorbent in the column.

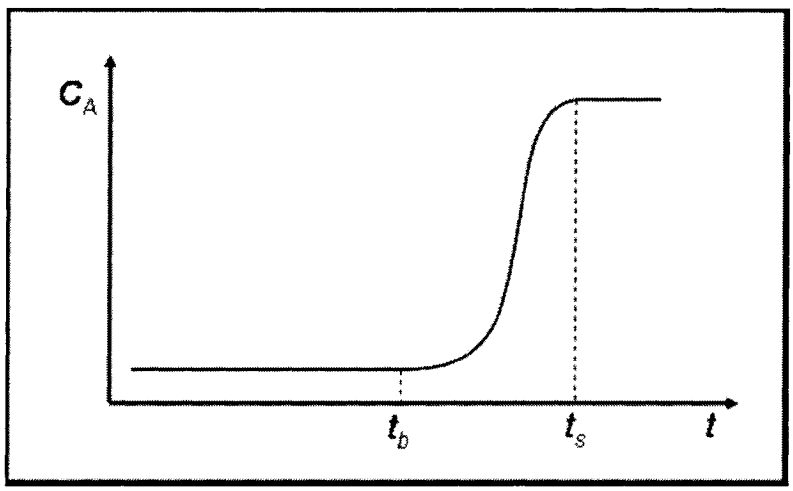

Figure 7.1. Typical profile of a breakthrough curve

By definition, the adsorption capacity is the amount of adsorbate (typically in mol) adsorbed onto a certain amount of adsorbent (typically in grams) at equilibrium, as represented in Eq. 7:

$$q = \frac{N_A}{W} \tag{7}$$

Where q is the adsorption capacity (commonly expressed in mol of adsorbate per gram of adsorbent), N_A is the maximum amount of adsorbate adsorbed and W is the total mass of adsorbent in the column. When a fixed bed column is used, the amount of adsorbent packed is constant at all times, and thus W is a variable easily determined by direct measurements. Additionally, if the volume of the packed portion of the column V is known, the volumetric capacity of adsorption can be expressed as:

$$q' = \frac{N_A}{V} \tag{8}$$

If a constant flow of gaseous mixture with a known concentration of adsorbate is sent through the column, the adsorbate flow can be calculated by:

$$F_A = F\ y_A \tag{9}$$

Where F_A is the molar flow of adsorbate in mol/min, F is the total flow of gases in mol/min and y_A is the molar fraction of adsorbate in the gaseous mixture. Since the flow

of gas is commonly measured in volumetric units, it can be transformed to molar flow making use of the ideal gas equation as expressed in Eq. 10:

$$F = \frac{v\,P}{R\,T} \tag{10}$$

Where v is the volumetric flow of gases, P is the total pressure of the system, R is the Universal Gas Constant, and T is the absolute temperature.

For being gaseous species, the molar fraction of adsorbate can be expressed as a function of its partial pressure:

$$y_A = \frac{P_{vap}}{P} \tag{11}$$

Where P_{vap} is the vapor pressure of the adsorbate. Substituting 10 and 11 in 9:

$$F_A = \frac{F}{R\,T} P_{vap} \tag{12}$$

Since the breakthrough curve represents the concentration of the column effluent from the beginning of the experiment until complete saturation, the amount of molecules adsorbed can be deduced with the flow of adsorbate and the stoichiometric time t_q, taken from the plots generated experimentally:

$$N_A = F_A \, t_q \tag{13}$$

Given that the area over the breakthrough curve is proportional to the moles adsorbed, t_q is calculated according to Equation 14 (A. Claudino et al., 2004):

$$t_q = \int_0^t \left(1 - \frac{C_A}{C_0}\right) dt \tag{14}$$

Where t is the time elapsed from the moment at which the flow of adsorbate was sent to the column. It is of interest for the present work to evaluate the amount adsorbed at breakthrough and at complete saturation of the adsorbent. For that reason, the limits of the integral will be set between times equal to zero up to t_b for the capacity at breakthrough and up to t_s for total capacity of the adsorbent. For practical purposes, t_b was considered as the time when C_A/C_0 increased over a value of 0.01, and t_s as the moment when the concentration of adsorbate entering the column is the same than the concentration at the column outlet (C_A/C_0=1), as represented schematically in Figure 7.1.

7.2 Experimental Setup

The experimental setup employed to determine the adsorption capacity of single components in dry environment is similar to the previously described arrangement used for the pulse chromatographic method. Most of the elements of this experimental setup (i.e. mass flow controllers, thermocouples, temperature controlled bath, electric oven, stainless steel column and FID) are the same ones utilized in the setup described in

Chapter 6.2. As can be appreciated from its schematic representation in Figure 7.2, the main difference between the systems for pulse chromatography and breakthrough curve consists in the use of a two-position four-way valve with no sample loop. In this case, the line "A" consists of nitrogen UHP level used as carrier gas during the adsorbent regeneration stages. A second nitrogen stream ("B") is bubbled at a constant flow of 30 ml/min into a glass saturator containing organic compounds in order to produce a mixed stream of nitrogen and VOC. The saturator is kept at a constant temperature using a bath of ethylene glycol and water in order to produce a stream of VOC with a of partial pressure of $P_{vap}/P = 0.13$. With such arrangement, when the valve is in Position 1, the saturated mixture of VOC and nitrogen flows directly into the venting stream while the pure nitrogen line enters the fixed bed column. When the valve is switched to Position 2, the pure nitrogen stream goes to ventilation while the organic compound is continuously carried to the column, eventually saturating the adsorbent. The required breakthrough profile is generated by monitoring C_A at the column outlet with a FID.

To produce a humid environment, a third stream of nitrogen ("C") is added to the system as presented in Figure 7.2. This stream flows into a second saturator containing water maintained at a constant temperature of 5 °C with the use of an ethylene glycol and water bath with controlled temperature. Simultaneously, a stream of nitrogen flows through the saturator containing the organic compound of interest and is afterwards mixed with the stream carrying water vapor. Once mixed, the resulting stream is directed into the fixed bed column. The column is placed inside an electric furnace where it is maintained at a constant temperature of 50 °C.

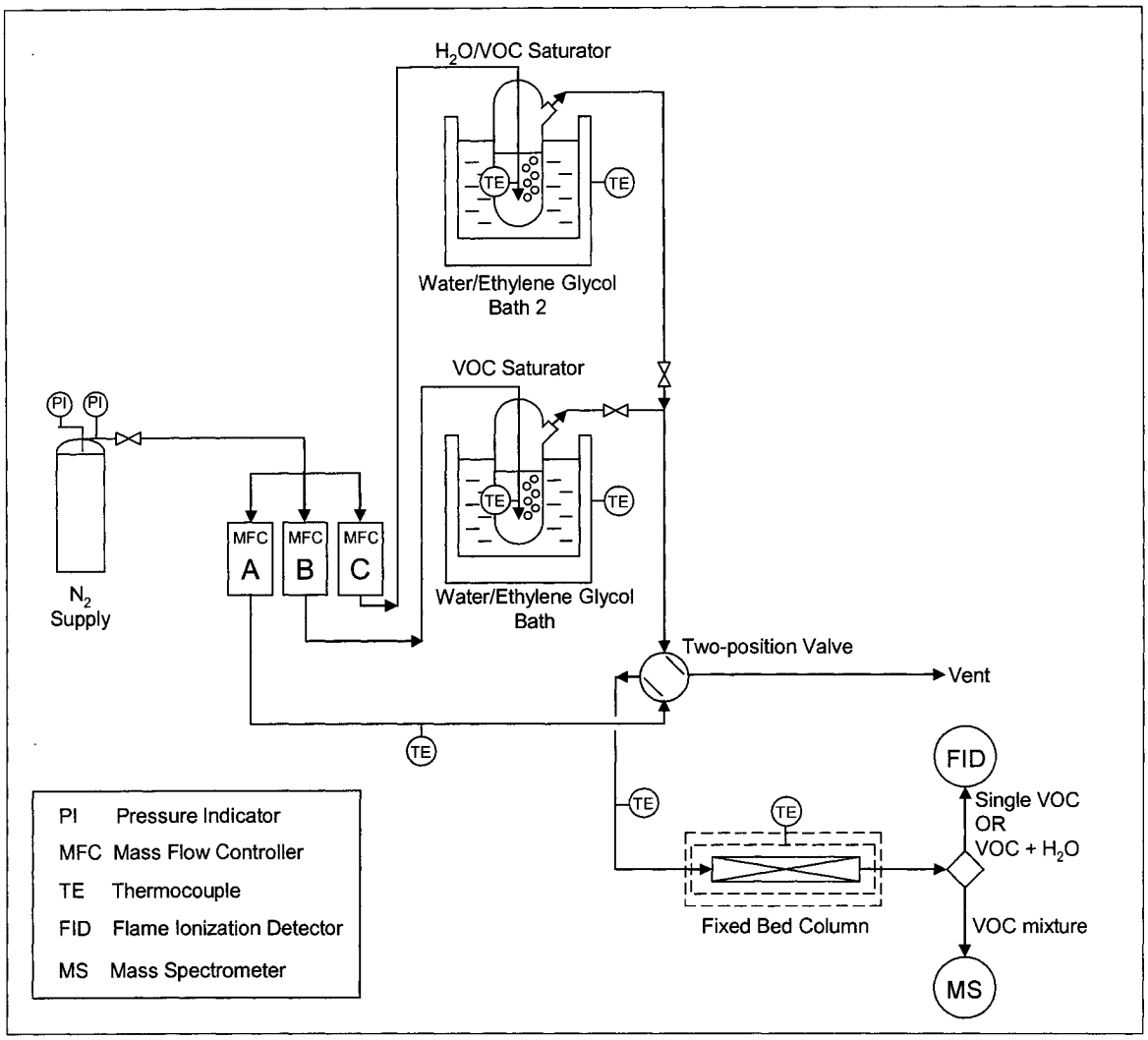

Figure 7.2. Experimental setup for the determination of adsorption capacity

Finally, to investigate adsorption with multiple components, a system similar to the one used for the evaluation of single components in humid environment was used. Two streams using nitrogen as carrier gas are bubbled into saturators containing each a different organic compound. The saturators are maintained at a constant temperature with the use of baths of water and ethylene glycol. The streams containing organic vapors are mixed and fed to the fixed bed column. In this case, however the column outlet is monitored using a mass spectrometer (MS) instead of a FID since the response of the

latter is not selective between organic species. Again, stream "A" contains pure nitrogen used as carrier for regeneration steps. The column temperature was maintained constant to 50 °C throughout the experiments with multiple components.

In all experiments involving one or two VOCs, the total flow and the concentration of the adsorbate at the entrance of the fixed bed column were maintained constant at 30 ml/min and $P/P_{vap} = 0.13$. In the case of binary mixtures, i.e. two VOCs or one VOC plus water vapor, the flow of a single stream of VOC or humid nitrogen was set at 15 ml/min before mixing the two streams. At the same time, the temperature of the saturator was adjusted to afford a VOC partial pressure of 0.26. After mixing, the total flow was 30 ml/min and the VOC partial pressure was 0.13, the same as in the single VOC experiments.

Before each experiment using pure silicieous adsorbents (i. e. MCM-41 and MCM-EC), the adsorbents were treated by increasing the column temperature at a minimum temperature of 100 °C under a flow of UHP nitrogen at a flow rate of 50 ml/min, until the detector presented a stable base line. A similar procedure was used for the regeneration of MCM-EE with the difference of column temperature, which was maintained at 50 °C to avoid thermal degradation of the surfactant layer on the adsorbent surface.

III. Results and Discussion

8. Characterization

The structural properties of the materials obtained were characterized with the method of nitrogen adsorption using a Coulter Omnisorp 100 gas sorption equipment by static measurements. Before each experiment, each sample of MCM-41 and MCM-EC was pretreated with vacuum (10^{-5} torr) at 100 °C. MCM-EE was pretreated with vacuum at ambient temperature to avoid any thermal degradation of the organic groups on its surface.

In addition, the density of the pelletized material and its apparent density in the bed were determined experimentally as explained next. The pellet density ρ_p was determined using a Micromeritics AccuPyc 1330 gas displacement pycnometer using UHP helium. Before any measurement each sample was purged with helium for at least 10 cycles. The pycnometer was programmed to perform a minimum of 5 consecutive determinations of sample volume until the values produced a difference less than 0.1%. To calculate the values of apparent density ρ_b, a vial of 2 ml was completely filled with pellets of each adsorbent and weighted using a Mettler Toledo AG 204 anlytical balance.

As can be seen in Figures 8.1a-8.3a, the adsorption isotherms of all the adsorbents produced correspond to the Type IV classification, which are representative of mesoporous materials with narrow pore size distribution (W. J. Thomas and B. Chrittenden, 1998; P. E. Yu-Chun Chiang et al., 2001). The shape of the adsorption isotherm for MCM-41 (Figure 8.1a) is very similar to the profiles reported by other authors (A. Corma et al., 1997; N. Lang and A. Tuel, 2004; J. W. Lee et al., 2004), which is a good indication of the successful production of an ordered silica type MCM-41.

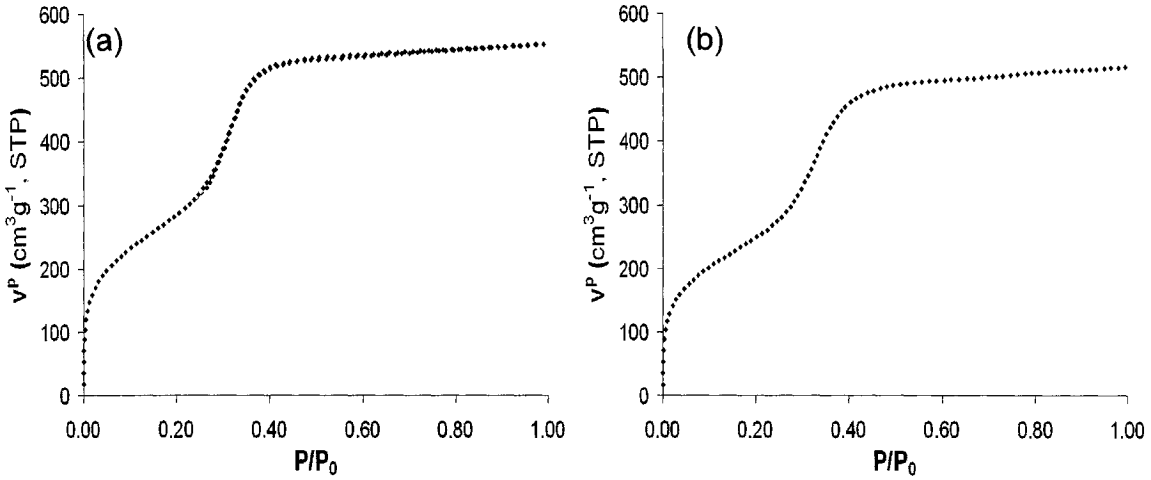

Figure 8.1. Nitrogen adsorption-desorption isotherms of MCM-41 (a) powder and (b) pellets

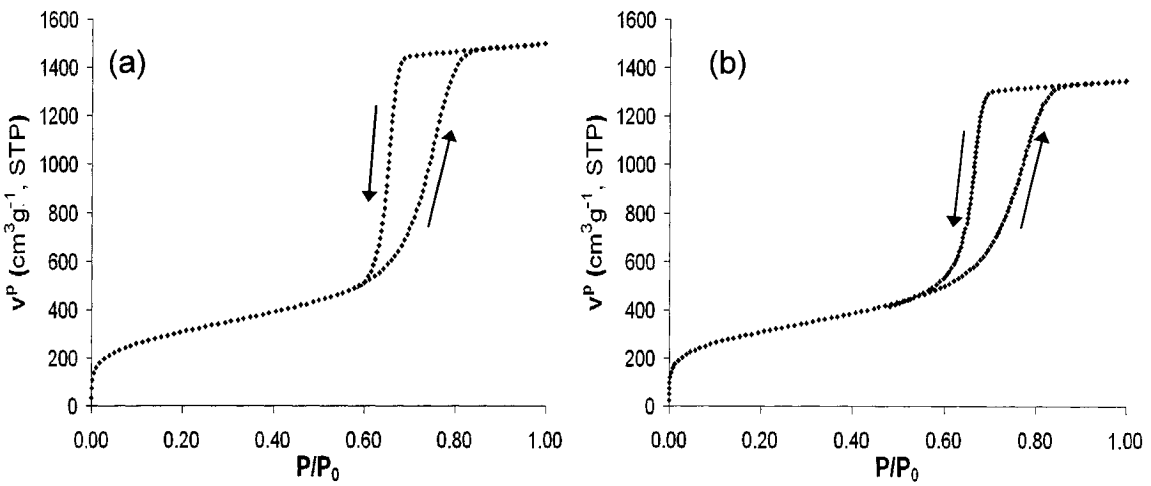

Figure 8.2. Nitrogen adsorption-desorption isotherms of MCM-EC (a) powder and (b) pellets

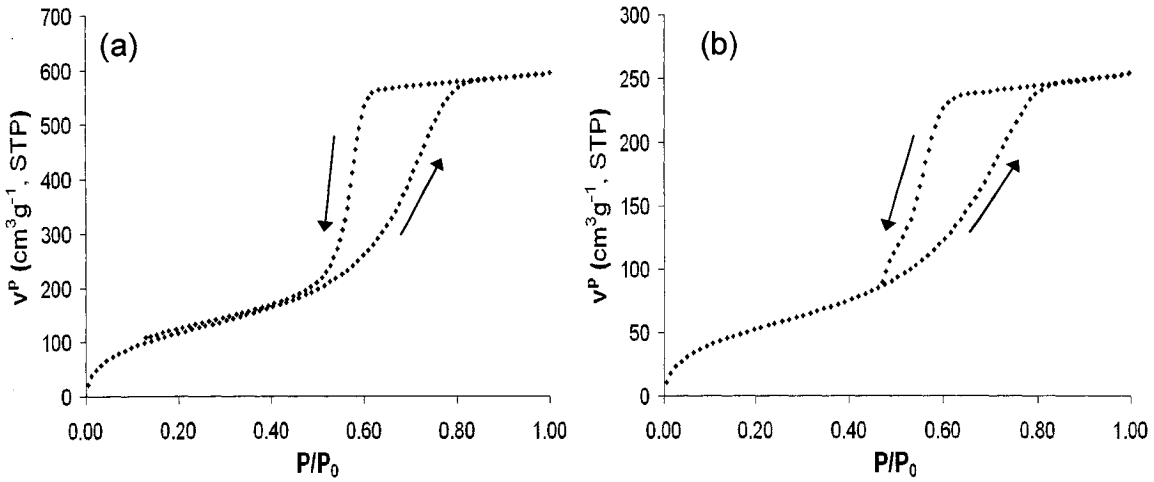

Figure 8.3. Nitrogen adsorption-desorption isotherms of MCM-EE (a) powder and (b) pellets

Table 8.1. Properties of synthesized adsorbents.

	Surface area ($cm^2 g^{-1}$)	Pore volume ($cm^3 g^{-1}$)	Mean pore size (nm)
MCM-41	1086	0.86	3.53
MCM-EE	379	0.83	7.30
MCM-EC	1119	2.35	9.18

As can be seen in Figure 8.1, the nitrogen adsorption-desorption isotherm of MCM-41 does not present a hysteresis loop. On the other hand, hysteresis loops appear in the isotherms for MCM-EC and MCM-EE, representing an alteration of the structure, and is mainly attributable in this case to the existence of longer pore sizes. The profiles obtained coincide with results published by other authors for nitrogen adsorption-desorption isotherms of MCM-41 type silicas with expanded pores (M. Kruk et al., 1997; M. Kruk et al. 2000, A. Sayari et al., 2005). The broadening of the hysteresis loop has also been related to a loss of pore diameter uniformity (Sayari et al., 1997). This

proposition coincides with the broader pore size distribution obtained with pore expanded silicas (plots of pore size distribution can be consulted in Appendix A).

The values of surface area were determined by the highly popular Brunauer-Emmett-Teller (BET) method (J. M. Thomas and W. J. Thomas, 1997) using the portion of the isotherm between P/P_0 =0.5 and P/P_0 = 0.3 and are presented in Table 8.1. The mean pore sizes were determined using the KJS method, based on the Barret-Joyner-Halenda (BJH) approach as modified by Kruk, Jaroniec and Sayari (M. Kruk et al., 1997). This method was developed with the use of well ordered mesoporous materials as model adsorbents. The properties determined are presented in Table 8.1. As can be seen, the lowest surface area and pore volume correspond to the hybrid mesoporous material MCM-EE. This can be explained based on the fact that the pore volume is partially occupied by the surfactant layer, thus the free pore volume appears lower compared to the pure pore expanded silica. It is interesting to notice that both the pore volume and the mean pore size of MCM-EC increased by a factor of around 2.6 with respect to MCM-41. This, however, is not the case for MCM-EE where even though the pore size was increased more than double compared to MCM-41, the pore volume was somewhat lower. This suggests the existence of organic molecules occupying space beyond a single layer of surfactant attached to the surface possibly altering the geometry of the pores.

The results of nitrogen adsorption characterization for the pelletized adsorbents are presented in Table 8.2. The adsorption-desorption isotherms are presented in Figures 8.1b-8.3b where they can be compared with their corresponding powder materials. Plots of pore size distribution for the pelletized adsorbents can be consulted in Appendix A.

Table 8.2. Properties of synthesized adsorbents after pelletization

	Surface area ($cm^2\ g^{-1}$)	Pore volume ($cm^3\ g^{-1}$)	Mean pore size (nm)
MCM-41	940	0.81	3.62
MCM-EE	208	0.40	7.10
MCM-EC	1129	2.11	9.62

Comparing the results in Tables 8.1 and 8.2, it can be suggested that both calcined materials MCM-41 and MCM-EC have a good mechanical stability with only slight changes in their pore volumes and surface areas after compression. However, the pelletization process evidently altered the properties of MCM-EE. While the isotherm shape and the mean pore size are very similar before and after compression, the mean pore size and the surface area diminished significantly, indicating that the hybrid variety has a lower mechanical stability than the other adsorbents. Since the only difference between the synthesis processes of MCM-EE and the rest of the materials studied is the calcination treatment, it is reasonable to suggest that whether this step confers better mechanical properties to the silica walls of the adsorbents or that the remaining organic groups attached to the surface of the hybrid adsorbent are fragile enough to collapse inside the pores during compression.

With the experimentally determined values of ρ_b and ρ_p, the bed porosity ε can be calculated with (M. D. Ruthven, 1984; W. J. Thomas and B. Chrittenden, 1998):

$$\varepsilon = 1 - \frac{\rho_b}{\rho_p} \tag{15}$$

The calculated values of ρ_b, ρ_p and ε for each material are presented in Table 8.3.

Table 8.3. Densities and bed porosity of adsorbent pellets

Material	ρ_p (g cm^{-3})	ρ_b (g cm^{-3})	ε
MCM-41	2.2944	0.5537	0.8126
MCM-EC	2.5362	0.3730	0.8857
MCM-EE	1.4399	0.7956	0.5694

Within the studied materials, MCM-EC is the one with highest particle density. MCM-41 presents a density very similar to that reported in the literature for amorphous silica (R. H. Perry and D. W. Green, 1997). MCM-EE presents a much lower particle density compared to the other materials. This can be explained by the fact that the density of the organic molecules attached on the surface (i. e. CTAB) is much lower than that of silica and thus affects directly the density of the hybrid silica walls. With respect to the void space in the column, it can be seen that MCM-EC has a lower apparent density than MCM-41 which can be attributed to its higher pore volume. Correspondingly, the bed porosity for MCM-EE is much lower than the other adsorbents, which is an expected effect since it presents the lowest pore volume.

The values of ρ_p and ε result in very different values of apparent density for each material. It is therefore useful to analyze the results of capacity in terms of volume of adsorbent, since the column used to perform dynamic analyses was of constant volume. The volumetric capacity q' provides an idea of the performance of a column with

constant volume in separation processes, independently of the mass of adsorbent packed into the column, accounting for the different densities of the adsorbents.

9 Determination of Mean Dead Time

Before performing the pulse chromatography experiments, it was necessary to determine the mean dead time (μ_D) of our particular system, since it is one of the factors required for the estimation of the mean retention time as expressed by Equation 3. Since μ_D represents the average time spent by a molecule inside the system in the absence of adsorption phenomena, it was required to send pulses of a tracing compound through the system described in Chapter 6.2 using a column packed with a non-adsorbent material. Therefore, the column was packed with crystal bins sieved between nets with openings of 40 and 60 mesh size. Pulses with known concentration of ethanol were subsequently sent to the column. In this way, the response of the detector in the absence of an adsorptive phenomenon was evaluated.

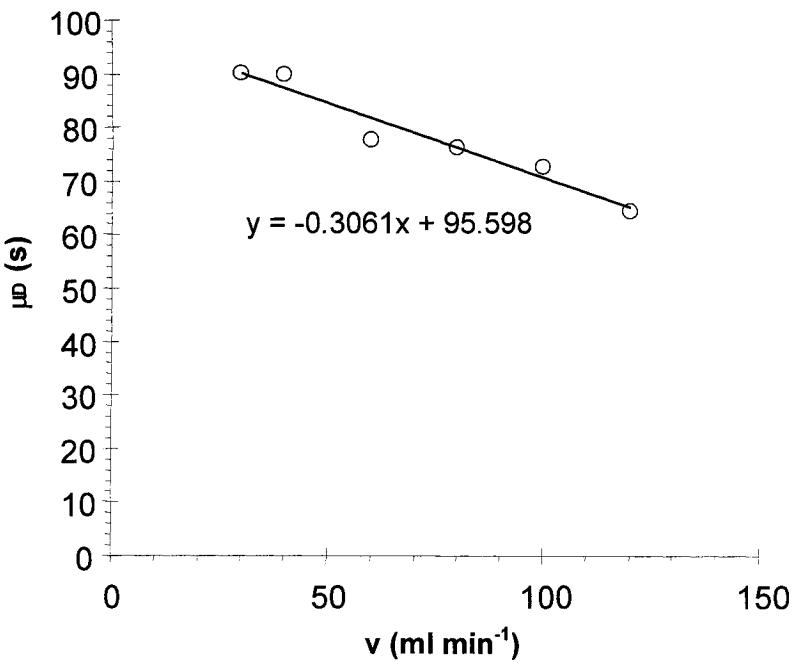

Figure 9.1. Mean dead time as a function of volumetric flow rate

The value of μ_D is calculated with Equation 16 from the profiles obtained in a system with negligible adsorptive properties (Harlick and Tezel, 2003):

$$\mu_D = \frac{\int t\, C_A\, dt}{\int C_A\, dt} \tag{16}$$

The results obtained experimentally of μ_D are presented as a function of the flow rates of carrier gas in Figure 9.1. With the data points obtained at a flow of 30 ml/min and higher, a linear function was generated to estimate the mean dead time in the system at any flow rate used within the range analyzed. It must be said that the values of μ_D obtained with flows lower than 30 ml/min were no longer a linear function of v, but an exponential type function tending to infinity as the flow rate approached zero.

A value of μ_D corresponding to the setup for breakthrough experiments was determined as well. In order to do so, the column in the experimental setup described in Chapter 7.2 was packed with crystal bins and the saturator was filled with ethanol to be used as tracing compound. The breakthrough curve thus obtained is assumed to be produced in the absence of any adsorptive phenomena. Hence, the stoichiometric time t_q hereby obtained is a measurement of the time necessary for the VOC to travel inside the system before reaching de detector, i.e. the dead time of the system. A representative breakthrough curve obtained experimentally is presented in Figure 9.2. The value of μ_D calculated for breakthrough experiments is 35 s and is accounted in all results of q presented in Section 6.5.

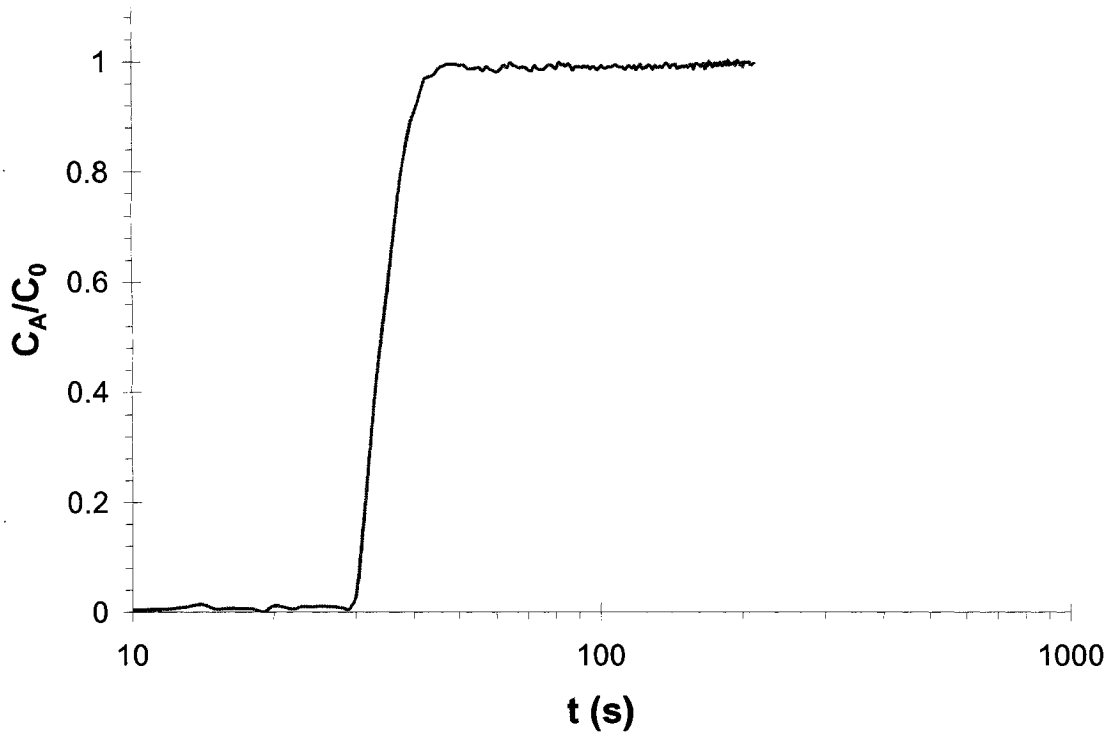

Figure 9.2 Normalized breakthrough curve of ethanol in a non-adsorbing system

10. Determination of Conditions for Infinite Dilution

Despite the small volume of the loop from which VOCs are injected into the column in pulse chromatography experiments, the possibility that the resulting mixture with the nitrogen stream does not present a sufficiently low concentration may occur. It was therefore necessary to verify experimentally that the infinite dilution conditions were met and to set limits for operating conditions. With this in mind, a set of pulse chromatography experiments were carried out to determine the adequate conditions to operate at infinite dilution, as required by this evaluation method. Using dichloromethane as reference compound, pulse chromatographic studies (as described in Chapter 6) were performed using a set of different temperatures in the saturator (T_s), and hence varied concentrations. The Arrhenius plots by which $-\Delta H_a$ was estimated for each case are presented in Figure 10.1, and the conditions of temperature and concentration with their respective results are presented in Table 10.1.

Table 10.1. Conditions and results of pulses of dichloromethane at different concentrations

T_s (°C)	P_{vap} (bar)	$-\Delta H_a$ (kJ mol^{-1})
5	0.24	55
4	0.23	52
2	0.21	52
-2	0.17	55
-4	0.16	54
-5	0.15	55

According to the work by Schneider and Smith (1968), when working at Henry's law region the mean retention time (and thus, $-\Delta H_a$) is independent of the concentration

of adsorbate in the fluid stream. The results presented in Table 10.1 show a very similar $-\Delta H_a$ in all cases, which is a good testimony of the fact that the infinite dilution conditions apply with any of the adsorbate vapor pressures analyzed. However, it can be seen in Figure 10.1 that the trend line presents an apparent shift of position from T_s= 4 °C and T_s= 2 °C. With lower concentrations beyond this point, there is no appreciable change in the trend line or in its slope. The latter suggests that at a vapor pressure lower than 0.17 bar (which corresponds to the vapor pressure of dichloromethane at -2 °C), the concentration of organic compound may be low enough to be confidently considered within the Henry's law region. Based on this evidence, the studies presented hereafter consider 0.17 bar as the maximum allowed vapor pressure to perform studies under Henry's law assumptions.

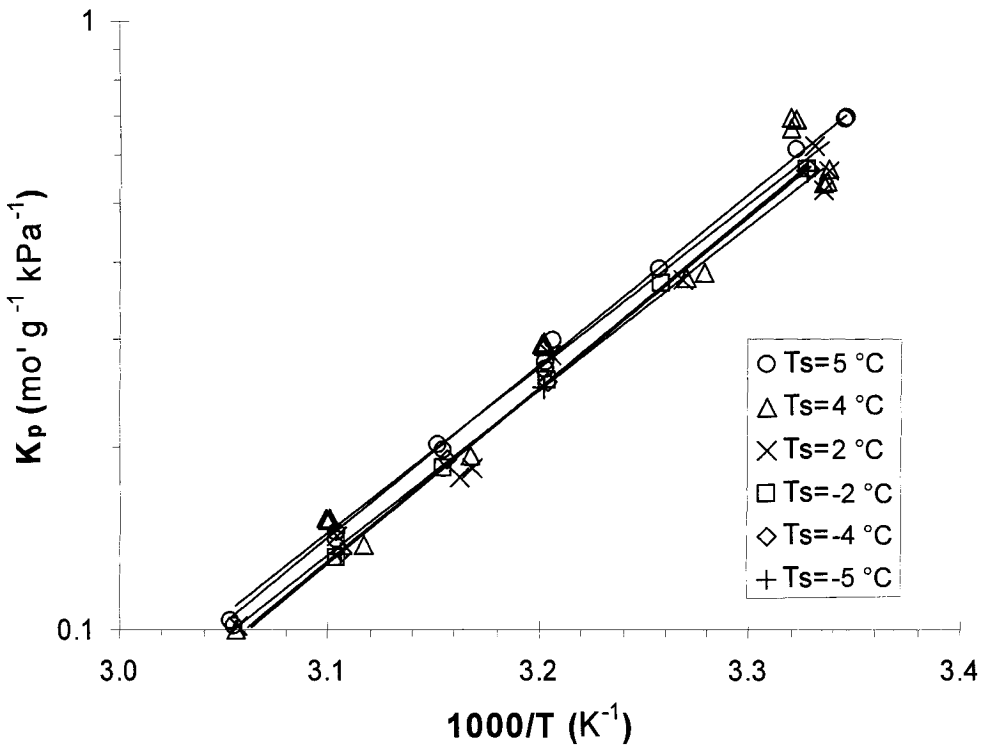

Figure 10.1. Arrhenius plots for dichloromethane on MCM-EE under different concentrations

11. Heat of Adsorption and Henry's Law Constant

The experimental results obtained for the adsorption of various volatile organic compounds using the pulse chromatographic method are presented next. As previously explained, it was determined that the limiting concentration that meet the Henry's Law assumption of infinite dilution corresponds to P_{vap} = 0.17 bar. Thus pressures were maintained below 0.17 bar throughout this work.

Organic compounds with diverse characteristics were chosen with the aim of studying the interaction between MCM-EE and some representative groups of organic pollutants. In the first place, two different halogenated compounds were studied: dichloromethane (99.96% purity, supplied by EM-Merck) and chloroform (99.8% purity supplied by BDH). In the second place, experiments with a series of cyclic compounds were performed. Benzene and toluene (99.9% and 99.8% purity respectively supplied by Aldrich), were analyzed for being aromatic compounds with different degrees of hydrophobicity. Cyclohexane (99.9% purity, Aldrich) was chosen to represent aliphatic cyclic hydrocarbons.

The results presented next include the Arrhenius plots from which $-\Delta H_a$ were estimated. Tables include the experimental results obtained in the present work and some values of $-\Delta H_a$ published in the literature, which were added for comparison purposes. The concentration profiles obtained from the response of the FID detector to each pulse injection of VOC into the adsorption column can be found in Appendix B.

11.1 Dichloromethane

From the plot presented in Figure 11.1, it is evident that MCM-EC has the highest K_p in the temperature range analyzed. It is possible that the comparatively larger pore size and pore volume of MCM-EC offer more space to accommodate adsorbate molecules inside its pores, resulting in an enhanced capacity compared to the non expanded MCM-41. This could account for the higher K_p for MCM-EC since it is directly associated to the adsorption capacity at low concentrations. While this proposition may seem contradictory when the values of K_p for MCM-EE and MCM-41 are compared (i. e. the former has a lower pore volume than the latter), it must be kept in mind that the pore volume is not the only influencing characteristic on the adsorption phenomena. The higher K_p of MCM-EE can be attributed to a better compatibility between dichloromethane and the organically modified surface rather than the calcined MCM-41.This is consistent with the higher adsorption enthalpy.

Table 11.1 Operating conditions and experimental results for the adsorption of dichloromethane by pulse chromatography

Adsorbent	T_c (°C)	P_{vap} (bar)	μ_1 (s)	K_p (mol g^{-1} kPa^{-1})
MCM-EE	54	0.16	592	0.12
	44	0.16	1118	0.24
	34	0.16	2173	0.49
	28	0.16	3256	0.75
MCM-41	55	0.16	193	0.08
	44	0.16	372	0.17
	34	0.16	671	0.31
	27	0.16	981	0.46
MCM-EC	75	0.16	503	0.33
	54	0.16	1719	1.21
	43	0.16	3258	2.37
	33	0.16	6093	4.57

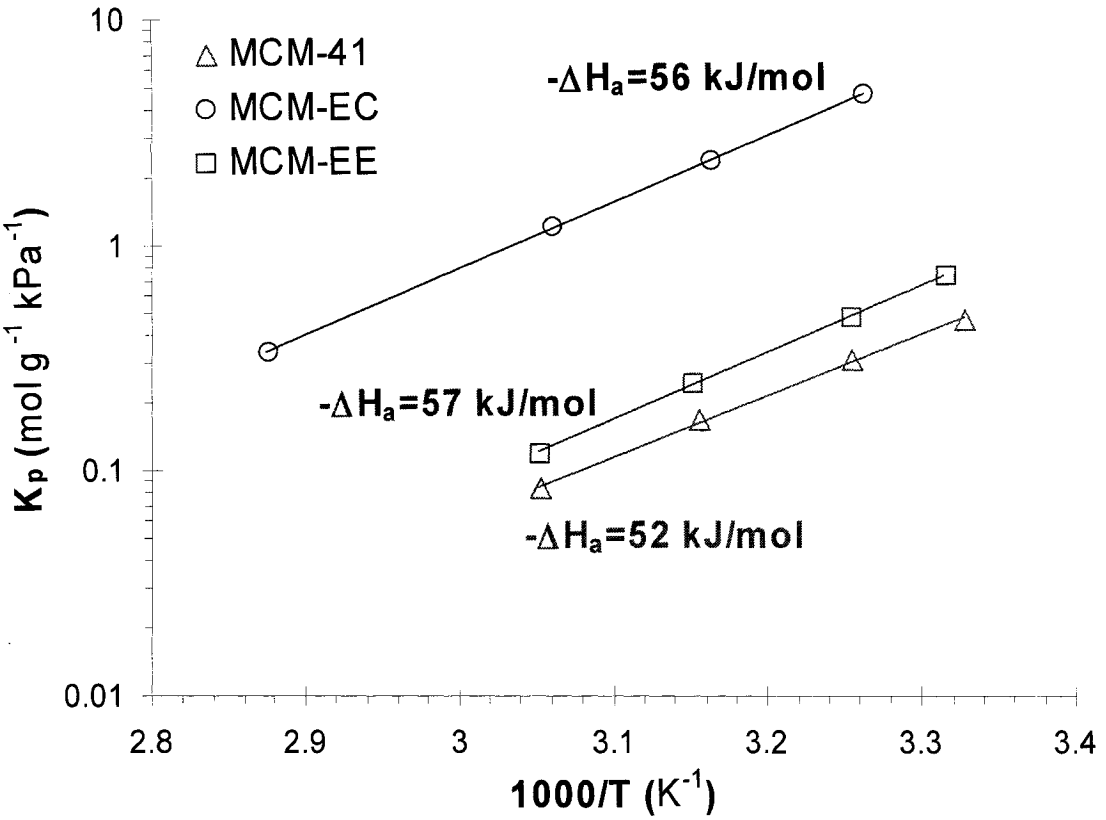

Figure 11.1. Arrhenius plots for the adsorption of dichloromethane

As seen in Table 11.2, compared with literature data, the current values of $-\Delta H_a$ for dichloromethane on mesoporous silicas are the highest. In particular, MCM-EE appears to have the strongest interaction with dichloromethane, slightly higher than the pore-expanded calcined material. It is believed that the functional groups attached to the silica surface in MCM-EE confer it with more hydrophobic character than that of purely siliceous adsorbents, resulting in a better compatibility with organic compounds like dichloromethane. The results obtained for dichloromethane are very positive for the purpose pursued in this work. For example, in terms of bonding energies, the three varieties of ordered mesoporous silicas are superior to activated carbon, a very popular adsorbent in industry. Moreover, both types of modified MCM-41, especially MCM-EE,

presented stronger interactions with the adsorbate than DAY zeolite, which is considered to exhibit a hydrophobic character; this is evidence of the enhanced hydrophobicity of the hybrid silica as a result of the organic groups on the silica surface.

Table 11.2. Heat of adsorption of dichloromethane on different adsorbents

Adsorbent	Name/Description	$-\Delta H_a$ (kJ mol^{-1})	Reference
Poly(ethylvinylbenzene-divinylbenzene)	Propak Q	43	N. M. Djordjevic et al. (1986)
DAY Zeolite	Regenerated at 423 K	28	J. H Yun et al. (1998)
DAY Zeolite	Regenerated at 573 K	52	B. Clausse et al. (1998)
Activated Carbon Fiber		25	J. H. Yun (2001)
Activated Carbon Fiber		40	J. W. Park et al. (2002)
MCM-41 hybrid expanded	MCM-EE	57	This work
MCM-41		52	This work
MCM-41 expanded calcined	MCM-EC	56	This work

11.2 Chloroform

The experimental results with chloroform are very similar to those obtained for dichloromethane. The values of K_p are found in the order MCM-EC>MCM-EE>MCM-41. Likewise, there are stronger interactions between the hybrid adsorbent MCM-EE and the adsorbate, than the other two mesoporous materials according to the calculated values of $-\Delta H_a$.

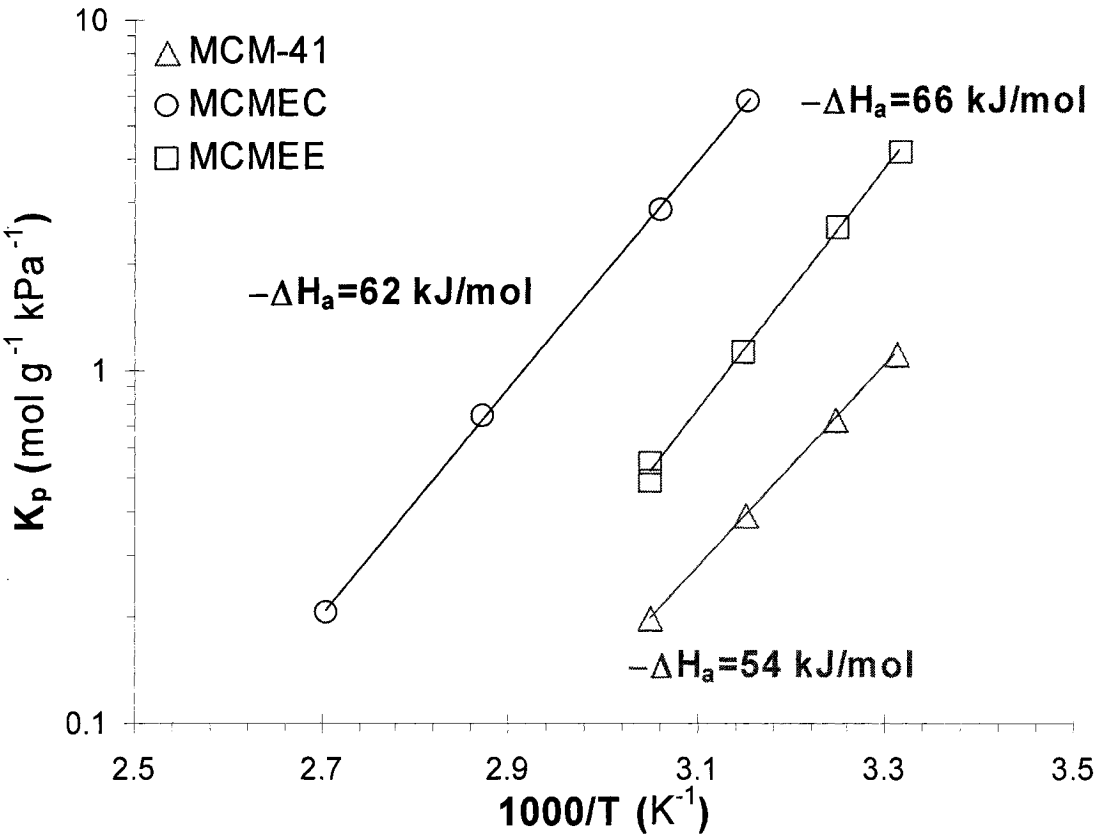

Figure 11.2. Arrhenius plots for the adsorption of chloroform

As seen in Table 11.4, compared with the results presented by other authors, the values of $-\Delta H_a$ for all current adsorbents are evidently superior. It is particularly

important to compare the mesoporous materials with the Carbon Molecular Sieve studied by Reid et al. (2001) since, even though it is a commercially available adsorbent, it presents a substantially weaker interaction with chloroform than the current materials.

Table 11.3 Operating conditions and experimental results for the adsorption of chloroform by pulse chromatography

Adsorbent	T_c (°C)	P_{vap} (bar)	μ_1 (s)	K_p (mol g^{-1} kPa^{-1})
MCM-EE	55	0.16	2582	0.54
	44	0.16	5191	1.13
	35	0.16	11366	2.55
	28	0.16	18005	4.13
MCM-41	55	0.16	462	0.20
	44	0.16	865	0.39
	35	0.16	1560	0.72
	29	0.16	2353	1.11
MCM-EC	97	0.16	331	0.21
	75	0.16	1133	0.75
	54	0.16	4079	2.87
	44	0.16	8034	5.82

The data obtained for both dichloromethane and chloroform suggest that there is an excellent compatibility between MCM-EE and halogenated compounds. It appears also, that the other two varieties of mesoporous materials have good interaction with chloroform, stronger than other adsorbents studied elsewhere, as presented in Table 11.4. It is interesting to notice that the values of $-\Delta H_a$ for chloroform are higher than those of dichloromethane. This is an expected behavior since it is believed that the mesoporous materials exhibit a hydrophobic surface that attracts more strongly the least polar compounds, in this case, chloroform.

Table 11.4. Heat of adsorption of Chloroform on different adsorbents.

Adsorbent	Name/Description	$-\Delta H_a$ (kJ mol^{-1})	Reference
Poly(ethylvinylbenzene-divinylbenzene)	Propak Q	43	N. M. Djordjevic et. al. (1986)
Polymethylsilsesquioxane		37	O. A. Kolyadina et. al. (2000)
Carbon Mol. Sieve		45	C. R. Reid et. al. (2001)
MCM-41 hybrid expanded	MCM-EE	66	This work
MCM 41		54	This work
MCM-41 expanded calcined	MCM-EC	62	This work

11.3 Benzene

The results obtained for the adsorption of benzene present a different tendency compared to that observed with halogenated hydrocarbons. As presented in Figure 11.3 and Table 11.5, while the values of K_p for MCM-EC are still the highest within the range of T analyzed, in this case the values of K_p are higher for MCM-41 than for MCM-EE. Additionally, MCM-EE presents an evidently lower $-\Delta H_a$ than MCM-41 and MCM-EC. It can also be seen that the $-\Delta H_a$ exhibited by MCM-EC and MCM-41 are much higher for benzene than halogenated compounds. Contrary to that, MCM-EE's $-\Delta H_a$ is lower for benzene, suggesting that the calcined materials are more suitable for the adsorption of benzene than the organically modified material.

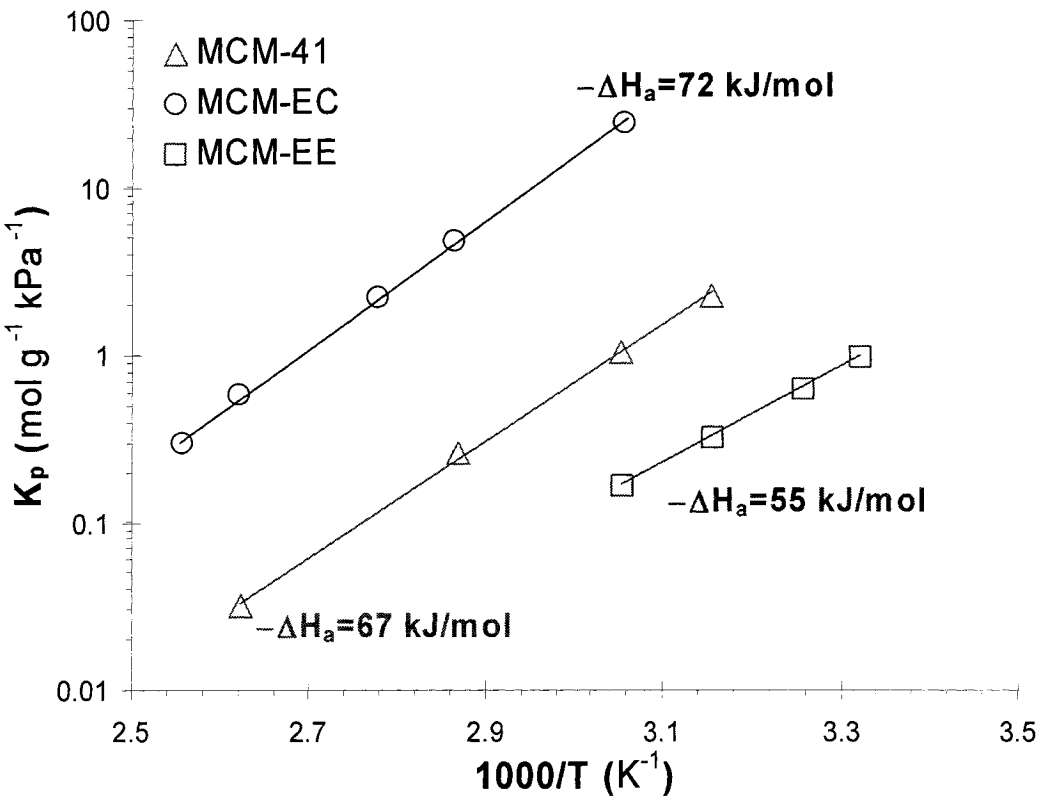

Figure 11.3. Arrhenius plots for the adsorption of benzene

As shown in Table 11.6, the results of $-\Delta H_a$ obtained for benzene adsorption on MCM-41 and MCM-EC show a better compatibility compared to activated carbons, silicas and alumina. However, some zeolites like 3A and 5A molecular sieves (Bilgic et al., 2003) appear to have a stronger adsorption of benzene. Care must be taken, however by suggesting that 3A and 5A zeolites are more appropriate for the adsorption of benzene than the mesoporous silicas studied. As can be seen, $-\Delta H_a$ are extremely high with these zeolites, up to 135 KJ/mol. Such extent of heat of adsorption is commonly attributed to chemisorption processes rather than physical adsorption with less energetic bonds. As explained in Chapter 3, this type of interaction may not be suitable for adsorption separation processes since the regeneration of the adsorbents may require an extreme demand of energy and, even with adsorbate recovery, it may not be an economically feasible process.

Table 11.5 Operating conditions and experimental results for the adsorption of benzene by pulse chromatography

Adsorbent	T_c (°C)	P_{vap} (bar)	μ_1 (s)	K_p (mol g^{-1} kPa^{-1})
MCM-EE	54	0.06	775	0.16
	44	0.06	1485	0.32
	34	0.06	2775	0.62
	28	0.06	4211	0.97
MCM-41	108	0.06	87	0.03
	76	0.06	646	0.26
	54	0.06	2441	1.06
	44	0.06	5068	2.27
MCM-EC	118	0.06	516	0.30
	108	0.06	963	0.58
	87	0.06	3493	2.23
	76	0.06	7279	4.79
	54	0.06	34695	24.39

Table 11.6 Heat of adsorption of benzene on different adsorbents

Adsorbent	Name/Description	$-\Delta H_a$ (kJ mol^{-1})	
Poly(ethylvinylbenzene-divinylbenzene)	Propak Q	48	N. M. Djordjevic et al. (1986)
Silicalite		21	J. R. Hufton et al. (1995)
Faujastite		45	J. Janchen et al. (1996)
Silicalite	MFI	58	
Silicalite	MEI	59	
VPI-5	VFI	40	
$AlPO_4$-5	AFI	54	
$AlPO_4$-11	AEI	62	
DAY zeolite		40	J. H. Yun et al. (1998)
MCM-41		56	V. R. Choudhary (2000)
Polymethylsilsesquioxane	PMS	40	O. A. Kolyadina et al. (2000)
Activated Carbon	Ajax type 976	53	D. D. Do et. al. (2001)
Carbon mol. Sieve.		42	C. R. Reid et al. (2001)
MCM-41		60	X. S. Zhao (2001)
4A zeolite		55	O. Inel et al. (2002)
13X zeolite		64	
SiO_2		39	K. B. Gurevich et al. (2002)
SiO_2-$Si(CH_3)_2$-(nC_8H_{17})		29	
SiO_2-$Si(CH_3)_2$-($nC_{16}H_{33}$)		28	
SiO_2-$Si(CH_2)_3$-$(CF_2)_3$-CF_3		30	
SiO_2-$Si(CH_2)_3$-$(CF_2)_5$-CF_3		29	
Alumina	F-1	50	C. Bilgic et. al (2003)
3A.zeolite	Molecular sieve	86	
5A zeolite	Molecular sieve	135	
Activated Carbon	AU-TU commercial	52	I. A. Bardina et. al. (2004)
MCM-41 expanded extracted	MCM-EE	55	This work
MCM-41		67	This work
MCM-41 expanded calcined	MCM-EC	72	This work

Table 11.6 shows that MCM-EE has the lowest -ΔH_a compared with MCM-41 from this and other works. A reasonable explanation can be found in the work by Inel et al. (2002) where it was suggested that the silica walls exhibit a weak acidic character due to the hydroxyl groups that exist on its surface. Such character produces a specific and

strong interaction between the silica surface and molecules containing π electrons. This accounts for the higher $-\Delta H_a$ of MCM-EC and MCM-41, since the organic molecules on the surface of MCM-EE inhibit such interaction. In fact, other silica-based adsorbents like the silicalites studied by Janchen et al. (1996) present higher $-\Delta H_a$ than MCM-EE. This is evidence that the organic molecules in MCM-EE effectively altered the surface chemistry of this adsorbent, producing a hybrid material with an adsorptive nature different to that of pure silica.

11.4 Toluene

The results exhibited in Figure 11.4 and Table 11.7 suggest a similar behavior of the adsorbents with toluene and benzene. Once again, MCM-EC presented both the highest K_p and $-\Delta H_a$. It is worth noticing that the values of K_p and $-\Delta H_a$ for toluene are higher for MCM-41 and MCM-EC than for benzene or any halogenated compound hereby studied. This behavior is in agreement with other works where siliceous adsorbents were studied. As explained in the discussion for benzene, toluene contains π electrons that allow it to be selectively attached on silica surfaces. Moreover, it has been proposed (Djordjevic et al., 1986; Kolyadina et al., 2000) that the attractive forces may be proportional to the number of carbons in the molecule, resulting in a stronger interaction with toluene than benzene, for example.

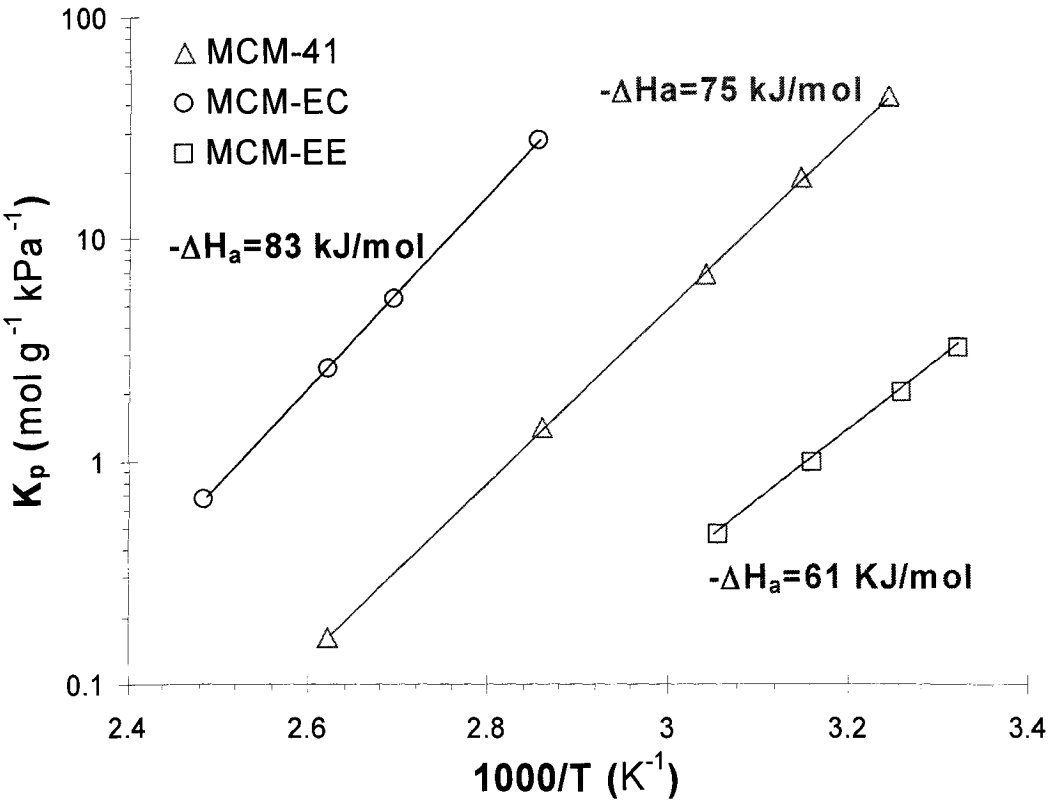

Figure 11.4. Arrhenius plots for the determination of the adsorption of toluene

Table 11.7 Operating conditions and experimental results for the adsorption of toluene by pulse chromatography

Adsorbent	T_c (°C)	P_{vap} (bar)	μ_1 (s)	K_p (mol g^{-1} kPa^{-1})
MCM-EE	54	0.01	2226	0.47
	43	0.01	4558	0.99
	34	0.01	9044	2.04
	28	0.01	14301	3.28
MCM-41	108	0.01	436	0.16
	77	0.01	3544	1.44
	56	0.01	16072	6.95
	45	0.01	42461	19.02
	35	0.01	97028	44.79
MCM-EC	129	0.01	1180	0.67
	108	0.01	4304	2.59
	98	0.01	8630	5.35
	77	0.01	43181	28.38

As exhibited in Table 11.8, the values of $-\Delta H_a$ for the materials investigated in the present work is lower in the case of MCM-EE than most of the zeolites reported by other authors. This is a similar behavior as the one observed with benzene, where the low interaction forces presented by MCM-EE are a consequence of the inaccessibility of toluene to the silica surface. The pore-expanded variety (MCM-EC) has the highest $-\Delta H_a$ of all ordered mesoporous silicas and, compared with all other materials, is only surpassed by 5A, ZSM-5 and 10X zeolites. Toluene appears to be extremely compatible with siliceous adsorbents, but once again the values of $-\Delta H_a$ with these materials fall within the range of chemisorption energy.

Table 11.8. Heat of adsorption of toluene on different adsorbents

Adsorbent	Name/Description	ΔH_a (kJ mol^{-1})	
Poly(ethylvinylbenzene-divinylbenzene)	Propak Q	56	N. M. Djordjevic et al. (1986)
Alumina	Commercial	46	E. Alpay et al. (1996)
3A zeolite	Commercial	68	
4A zeolite	Commercial	74	
5A zeolite	Commercial	90	
ZSM-5	Commercial	98	
10X zeolite	Commercial	98	
NaY zeolite	Commercial	76	
KY	Commercial	64	
DAY zeolite		73	J. H. Yun et al. (1998)
MCM-41		62	V. R. Choudary et al. (2000)
Activated Carbon	Picatiff	79	F. Delage et al. (2000)
Activated Carbon	Fiber	26	J. W. Park et al. (2002)
Granular Activated Carbon	Picatiff NC60	63	P. Pre et al. (2002)
MCM-41 hybrid expanded	MCM-EE	61	This work
MCM-41		75	This work
MCM-41 expanded calcined	MCM-EC	83	This work

11.5 Cyclohexane

As can be observed in Figure 11.5, within the adsorbents studied in the present work, MCM-EC presents the highest values K_p and $-\Delta H_a$ and MCM-EE the lowest. It is interesting to observe that even though cyclohexane is the most hydrophobic of the organic components analyzed, $-\Delta H_a$ in all adsorbents is lower that those calculated for aromatic hydrocarbons. These results suggest that the strength of the adsorption interactions on the adsorbent surface is not dependent only on the hydrophobicity of the VOC adsorbate. In fact, the values of $-\Delta H_a$ are very similar to those obtained for dichloromethane (from 50 to 57 kJ/mol, as seen in Table 11.1) which is the least hydrophobic of the organic compounds studied.

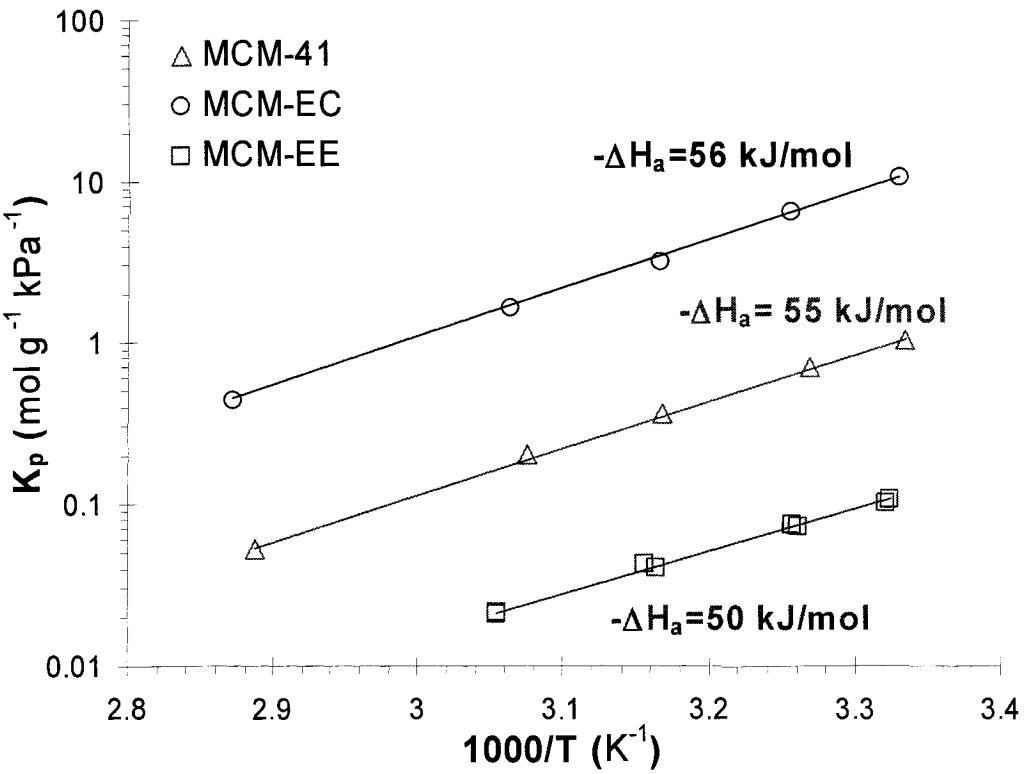

Figure 11.5. Arrhenius plots for the adsorption of cyclohexane

A simple explanation for such behavior was proposed in the work of Bilgic et al. (2003), where experimental results with zeolites showed higher values of K_p and $-\Delta H_a$ in the adsorption of benzene than those for cyclohexane. Such difference was attributed to the smaller size of the benzene molecule, which would permit a greater load of benzene molecules inside the same void space. This explanation, while simple, may not be appropriate according to the results of the present work, since toluene for example has a larger molecule than benzene (Y. C. Chiang et al., 2001), but presents both higher $-\Delta H_a$ and capacity at low adsorbate concentration.

Table 11.9 Operating conditions and experimental results for the adsorption of cyclohexane by pulse chromatography

Adsorbent	T_c (°C)	P_{vap} (bar)	μ_1 (s)	K_p (mol g^{-1} kPa^{-1})
MCM-EE	54	0.06	102	0.02
	44	0.06	197	0.04
	34	0.06	337	0.08
	28	0.06	479	0.11
	73	0.06	132	0.05
MCM-41	52	0.06	473	0.21
	43	0.06	815	0.37
	33	0.06	1515	0.70
	27	0.06	2245	1.06
MCM-EC	75	0.06	664	0.44
	53	0.06	2334	1.64
	43	0.06	4380	3.19
	34	0.06	8691	6.51
	27	0.06	13968	10.69

The results however, are consistent once again with the proposal of Inel et al. (2002), where the lower $-\Delta H_a$ in the adsorption of cyclohexane with silica adsorbents was attributed to the absence of double bonds in its molecules. It can be seen from Table 11.9 that all siliceous materials, whether studied in this or other works presented a much lower $-\Delta H_a$ with cyclohexane than with benzene. It is interesting to notice that such decrease in the heat of adsorption is less dramatic in the case of adsorbents like

polymethylsilsesquioxane (O. A. Kolyadina et al., 2000) or MCM-EE, where benzene and cyclohexane exhibit very similar $-\Delta H_a$.

Table 11.10 Heat of adsorption of cyclohexane on different adsorbents

Adsorbent	Name/Description	$-\Delta H_a$ (kJ mol^{-1})	
Poly(ethylvinylbenzene-divinylbenzene)	Propak Q	51	N. M. Djordjevic et. al. (1986)
Polymethylsilsesquioxane	PMS	41	O. A. Kolyadina et. al. (2000)
4A zeolite		50	O. Inel et. al. (2002)
13 X zeolite		47	
Alumina	F1	32	C. Bilgic et. al. (2003)
3A zeolite	Mol. Sieve	29	
5A zeolite	Mol. Sieve	45	
MCM-41 hybrid expanded	MCM-EE	50	This work
MCM-41		55	This work
MCM-41 expanded calcined	MCM-EC	56	This work

The results presented in Table 11.10 show that in general, all the mesoporous silicas present a good interaction with cyclohexane. MCM-EC and MCM-41 present higher values of $-\Delta H_a$ than any other adsorbent reported in literature, even when compared with adsorbents that presented higher $-\Delta H_a$ with benzene or toluene (i.e., 3A and 5A). This provides evidence of the suitability of mesoporous silicas as adsorbents of alicyclic compounds.

12. Adsorption Capacity

The adsorption capacity (q) of the adsorbents was evaluated from experimentally generated breakthrough curves. For this analysis, a continuous flow of VOC with known concentration was fed to the column until a saturated state was achieved, as explained in Chapter 5. To obtain suitable results, some operational conditions were changed with respect to the pulse chromatography experiments previously described. Since it was expected that the amount of VOC received in the FID is much higher with a continuous flow than with a single pulse, the sensitivity of the detector was changed into a medium gain to avoid off-scale measurements. The gas flow was also reduced from 50 to 30 ml/min to obtain more detailed breakthrough profiles while decreasing the possibility of premature breakthrough of the column.

It must be said that, due to the difference of densities between the adsorbents, the mass of packed material (W) in the column was dissimilar. For each adsorbent, the total amount of adsorbent packed in the column was measured using an analytical balance and the values obtained are presented in Table 12.1.

Table 12.1. Actual amount of adsorbent packed in the adsorption column

Adsorbent	W (g)
MCM-EE	0.80
MCM-41	0.55
MCM-EC	0.37

The results presented in this section include the normalized breakthrough curves, followed by tables containing the estimated values of time at breakthrough (t_b), of

stoichiometric time calculated at saturation (t_q), and of adsorption capacity at breakthrough (q_b) and at complete saturation (q). In Chapters 12.2 and 12.3, an additional column presenting an efficiency factor, expressed as the ratio of capacity in the presence of water over capacity in dry environments (q_{humid}/q) or as the capacity for multiple adsorbates over the capacity for a single adsorbate (q_{mix}/q) is included. Such column is intended as a benchmark to compare the results under different environments, and is a measurement of efficiency of the adsorbents towards a particular adsorbate.

12.1 Adsorption Capacity of Single VOCs in inert environment

12.1.1 Dichloromethane

From the breakthrough curves presented in Figure 12.1, it is evident that MCM-41 presented the longest breakthrough time, resulting in the highest q of the adsorbents studied. It can be seen that even though the breakthrough of dichloromethane with MCM-EE occurs earlier than for any other adsorbent, C_A increases at a very low and steady rate until a time around 130 s when the slope of the curve presents an evident change, and hence its final capacity q' is higher than MCM-EC as presented in Table 12.2. In fact, the evident appearance of an early breakthrough of MCM-EE can be attributed to other effects rather than the proximity of saturation. A premature breakthrough may appear if the adsorbate is pushed through the fixed bed at a velocity too high to allow the adsorption of some VOCs. MCM-EE is more likely to present this effect since (according to Eq. 5) its smaller ε produces a higher interstitial velocity of the fluid than any other adsorbent. However, since the value of q' for MCM-EE is higher than MCM-EC, a better performance of a column packed with the hybrid silica is suggested.

Table 12.2. Dichloromethane breakthrough curves data

Adsorbent	t_b (s)	q_b (mol g^{-1})	t_q (s)	N_A (mmol)	q (mmol g^{-1})	q' (mmol ml^{-1})
MCM-EE	112	0.50	193	0.70	0.88	0.54
MCM-41	231	1.51	289	1.04	1.88	0.80
MCM-EC	142	1.37	160	0.59	1.55	0.45

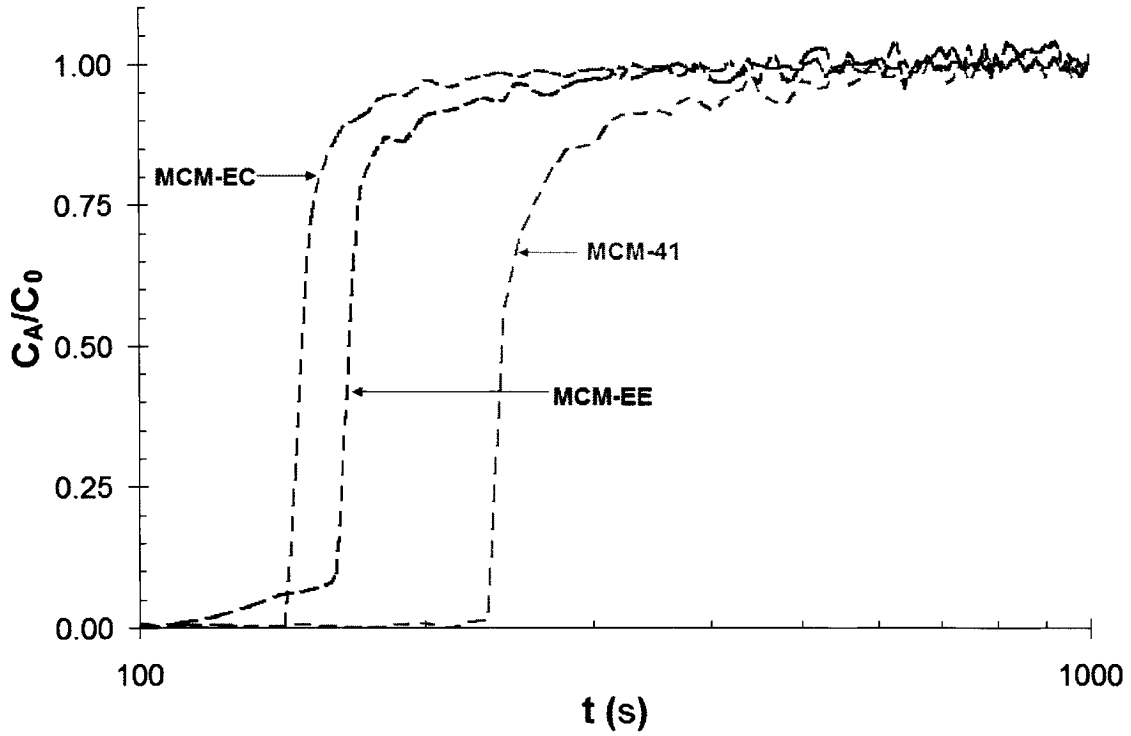

Figure 12.1. Normalized breakthrough curves of dichloromethane on ordered mesoporous adsorbents.

It is important to notice that the values of adsorption capacity in terms of mass of adsorbent may seem contradictory to the results of chromatographic analysis since MCM-EE has the lowest q of all the adsorbents but presented higher $-\Delta H_a$ and K_p than MCM-41. An explanation to this is the fact that MCM-EE presents significantly lower surface area and pore volume, resulting in a smaller number of sites for VOC adsorption and a more constrained space for the molecules to enter inside the pores. While these characteristics may not be significant in the analysis of a pulse in infinite dilution, its influence on the adsorption capacity becomes evident at saturation conditions.

12.1.2 Chloroform

For chloroform, the breakthrough curves obtained were sharp and well defined for the three adsorbents studied, as observed in Figure 12.2. MCM-41 presents the highest capacity with a q' equal to 0.29 mol/ml, slightly over the rest of the adsorbents whose q' was very similar at around 0.27 mol/ml. As seen in Table 12.3, even though t_b for MCM-41 was the shortest, its breakthrough curve presented a lower saturation rate, resulting in the aforementioned superior capacity. Its earlier breakthrough, however, may not be suitable when intended for purification purposes, since it may exceed the requested concentration at the column outlet faster than the other adsorbents.

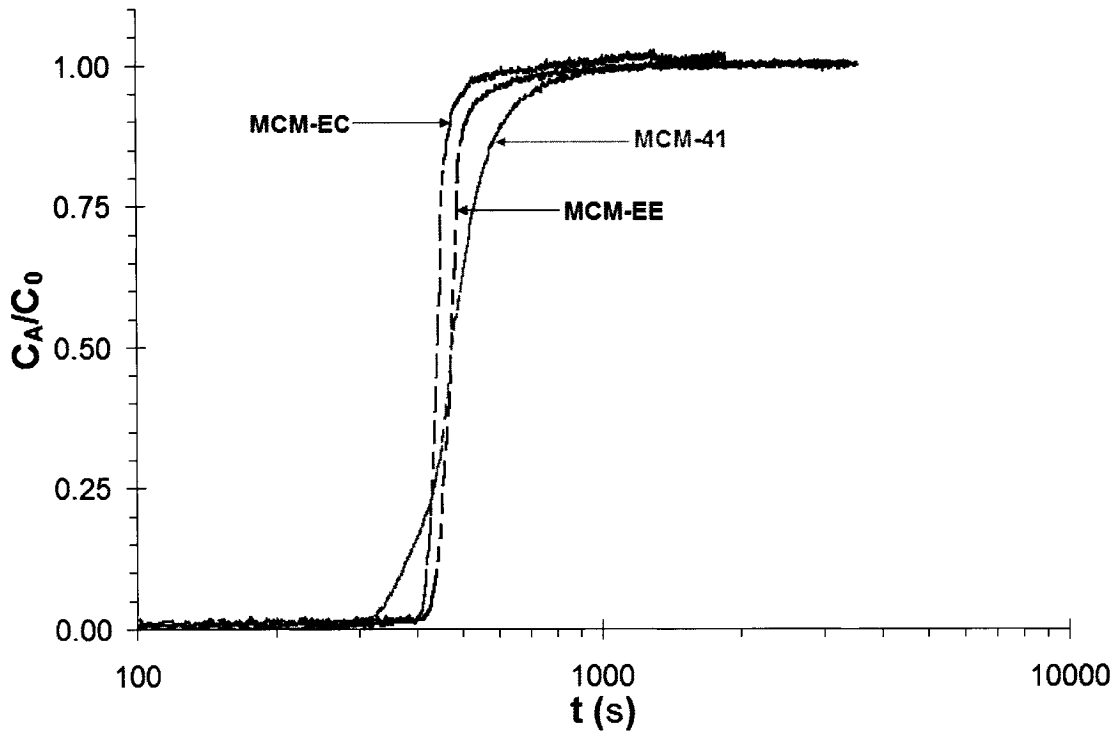

Figure 12.2. Normalized breakthrough curves of chloroform on ordered mesoporous adsorbents.

Table 12.3. Chloroform breakthrough curves data

Adsorbent	t_b (s)	q_b (mol g^{-1})	t_q (s)	N_A (mmol)	q (mmol g^{-1})	q' (mmol ml^{-1})
MCM-EE	413	0.35	489	0.35	0.44	0.27
MCM-41	291	0.40	524	0.38	0.69	0.29
MCM-EC	398	0.80	490	0.35	0.92	0.27

12.1.3 Benzene

The breakthrough curves for benzene in Figure 12.3 show a higher capacity of MCM-41, over the other adsorbents. MCM-EE presents a sharp curve at its t_b resulting in a shorter q' than any other adsorbent, as seen in Table 12.4. This coincides with the results from chromatographic analyses, where it showed the lowest compatibility for aromatic hydrocarbons among the adsorbents analyzed in this work.

Table 12.4. Benzene breakthrough curves data

Adsorbent	t_b (s)	q_b (mol g^{-1})	t_q (s)	N_A (mmol)	q (mmol g^{-1})	q' (mmol ml^{-1})
MCM-EE	512	0.66	568	0.57	0.77	0.44
MCM-41	1072	1.93	1331	1.34	2.43	1.04
MCM-EC	443	1.19	767	0.77	2.07	0.60

An interesting behavior is exhibited by the breakthrough curve for MCM-EC, since the curve reaches an apparent plateau when C_A/C_0 reaches 0.15 at approximately 700 s right before a sudden increase of concentration. While slightly less evident, a similar effect can be noticed for MCM-41 at 1200 s. This type of behavior has been observed by other authors and was attributed to the existence of capillary condensation of

the adsorbate inside the pores of the adsorbent (M. Hartmann and C. Bischof, 1999). It is worth saying that this effect appears only with the purely siliceous (i. e. calcined) adsorbents, and not with the hybrid MCM-EE. It is then possible that this effect is present as a consequence of the interaction between benzene and the bare silica surface. Another possibility is a greater similarity between the calcined materials in terms of their particle structure, since it is possible that the aforementioned condensation takes place in the interparticle void rather than inside the pores of the adsorbent.

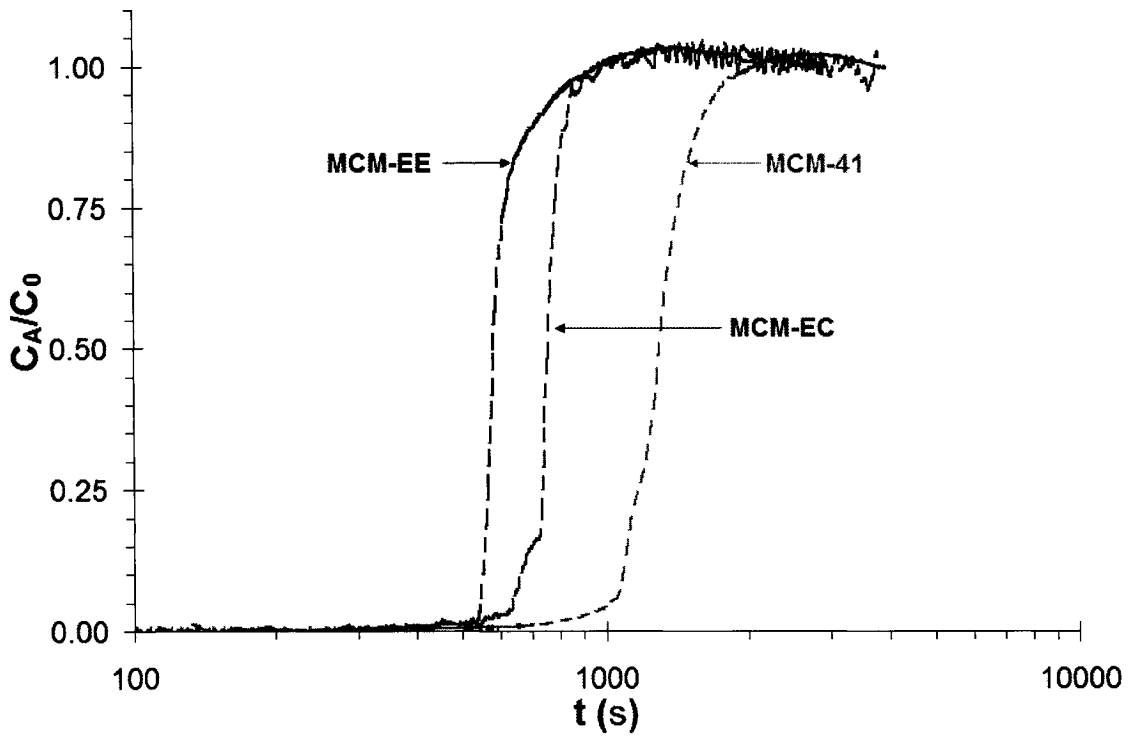

Figure 12.3. Normalized breakthrough curves of benzene on ordered mesoporous adsorbents.

12.1.4 Toluene

The values of q' calculated from the breakthrough curves presented in Figure 12.4 show a high capacity for toluene with MCM-41, while MCM-EE exhibits the lowest capacity. A breakthrough with a low rate of increase is observed in these experiments with all the adsorbents used. Similarly to the case of adsorption of dichloromethane on MCM-EE (presented in Figure 12.2), this behavior can be attributed to a high flow rate of the fluid phase in the column.

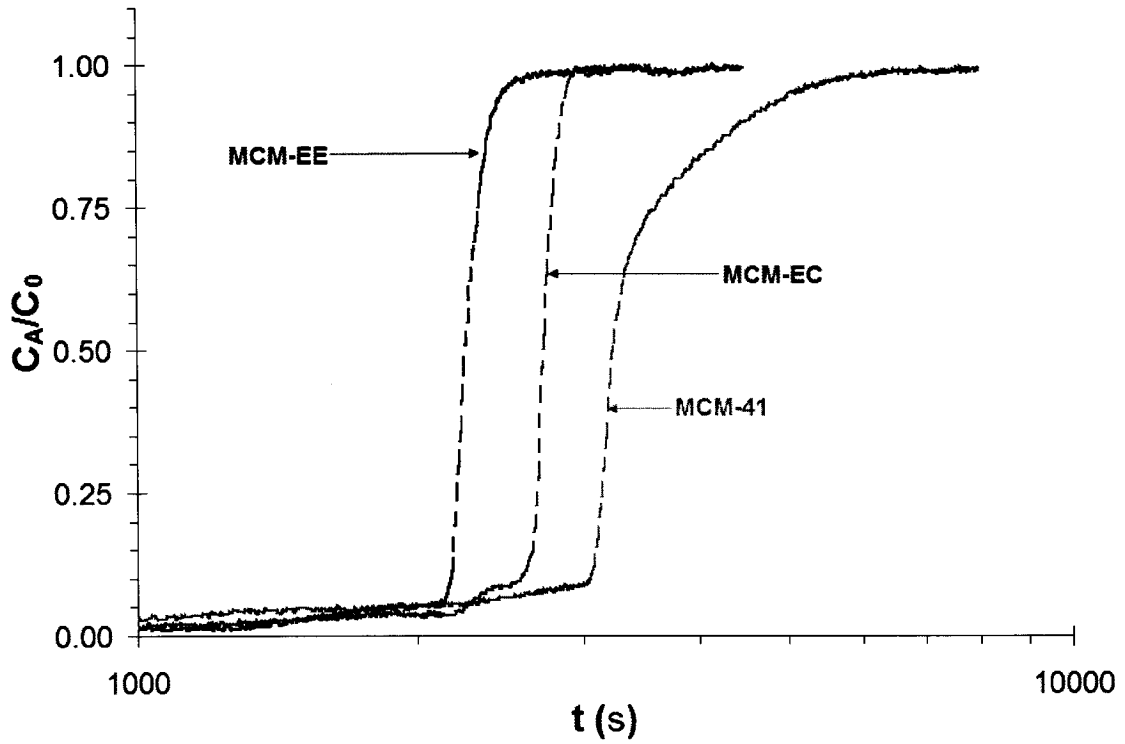

Figure 12.4. Normalized breakthrough curves of toluene on ordered mesoporous adsorbents.

Considering the adsorption data for both toluene and benzene, it is evident that MCM-EE is not an adsorbent as effective as the purely siliceous materials for aromatic hydrocarbons. This is in agreement with the results of $-\Delta H_a$ and K_p calculated in Chapter 11 (Figures 11.3 and 11.4), where it was observed that MCM-EC and MCM-41 exhibit much stronger interactions with both benzene and toluene.

Table 12.5. Toluene breakthrough curves data

Adsorbent	t_b (s)	q_b (mol g^{-1})	t_q (s)	N_A (mmol)	q (mmol g^{-1})	q' (mmol ml^{-1})
MCM-EE	1445	0.22	2240	0.27	0.35	0.21
MCM-41	3052	0.75	3401	0.41	0.87	0.32
MCM-EC	2164	0.73	2573	0.33	0.89	0.26

12.1.5 Cyclohexane

Finally, it can be seen in Table 12.6 that the highest adsorption capacity for cyclohexane is shown by MCM-41. As can be appreciated in Figure 12.5, while MCM-EC presents a shorter breakthrough time t_b than MCM-EE, the shape of its isotherm is less sharp, allowing it to accomplish saturation after a longer time and resulting in a higher q'. It can be seen that MCM-EE has a sharper breakthrough curve compared with the other varieties.

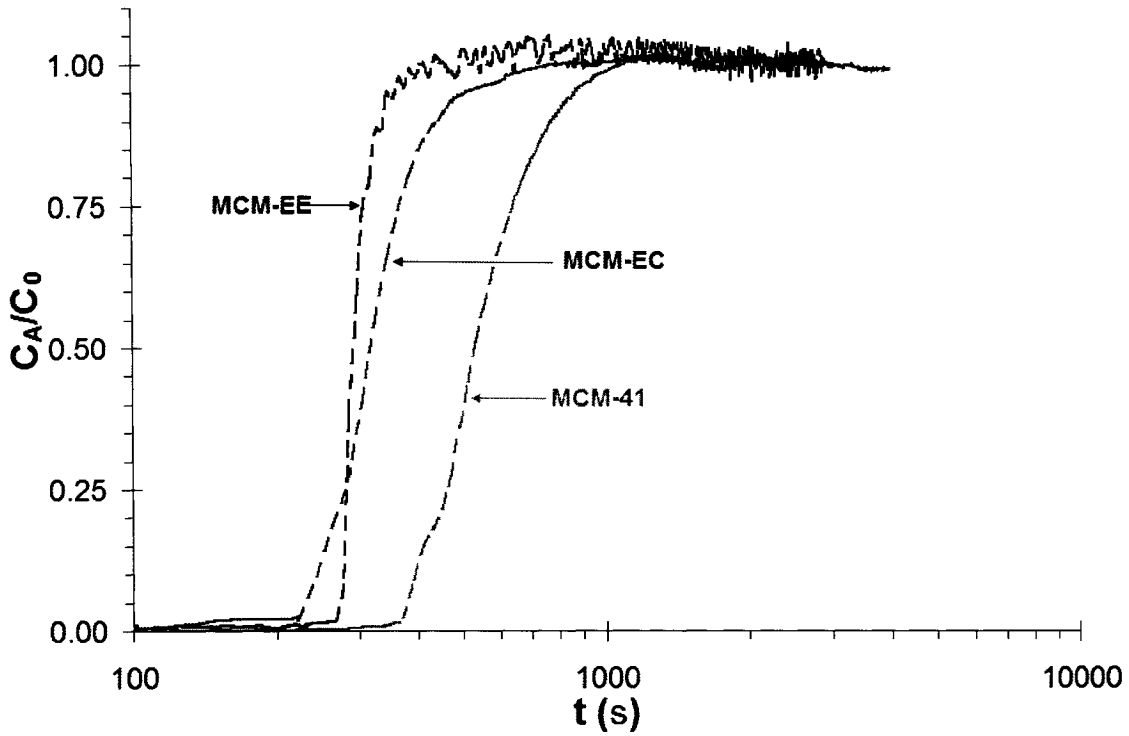

Figure 12.5. Normalized breakthrough curves of cyclohexane on ordered mesoporous adsorbents.

It is interesting to observe in Figure 12.5 that the shape of the breakthrough curves for MCM-41 and MCM-EC is very similar with an inflection point at a C_A/C_0 of around 0.2. MCM-EC appears to be a reproduction of the breakthrough curve of MCM-41 displaced 120 seconds earlier. Since both adsorbents are purely siliceous calcined materials, a reasonable explanation for this could be that the adsorption of cyclohexane is strongly influenced by the surface chemistry of the adsorbent. In fact, the capacity q estimated for both adsorbents is both cases similar, with 1.08 mmol/g for MCM-41 and 0.90 mmol/g for MCM-EE (Table 12.6). It can be said that the adsorption process taking place in the case of cyclohexane is extremely similar with both MCM-41 and MCM-EC.

Table 12.6. Cyclohexane breakthrough curves data

Adsorbent	t_b (s)	q_b (mol g^{-1})	t_q (s)	N_A (mmol)	q (mmol g^{-1})	q' (mmol ml^{-1})
MCM-EE	142	0.16	318	0.34	0.45	0.26
MCM-41	231	0.76	569	0.60	1.08	0.46
MCM-EC	112	0.72	340	0.36	0.90	0.28

12.2 Adsorption of single VOCs in humid environment

12.2.1 Dichloromethane

From the results presented in Table 12.7, it is seen that even though MCM-EE does not present the highest capacity, it is the most efficient for dichloromethane in a humid environment. In the presence of water, MCM-EE is capable of adsorbing around 89% of its total capacity under dry conditions. This ratio is 80% and 84% for MCM-41 and MCM-EC, respectively. This efficiency can be easily appreciated in Figure 12.6 where the breakthrough curves for dry and humid streams with MCM-EE appear much closer than with the other adsorbents.

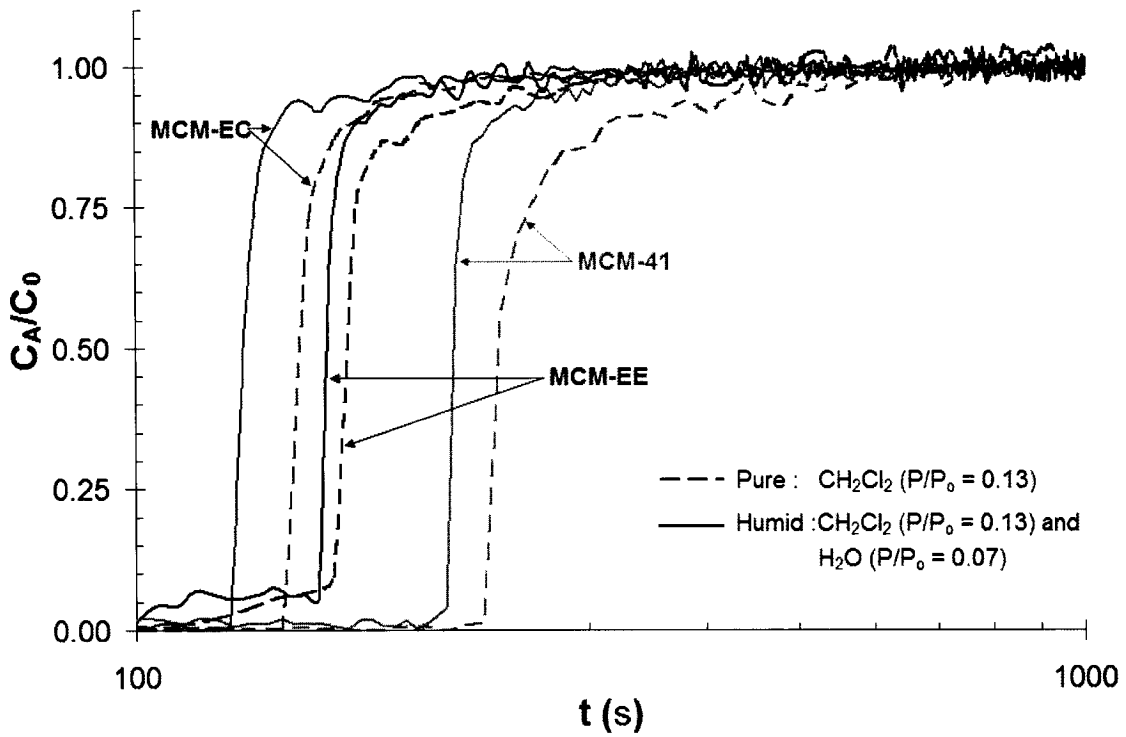

Figure 12.6 Normalized breakthrough curves for dichloromethane under dry and humid environments

12.2.2 Benzene

The breakthrough curves presented in Figure 12.7 show a very high efficiency of MCM-41 for benzene. The curves of both dry and wet environments with MCM-41 broke through at a very similar time and following the same path up to a C_A/C_0 of 0.2. The slight decrease of adsorption capacity can be accounted for by the slower rate of the effluent gas to achieve equilibrium under dry conditions.

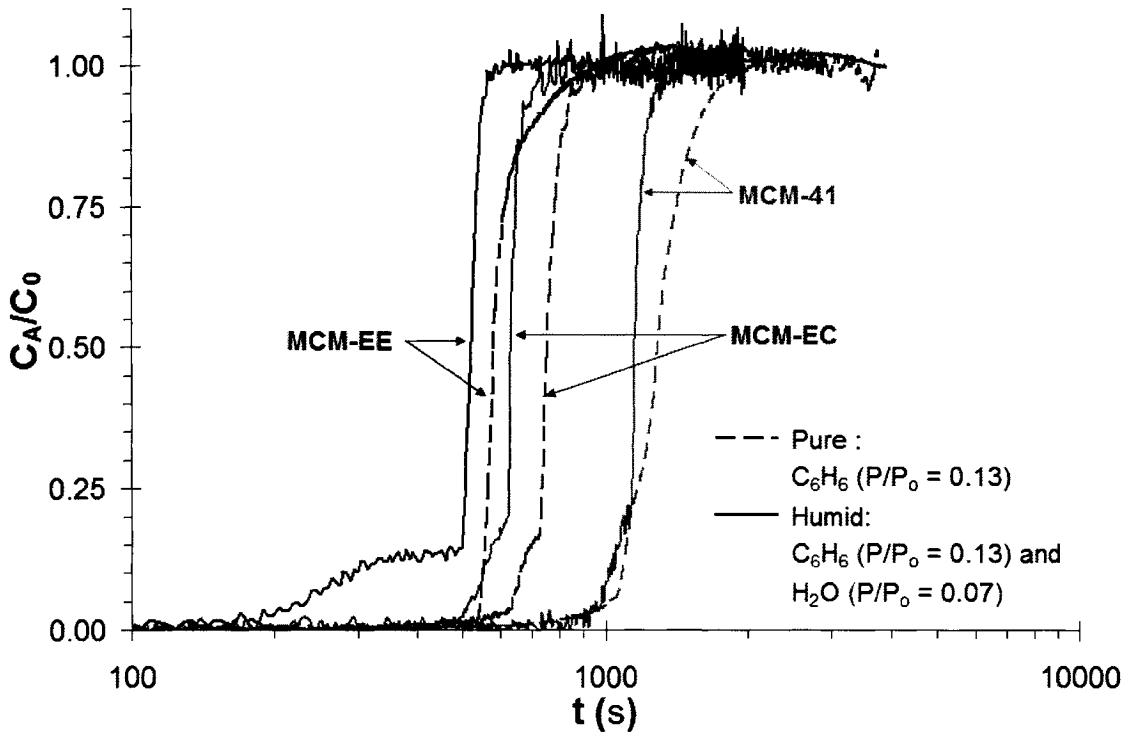

Figure 12.7 Normalized breakthrough curves for benzene under dry and humid environments

MCM-EC presented a lower efficiency than MCM-41, with a value of q_{humid}/q_{dry} = 0.84 which, surprisingly, is the same value obtained for the adsorption of

dichloromethane. As can be seen in Figure 12.7, the shape of the breakthrough curves of MCM-EE and MCM-41 obtained under humid and dry conditions are very similar, including a small plateau at C_A/C_0 = 0.2. As mentioned for the adsorption of dichloromethane in Section 12.2.1, these similarities suggest that the presence of water is not affecting the adsorption mechanism by which purely siliceous materials adsorb benzene. This, however, is not observed with MCM-EE, where an evident change of shape is presented. While MCM-EE presented a sharp breakthrough curve in dry conditions, a sudden breakthrough appears with a plateau extending from t = 300 to 500 s in the presence of humidity. MCM-EE is the adsorbent with lowest efficiency for benzene in humid streams, as presented in Table 12.8.

Table 12.8 Adsorption capacity for benzene in humid environment

Adsorbent	N_A (mmol)	q (mmol g^{-1})	q' (mmol ml^{-1})	q_{humid}/q_{dry}
MCM-EE	0.49	0.62	0.38	0.81
MCM-41	1.16	2.10	0.90	0.87
MCM-EC	0.65	1.73	0.50	0.84

12.2.3 Cyclohexane

Compared to the other VOCs studied, the efficiency for cyclohexane in the presence of humidity was unexpectedly much lower in all cases, despite the highly hydrophobic nature of the adsorbate. It is interesting to notice that the efficiency observed in the presence of water is very similar in all cases, according to the results presented Table 12.9. It can also be seen in Figure 12.8, that the breakthrough curves obtained for MCM-41 and MCM-EC are once again extremely similar in shape, which is indicative of the similarities between the adsorptive phenomena occurring with the calcined adsorbents.

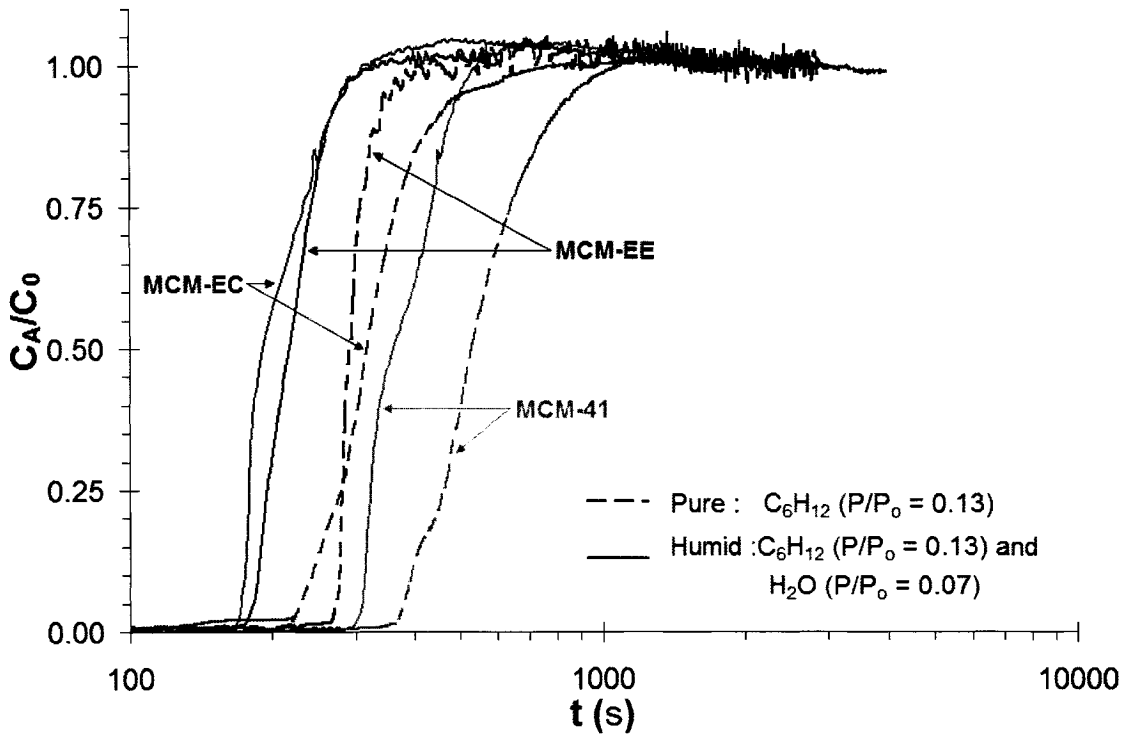

Figure 12.8 Normalized breakthrough curves for cyclohexane under dry and humid environments

The results obtained with cyclohexane are extremely relevant, since they present evidence that a highly hydrophobic adsorbent may not necessarily be more efficiently adsorbed.

Table 12.9 Adsorption capacity for cyclohexane in humid environment

Adsorbent	N_A (mmol)	q (mmol g^{-1})	q' (mmol ml^{-1})	q_{humid}/q_{dry}
MCM-EE	0.24	0.30	0.18	0.66
MCM-41	0.41	0.73	0.31	0.68
MCM-EC	0.23	0.61	0.18	0.68

12.3 Adsorption Capacity for mixtures of two VOCs

12.3.1 Dichloromethane – Benzene Mixture

The objective of performing analyses with systems containing two VOCs is to evaluate the influence of a second organic compound on the adsorption capacity of the adsorbents for a given adsorbate and the possible occurrence of competitive adsorption. The breakthrough curves presented in Figure 12.9 correspond to the adsorption of dichloromethane in a mixture containing benzene. The breakthrough curves of dichloromethane as a single component are also presented for comparison.

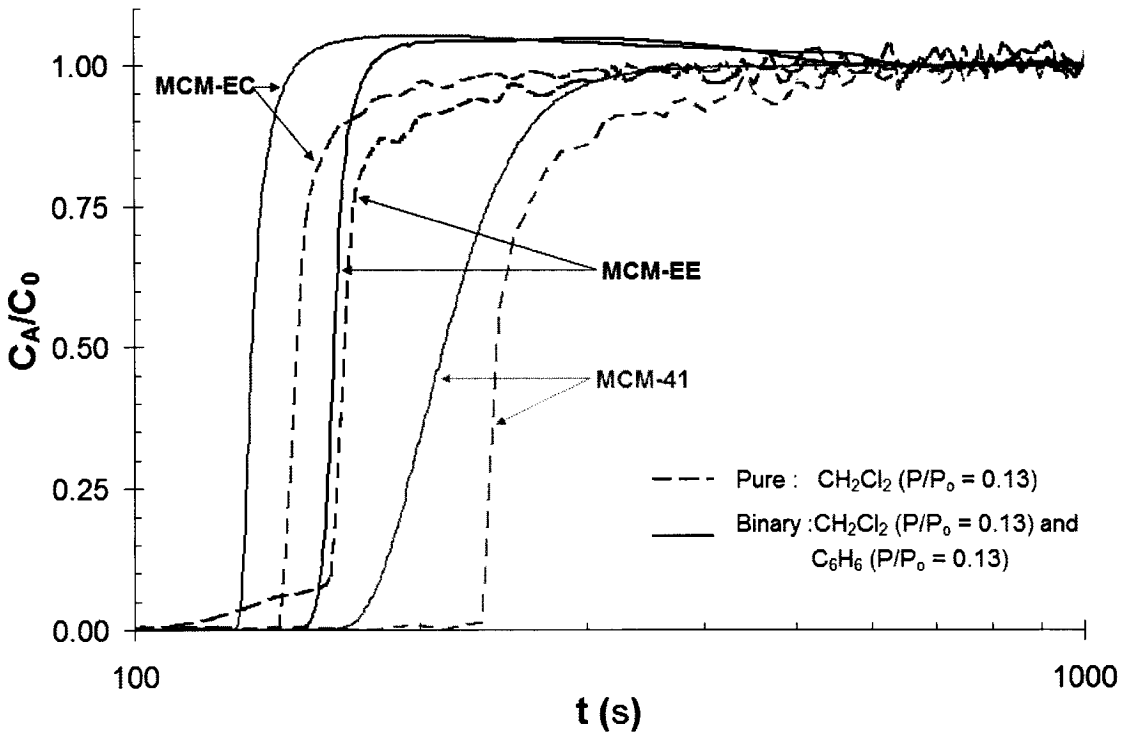

Figure 12.9 Normalized breakthrough curves for dichloromethane as a single component and in a mixture containing benzene

While in all cases the breakthrough curves appeared at an earlier t_b for the two-component system, it can be seen that the curves of dichloromethane with MCM-EE have a much smaller shift than the other adsorbents. This may indicate a lower influence exerted by benzene on the adsorption of dichloromethane over the hybrid silica. On the other hand, the evident differences in the curves with MCM-41 and MCM-EC represent a lower efficiency for halogenated compounds by these adsorbents. This is confirmed by the values of q_{mix}/q_{dry} presented in Table 12.10 where a value of 0.86 was found for MCM-EE while the efficiencies for MCM-EC and MCM-41 were only 0.83 and 0.76.

Table 12.10 Adsorption capacity for dichloromethane in a mixture containing benzene

Adsorbent	N_A (mmol)	q (mmol g^{-1})	q' (mmol ml^{-1})	q_{mix}/q_{single}
MCM-EE	0.60	0.75	0.46	0.86
MCM-41	0.79	1.44	0.61	0.76
MCM-EC	0.49	1.31	0.38	0.83

A very interesting effect observed in the breakthrough curves of dichloromethane with MCM-EE and MCM-EC is their sharp profile in the presence of benzene. As can be seen in Figure 12.9, the concentration downstream the column reaches complete saturation quickly after t_b. When these breakthrough curves are compared with those of benzene in Figure 12.10, a time span can be found where the only VOC detected in significant amounts at the column outlet is dichloromethane. This behavior is relevant for the use of these adsorbents in gas separation applications, since it represents the capacity of these adsorbents to separate a high purity dichloromethane even if the stream intended to be treated contains other organic compounds.

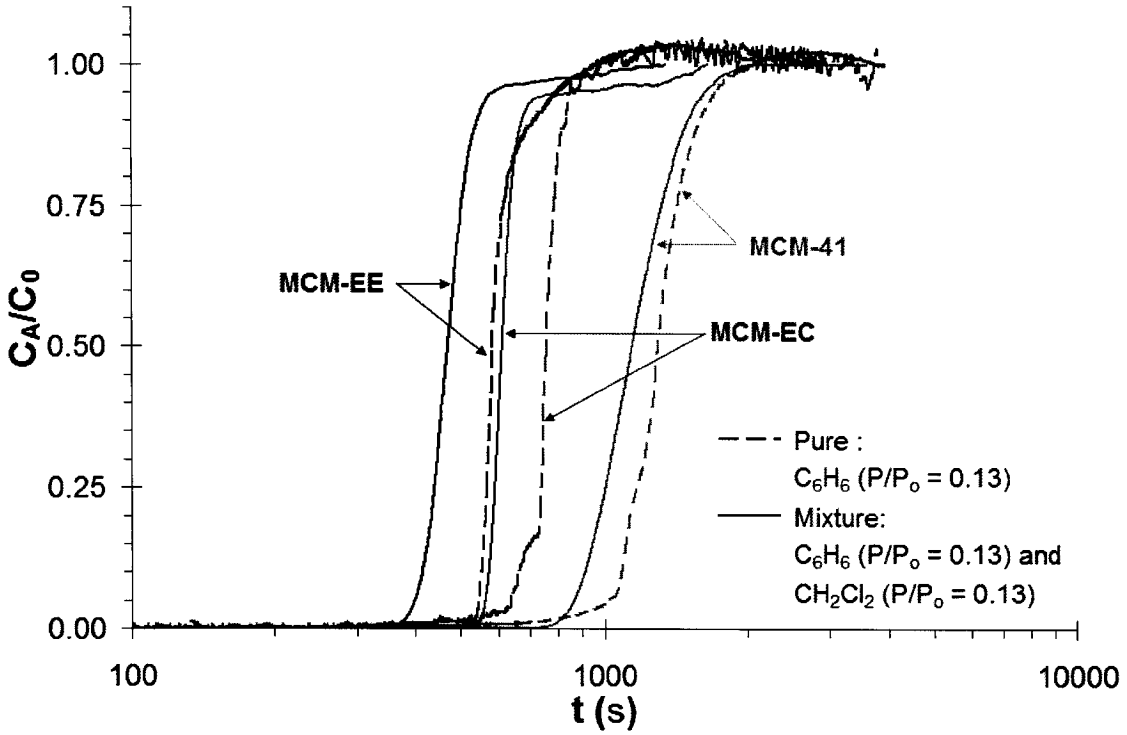

Figure 12.10 Normalized breakthrough curves for benzene as a single component and in a mixture containing dichloromethane

A completely contrary tendency of efficiency is observed with respect to the adsorption of benzene (Figure 12.10). In this case, the breakthrough curves of the purely siliceous materials appeared closer to their corresponding curves for single component adsorption than the hybrid MCM-EE, resulting in a better efficiency as presented in Table 12.11. Particularly, MCM-41 presents the highest efficiency for benzene with up to 89% of the capacity for benzene as a single component (Table 12.11).

These results exhibit the particular selectivity of the different adsorbents studied, corroborating the compatibility of MCM-EE towards halogenated hydrocarbons and MCM-41 towards aromatic compounds. They also suggest the existence of particular sites for the adsorption of chlorinated and aromatic hydrocarbons. This can be stated assuming each molecule adsorbed occupies one available site; hence the total amount of

adsorption sites (i.e. N_{TOT} of benzene plus N_{TOT} of dichloromethane) in the mixture of two organic compounds is higher than the molecules adsorbed during experiments with a single VOC. It is also possible that some adsorbate molecules condense inside the pores, acting as solvent for additional molecules of a second VOC in the fluid stream.

Table 12.11 Adsorption capacity for benzene in a mixture containing dichloromethane

Adsorbent	N_A (mmol)	q (mmol g^{-1})	q' (mmol ml^{-1})	q_{mix}/q_{single}
MCM-EE	0.48	0.61	0.37	0.79
MCM-41	1.19	2.15	0.92	0.89
MCM-EC	0.62	1.68	0.48	0.81

12.3.2 Benzene – Toluene Mixture

At first glance, the results presented in Figure 12.11 and Table 12.12 corresponding to the adsorption of benzene in the presence of toluene could appear contradictory to the results of the mixture dichloromethane-benzene, since MCM-EE exhibits an efficiency towards benzene of 83% which is higher than the 77% presented by MCM-EC and the 70% with MCM-41 (Table 12.12). This apparent contradiction however, can be explained by taking in count that benzene is the least hydrophobic of the components in the mixture and that the evidence presented so far suggests a good compatibility of MCM-EE with VOCs of low hydrophobic character.

Table 12.12 Adsorption capacity for benzene in a mixture containing toluene

Adsorbent	N_A (mmol)	q (mmol g^{-1})	q' (mmol ml^{-1})	q_{mix}/q_{single}
MCM-EE	0.51	0.64	0.39	0.83
MCM-41	0.94	1.70	0.73	0.70
MCM-EC	0.60	1.60	0.46	0.77

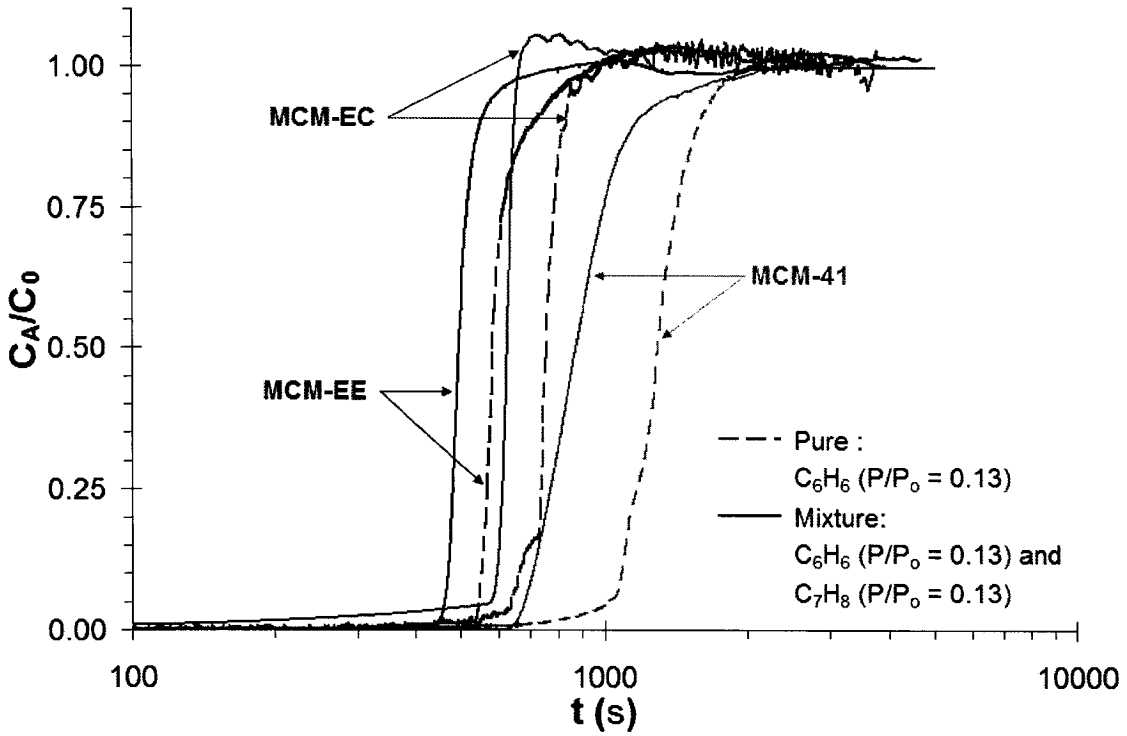

Figure 12.11 Normalized breakthrough curves for benzene as a single component and in a mixture containing toluene

With respect to toluene, a large deviation from the breakthrough curve of a single component can be observed for MCM-EE, as a consequence of its selectivity towards benzene. Opposite to that, the breakthrough curve of MCM-41 shows an earlier t_b but increases at a rate low enough to eventually overlap the curve for adsorption of single component, resulting in a high efficiency of around 86% (Table 12.13).

Table 12.13 Adsorption capacity for toluene in a mixture containing benzene

Adsorbent	N_A (mmol)	q (mmol g^{-1})	q' (mmol ml^{-1})	q_{mix}/q_{single}
MCM-EE	0.17	0.22	0.13	0.62
MCM-41	0.36	0.65	0.28	0.86
MCM-EC	0.23	0.62	0.35	0.70

The results obtained with the different mixtures of organic compounds show a clear compatibility of MCM-EE and the least hydrophobic compound of the mixture. MCM-41 on the other hand presented a better compatibility with the most hydrophobic compounds in all cases. It is interesting to observe that MCM-EC presents intermediate efficiencies between MCM-41 and MCM-EE in all cases, and that for the two-component systems, its efficiency towards the most hydrophobic compound was more similar to MCM-EE than to MCM-41.

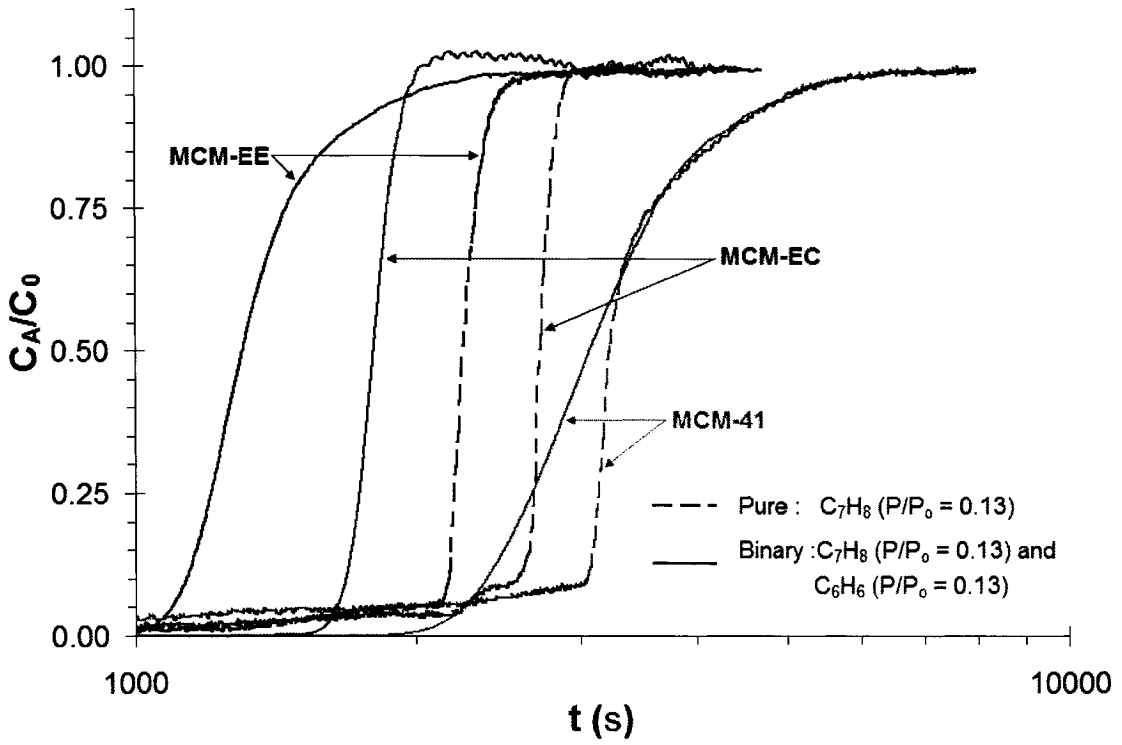

Figure 12.12 Normalized breakthrough curves for toluene as a single component and in a mixture containing benzene

IV. Conclusions

The exceptional characteristics of ordered mesoporous silicas, in particular the MCM-41 type, have made them an important subject of research in recent years. These materials present features that offer a wide range of possibilities in diverse fields like materials science and separation technologies. Both its recent discovery and the possibility to engineer its structural and chemical properties have make necessary the exploration of MCM-41 varieties with different characteristics to gain a better understanding of their performance and determine their suitability for particular applications. For that reason, the present work dealt with the analysis of three different varieties of mesoporous silicas as adsorbents of volatile organic compounds, in order to find an efficient alternative to minimize industrial emissions of air pollutants while studying the advantages offered by MCM-41 silicas.

A highly ordered MCM-41 mesoporous silica was successfully synthesized, and characterized by nitrogen adsorption. The MCM-41 produced was used as adsorbent of representative organic compounds and as parent material for two other varieties of mesoporous silicas. The results obtained via characterization by nitrogen adsorption demonstrate that the hydrothermal post-synthesis treatment of MCM-41 effectively produced a material with expanded pore size and high pore volume (MCM-EC). It showed as well that the selective extraction of the expander agent with ethanol generated a material with large pore size and a relatively low pore volume, attributed to the existence of a surfactant layer attached to the internal silica surface, hence resulting in a hybrid organic-inorganic adsorbent (MCM-EE).

It is interesting to notice that despite the fact that the adsorbents studied were produced from the same mesoporous silica, each of these materials exhibited a very particular adsorptive behavior. The hybrid silica MCM-EE presented characteristics that make it a very good adsorbent for halogenated hydrocarbon. It presented stronger interactions with dichloromethane and chloroform than any other mesoporous silica hereby studied or any other adsorbent previously published, as implied from its high heat of adsorption. In addition, the performance of a column packed with pellets of MCM-EE was better than that of MCM-EC for the adsorption of halocarbons since it presented longer breakthrough times under the same conditions. Another particularly important characteristic offered by MCM-EE is its efficiency in the adsorption of halogenated hydrocarbons in humid environments, as up to 89% of its total adsorption capacity for dichloromethane was retained. This is a very attractive behavior for industrial use since humidity is regularly present in air streams and it is known to affect the performance of popular adsorbents like activated carbon, for example. It was also found that the hybrid silica presented a characteristic selectivity towards the less hydrophobic component in mixtures of VOCs.

It must be acknowledged, however, that MCM-EE presented some disadvantages with respect to the rest of the adsorbents studied in this work. The nitrogen adsorption data revealed a much lower surface area of MCM-EE than the other two mesoporous silica. In addition, a lower mechanical stability is inferred since its structural properties were significantly altered after compression with a force that barely modified the pure siliceous varieties. It is possible that such disadvantages affect directly the availability of active site for adsorption, resulting in the observed lower values of q.

The pore expanded variety MCM-EC presented its own advantages as well. The pulse chromatographic studies revealed high values of $-\Delta H_a$ with aromatic hydrocarbons, an effect attributed to the interaction of silica walls and the unsaturated bond system in the molecules of this type of adsorbates. It is interesting to notice that MCM-EC exhibited stronger interactions vis-à-vis aromatics than MCM-41, even though the surface of this material is constituted in both cases by silica walls. It was also found that MCM-EC presents the highest adsorption capacity at low concentrations for every adsorbate studied, as can be implied from the values of K_p determined. With respect to the results obtained with breakthrough curves, it is worth noticing that the values of q were very similar to those of MCM-41, which may be a consequence of the similar chemical structures in the surface of both adsorbents. Such likeness in capacity, however, have an impact on the performance of a column packed with MCM-EC since, as a consequence of its lower bulk density, the breakthrough curves of MCM-EC appear earlier than with MCM-41 in all cases. These results make a good example of the convenience of each material for particular applications, since they demonstrate that MCM-EC can be a good alternative in purification processes where low concentrations of pollutants are considered, while MCM-41 may be the best choice in separation of streams with higher concentrations.

With respect to efficiency in humid environments it was found that MCM-41 offers the highest efficiency for aromatic hydrocarbons. It is very interesting to notice that MCM-EC presented the same efficiency for the adsorption of halogenated or aromatic hydrocarbons at around 84% of its capacity in dry environments. The results obtained with mixtures of VOCs demonstrated that MCM-41 has a clear selectivity

towards the most hydrophobic compound. Surprisingly, all hydrocarbons presented a more competitive adsorption on MCM-EC, resulting in lower efficiencies for aromatic adsorbates than MCM-41 and halocarbons with respect to MCM-EE. This represents a lower selectivity of MCM-EC towards any particular type of VOC, which may be a consequence of an indiscriminate compatibility with any type of adsorbents, which coincides with the aforementioned results for adsorption in humid streams.

The results with cyclohexane revealed some relevant features regarding the adsorptive behavior of the mesoporous materials. It was demonstrated that, despite the expected non-polar character of the adsorbents, the best efficiency was not necessarily obtained with the most hydrophobic adsorbate. The results of chromatographic analysis presented values of heat of adsorption for cyclohexane similar to that of dichloromethane, a less hydrophobic adsorbate. In addition, the efficiency for the adsorption of cyclohexane in humid environments was significantly lower with all the adsorbents than that of dichloromethane or benzene, and the values obtained of q_{humid}/q were very similar with all the mesoporous silicas.

As can be seen, mesoporous materials offer in general distinct advantages over other adsorbents, even when they are compared with commercially available materials. This represents an extremely relevant success in the search for better and more efficient VOC adsorbents, since the mesoporous silicas can be modified to adjust their properties in order to achieve an enhanced performance for a particular purpose, a feature rarely offered by other adsorbents.

References

A. Adachi, T. Komiyama, T. Tanaka, M. Nakatani, R. Muguruma, T. Okano, "Removal efficiency of defatted seed for organochlorine compounds" J. Health Science, 47, 1 (2001) 1717-1729.

M. Ahmenda, W. E. Marshall, A. A. Husseiny, I. Goktepe, R. M. Rao, "The use of nutshell carbons in drinking water filters for removal of chlorination by-products" J. Chem. Technology and Biotechnology, 79 (2004) 1092-1097.

A. Aizupuru, L. Malhauter, J. C. Roux, J. L. Fanlo, "Biofiltration of a mixture of volatile organic compounds on granular activated carbon" Biotechnology and Bioengineering, 83, 4 (2003) 479-488.

E. Alpay, N. Haq, L. S. Kershenbaum, N. F. Kirkby, "Adsorption parameters for strongly adsorbed hydrocarbon vapours on some commercial adsorbents" Gas Sep. Purif. 10, 1 (1996) 25-33.

M.-M. C. M. Alvim Ferraz, S. Möser, M. Tonhäueser, "Control of atmospheric emissions of volatile organic compounds using impregnated active carbons" Fuel, 78 (1999) 1567-1573.

T. V. Anurova, V. N. Klushin, V. M. Mukhin, V. E. Myshkin, S. A. Anurov, M. A. Suare, "Adsorption of hydrocarbon vapors on activated carbons obtained from vegetable raw materials" Russian J. Applied Chemistry, 77, 5 (2004) 739-744.

R. R. Bansode, J. N. Losso, W. E. Marshall, R. M. Rao, R. J. Portier, "Adsorption of volatile organic compounds by pecan shell- and almond shell-based granular activated carbons" Bioresour. Technol. 90, 2 (2003) 175-184.

I. A. Bardina, N. V. Kovaleva, Y. S. Nikitin, "Physical chemistry of separation processes – Chromatographic retention and the thermodynamic characteristics of adsorption on active carbon" Russ. J. Phys. Chem. 78, 6 (2004) 970-974.

O. Baroja, E. Rodriguez, Z. Gomez de Balguera, A. Goicolea, N. Undeta, C. Sampedro, A. Alonso, R. J. Barrio, "Speciation of volatile aromatic and chlorinated hydrocarbons in urban atmosphere using TCT-GC/MS" J. Env. Sci. Health A, A40, 2 (2005) 343-367.

J. S. Beck, J. C. Vartuli, W. J. Roth, M. E. Leonowicz, C. T. Kresge, K. D. Schmitt, C. T-W Chu, D. H. Olson, E. W. Sheppard, S. B. McCullen, J. B. Higgins, J. L. Schlenker, "A new family of mesoporous molecular sieves prepared with liquid crystal templates" J. Am. Chem. Soc. 144 (1992) 10834-10843.

J. Benkhedda, J. N. Jaubert, D. Barth, L. Perrin, "Experimental and modeled results describing the adsorption of toluene onto activated carbon" J. Chem. Eng. Data, 45, 4 (2001) 650-653.

C. Bilgic¸ A. Askýn, "Evaluation of the thermodynamic parameters for the adsorption of some hydrocarbons on alumina and molecular sieves 3A and 5A by inverse gas chromatography" J. Chromatography A, 1006 (2003) 281-286.

N. Brautbar, J. Williams, "Industrial solvents and liver toxicity: Risk assessment, risk factors and mechanisms" Int. J. Hyg. Environ. Health 205, 6 (2002) 479-491.

R. J. Brennan, R. H. Schiestl, "Chloroform and carbon tetrachloride induce intrachromosomal recombination and oxidative free radicals in Saccharomyces cerevisiae" Mutation Research – Fundamental and Molecular Mechanisms of Mutagenesis, 397, 2 (1998) 271-278.

A. C. Capleton, L. S. Levy, "An overview of occupational benzene exposures and occupational exposure limits in Europe and North America" Chemico-Biological Interactions 153-154 (2005) 43-53.

M. P. Cal, M. J. Rood, S. M. Larson, "Removal of VOCs from humidified gas streams using activated carbon cloth" Gas. Sep. Purif. 10, 2 (1996) 117-121.

C. F. Cheng, W. Zhou, D. H. Park, J. Klinowski, M. Hargreaves, L. F. Gladden, "Controlling the channel diameter of the mesoporous molecular sieve MCM-41" J. Chem. Soc. Faraday Trans. 93, 2 (1997) 359-363.

N. P. Cheremisinoff, "Handbook of Air Pollution Prevention and Control", Elsevier Science, USA (2000).

Y. C. Chiang, P. C. Chiang, E. E. Chang, "Effects of surface characteristics of activated carbons on VOC adsorption" J. Env. Eng. 127, 1 (2001) 54-62.

V. R. Choudhary, K. Mantri, "Adsorption of aromatic hydrocarbons on highly siliceous MCM-41" Langmuir 16 (2000) 7031-7037.

U. Ciesla, F. Schüth, "Ordered Mesoporous Materials" Microporous Mesoporous Mater. 27 (1999) 131-149.

A. Claudino, J. L. Soares, R. F. P. M. Moreira, H. J. Jose, "Adsorption equilibrium and breakthrough analysis for NO adsorption on activated carbons at low temperatures" Carbon 42 (2004) 1483-1490.

B. Clausse, B. Garrot, C. Cornier, C. Paulin, M. H. Simonot-Grange, F. Boutros, "Adsorption of chlorinated volatile organic compounds on hydrophobic faujasite: correlation between the thermodynamic and kinetic properties and the prediction of air cleaning" Microporous Mesoporous Mater. 25 (1998) 169-177.

D. O. Cooney "Adsorption Design for Wastewater Treatment", CRC Press, USA (1999).

A. Corma, Q. Kan, M. T. Navarro, J. Perez-Pariente, F. Rey, "Synthesis of MCM-41 with Different Pore Diameters without Addition of Auxiliary Organics" Chem. Mater. 9 (1997) 2123-2126.

F. Delage, P. Pre, P. LeCloirec, "Mass transfer and warming during adsorption of high concentrations of VOCs on an activated carbon bed: experimental and theoretical analysis" Environ. Sci. Technol. 34 (2000) 4816-4821.

N. de Nevers, "Air Pollution Control Engineering" 2nd Ed. McGraw-Hill, USA (2000).

R. Denoyel, E. Sabio Rey, "Solubilization in Confined Surfactant Mesophases" Langmuir 14 (1998) 7321-7323.

N. M. Djordjevic, R. J. Laub, M. M. Kopecni, S. K. Milonjic, "Adsorption of aliphatic, alicyclic, and aromatic hydrocarbons on poly(ethylvinylbenzene-divinylbenzene) adsorbent from effective zero to finite adsorbate surface coverage" Anal. Chem. 58 (1986) 1395-1404.

D. D. Do, H. D. Do, "Surface diffusion of hydrocarbons in activated carbon: Comparison between constant molar flow, differential permeation and differential adsorption bed methods" Adsorption, 7 (2001) 189-209.

G. Dogu, J. M. Smith, "Rate parameters from dynamic experiments with single catalyst pellets" Chemical Engineering Science, 31 (1976) 123-135.

Environment Canada "Priority Substances List Assessment Report, Benzene", Electronic version available at http://www.hc-sc.gc.ca/ewh-semt/pubs/contaminants/psl1-lsp1/benzene/index_e.html (1993a).

Environment Canada "Priority Substances List Assessment Report, Dichloromethane", Electronic version available at http://www.hc-sc.gc.ca/ewh-semt/pubs/contaminants/psl1-lsp1/dichloromethane/index_e.html (1993b).

Environment Canada "Priority Substances List Assessment Report, Toluene", Electronic version available at http://www.hc-sc.gc.ca/ewh-semt/pubs/contaminants/psl1-lsp1/toluene/index_e.html (1993c).

Environment Canada "Canadian Environmental Protection Act, 1999" Electronic version available at http://laws.justice.gc.ca/en/C-15.31/text.html (1999).

Environment Canada "Priority Substances List Assessment Report, Chloroform", electronic version available at http://www.hc-sc.gc.ca/ewh-semt/pubs/contaminants/psl2-lsp2/chloroform/index_e.html (2000).

R. Florida, "Lean and green: the move to environmentally conscious manufacturing", California Management Review, 39, 1 (1996) 80-105.

B. Garrod, P. Chadwick, "Environmental management and business strategy: towards a new strategic paradigm", Futures, 28, 1 (1996) 37-50.

P. A. Gauden, A. P. Terzyk, G. Rychlicki, P. Kowalczyk, M. S. Cwiertnia, J. K. Garbacz, "Estimating the pore size distribution of activated carbons from adsorption data of different adsorbates by various methods" J. Colloid. Interface Sci. 273, 1 (2004) 39-63.

A. Giaya, R. W. Thompson, "Liquid and vapor phase adsorption of chlorinated volatile organic compounds on hydrophobic molecular sieves" Microporous Mesoporous Mater. 40 (2000) 205-218.

T. Godish "Air Quality" 4th Ed. CRC Press, USA (2004).

M. C. Gomez, N. Durana, M. Navazo, L. Alonso, J. A. Garcia, J. L. Ilaroya, "Application of validation data tests from an on-line volatile organic compound analyser to the detection of air pollution episodes in urban areas" Analytica Chimica Acta, 524 (2004) 41-49.

H. Guo, T. Wang, I. J. Simpson, D. R. Blake, X. M. Yu, Y. H. Kwok, Y. S. Li, "Source contributions to ambient VOCs and CO at a rural site in eastern China" Atmospheric Environment, 38 (2004) 4551-4560.

K. B. Gurevich, T. M. Roschina, N. K. Shoniya, L. M. Kustov, A. V. Ivanov, "Peculiarities of adsorption of organic compounds and water on silicas with bonded polyfluoroalkyl groups" J. Colloid. Interface Sci. 254, 1 (2002) 39-48.

K. Hanna, I. Beurroies, R. Denoyel, D. Desplantier-Giscard, A. Galarneau, F. Di Renzo, "Sorption of Hydrophobic Molecules by Organic/Inorganic Mesostructures" J. Colloid. Interface Sci. 252 (2002) 276-283.

P. J. E. Harlick, F. H. Tezel, "Adsorption of carbon dioxide, methane and nitrogen: pure and binary mixture adsorption for ZSM-5 with SiO_2/Al_2O_3 ratio of 280" Sep. Purif. Technol. 33 (2003) 199-210.

M. Hartmann, C. Bischof, "Mechanical stability of mesoporous molecular sieve MCM-48 studied by adsorption of benzene, *n*-heptane and cyclohexane" J. Phys. Chem. B, 103 (1999) 6230-6235.

R. J. Heinsohn, R. L. Kabel "Sources and Control of Air Pollution", Prentice Hall, USA (1999).

X. Hu, S. Qiao, X. S. Zhao, G. Q. Li, "Adsorption study of benzene in ink-bottle-like MCM-41" Ind. Eng. Chem. Res. 40 (2001) 862-867.

J. R. Hufton, D. M. Ruthven, R. P. Danner, "Adsorption and diffusion of hydrocarbons in silicate at very low concentration: effect of defect sites" Microporous Mater. 5 (1995) 39-52.

P. Hunter, S. T. Oyama "Control of Volatile Organic Compound Emissions: Conventional and Emerging Technologies", Wiley Interscience, USA (2000).

O. Inel, D. Topaloglu, A. Askin, F. Yumsek, "Evaluation of the thermodynamic parameters for the adsorption of some hydrocarbons on 4A and 13 X zeolites by inverse gas chromatography" Chem. Eng. J. 88 (2002) 255-262.

S. K. Jana, R. Nishida, K. Shindo, T. Kugita, S. Namba, "Pore size control of mesoporous molecular sieves using different organic auxiliary chemicals" Microporous Mesoporous Mater. 68 (2004) 133-142.

J. Jänchen, H. Stach, L. Uytterhoeven, W. J. Mortier, "Influence of the framework density and the effective electronegativity of silica and aluminophosphate molecular sieves on the heat of adsorption of nonpolar molecules" J. Phys. Chem. 100 (1996) 12484-12493.

B. T. Jobson, C. M. Berkowitz, W. C. Kuster, P. D. Goldan, E. J. Williams, F. C. Fesenfeld, E. C. Apel, T. Karl, W. A. Lonneman, D. Riemer, "Hydrocarbon source signatures in Houston, Texas: Influence of the petrochemical industry" J. Geophysical Research D, 109 D24 (2004) D24305.

F. I. Khan, A. K. Ghoshal, "Removal of volatile organic compounds from polluted air", J. Loss Preven. Process Ind. 13 (2000) 527-545.

E. Klumpp, C. Contreras-Ortega, P. Klahre, F. J. Tino, S. Yapar, C. Portillo, S. Stegen, F. Quierolo, M. J. Schwuger, "Sorption of 2,4-dichlorophenol on modified hydrotalcites" Colloids and Surfaces A 230 (2004) 116-126.

C. A. Koh, R. E. Westacott, R. I. Nooney, V. Boissel, S. Tamir, V. Tricarico, "Separation of dichloromethane-nitrogen mixtures by adsorption: experimental and molecular simulation studies" Molecular Physics 100, 13 (2002) 2057-2095.

O. A. Kolyadina, Y. I. Murirov, M. G. Voronkov, Y. N. Pozhidaev, "Thermodynamic characteristics of hydrocarbon and chloroalkane adsorption by polymethylsilsesquioxane" Russ. Chem. Bulletin Int. Ed. 49, 12 (2000) 2000-2002.

T. Kopac, G. Dogu, T. Dogu, "Single pellet reactor for the dynamic analysis of gas-solid reactions: reaction of SO_2 with activated soda" Chem. Eng. Sci. 51, 10 (1996) 2201-2209.

C. T. Kresge, M. E. Leonowicz, W. J. Roth, J. C. Vartuli, J. S. Beck, "Ordered mesoporous molecular sieves synthesized by a liquid-crystal template mechanism" Nature, 359 (1992) 710-712.

M. Kruk, M. Jaroniec, A, Sayari, "Application of large pore MCM-41 molecular sieves to improve pore size analysis using nitrogen adsorption measurements" Langmuir 13 (1997) 6267-6273.

M. Kruk, M. Jaroniec, A. Sayari, "New insights into pore-size expansion of mesoporous silicates using long-chain amines" Microporous Mesoporous Mater. 35-36 (2000) 545-553.

M. Kruk, M. Jaroniec, "Characterization of modified mesoporous silicas using argon and nitrogen adsorption" Microporous Mesoporous Mat. 44-45 (2001) 725-732.

M. Kruk, M. Jaroniec, V. Antochshuk, A. Sayari, "Mesoporous silicate-surfactant composites with hydrophobic surfaces and tailored pore sizes" J. Phys. Chem. B 106 (2002) 10096-10101.

J. H. C. M. Lammers, J. van Asperen, D. de Groot, W. R. P. Rijcken, "Behavioral effects and kinetics in brain in response to inhalation of constant or fluctuating toluene concentrations in the rat" Environmental Toxicology and Pharmacology, 19, 3 (2005) 625-634.

N. Lang, A. Tuel, "A fast and efficient ion-exchange procedure to remove surfactant molecules from MCM-41 materials" Chem. Mater. 16 (2004) 1961-1966.

A. Latella, G. Stani, L. Cobelli, M. Duane, K. Junninen, C. Astorga, B. R. Larsen, "Semicontinuous GC analysis and receptor modelling for source apportionment of ozone precursor hydrocarbons in Bresso, Milan, 2003" J. Chromatography A, 1071 (2005) 29-39.

C. H. Lao, I. M. Chen, Y. F. Chang, M. C. Lu, "Removal of trichloromethane and trichloroethylene by suspended zero valent iron and ultraviolet radiation" J. Environmental Science and Health A, A38, 9 (2003) 1717-1729.

J. G. Leahy, T. E. Carrington, M. H. Eley, "Analysis of volatile and semivolatile hydrocarbons recovered from steam-classified municipal solid waste" J. Environmental Quality 33, 4 (2004) 1556-1561.

J. W. Lee, H. J. Jung, D. H. Kwak, P. G. Chung, "Adsorption of dichloromethane from water onto a hydrophobic polymer resin XAD-1600" Water Res. 39 (2005) 617-629.

S. Y. Lee, S. J. Kim, S. Y. Chung, C. H. Jeong, "Sorption of hydrophobic organic compounds onto organoclays" Chemosphere 55 (2004) 781-785.

W. Lei, R. Zhang, X. Tie, P. Hess, "Chemical characterization of ozone formation in the Houston-Galveston area: A chemical transport model study" J. Geophysical Research D, 109, D12 (2004) D12301.

M. A. Lillo-Rodenas, J. Carratala-Abril, D. Cazorla-Amoros, A. Linares-Solano, "Usefulness of chemically activated anthracite for the abatement of VOC at low concentrations" Fuel Process. Technol. 77-78 (2002) 331-336.

H. P. Lin, Y. R. Cheng, S. B. Liu, C. Y. Mou, "The effect of alkan-1-ols addition on the structural ordering and morphology of mesoporous silicate MCM-41" J. Mater. Chem. 9, 5 (1999) 1197-1202.

T. J. Lopes, D. A. Bender, "Nonpoint sources of volatile organic compounds in urban areas--relative importance of land surfaces and air" Environmental Pollution 101, 2 (1998) 221-230.

M. Lordgooei, M. S. Kim, "Modeling volatile organic compound sorption in activated carbon. I: Dynamics and single-component equilibrium" J. Env. Eng. 130, 3 (2004) 212-222.

M. Luechinger, G. D. Pirngruber, B. Lindlar, P. Laggner, R. Prins "The effect of the hydrophobicity of aromatic swelling agents on pore size and shape of mesoporous silicas" Microporous Mesoporous Mater. 19 (2005) 41-25.

C. N. Madu, C. Kuei, P. Winokur, "Environmental quality planning: A strategic total quality management (STQM) approach", Futures, 27, 8 (1995) 834-856.

J. Mather, D. Banks, S. Dumpleton, M. Fermor "Groundwater Contamination" The Geological Society, Great Britain (1998).

A. McCulloch, M. L. Aucott, T. E. Graedel, G. Kleiman, P. M. Midgley, Y. F. Li, "Industrial emissions of trichloroethene, tetrachloroethene, and dichloromethane: reactive chlorine emissions inventory" J. Geophysical Res. D 104, D7 (1999) 8417-8427.

Y. Miyake, T. Yumoto, H. Kitamura, T. Sugimoto, "Solubilization of organic compounds into as-synthesized spherical mesoporous silica" Phys. Chem. Chem. Phys. 4 (2002) 2680-2684.

M. Molina-Sabio, F. Rodriguez-Reinoso, F. Cartula, M. J. Selles, "Development of porosity in combined phosphoric acid-carbon dioxide activation" Carbon, 34, 4 (1996) 457-462.

C. S. Moon, J. T. Lee, J. H. Chun, M. Ikeda, "Use of solvents in industries in Korea: experience in Sinpyeong-Jangrim industrial complex" Int. Arch. Occup. Environ. Health 74, 2 (2001) 148-152.

C. Moreno-Castilla, F. Carrasco-Marin, M. V. Lopez-Ramon, "Micropore Structure of Activated Carbons Prepared From a Spanish Subbituminous Coal Studied by CO2, Benzene, and Cyclohexane Adsorption" Langmuir 11 (1995) 247-252.

K. Morishige, Y. Nakamura, "Nature of adsorption and desorption branches in cylindrical pores" Langmuir 20 (2004) 4503-4506.

J. C. Mycock, J. D. McKenna, L. Theodore "Handbook of Air Pollution Control Engineering and Technology", CRC Press, USA (1995).

B. S. Nielsen, H. R. Lam, O. Ladefoged, "Developmental neurotoxicity of toluene in rats as measured by l-ornithine decarboxylase in cerebellum" Pharmacology Toxicology 92 (2003) 51-54.

J. Nokerman, X. Canet, P. Mougin, S. Limborg-Noetinger, M. Frère "Comparative study of the dynamic gravimetric and pulse chromatographic methods for the determination of Henry constants of adsorption for VOC-zeolite systems" Meas. Sci. Technol. 16 (2005) 1802-1812.

C. Ooka, H. Yoshida, K. Suzuki, T. Hattori, "Effect of surface hydrophobicity of TiO_2-pillared clay on adsorption and photocatalysis of gaseous molecules in air" Appl. Catal. A, 260 (2004) 47-53.

J. W. Park, S. S. Lee, D. K. Choi, Y. W. Lee, Y. M. Kim, "Adsorption equilibria of toluene, dichloromethane and trichloroethylene onto activated carbon fiber" J. Chem. Eng. Data 47 (2002) 980-983.

R. H. Perry, D. W. Green, "Chemical Engineer's Handbook" 7^{th} ed. McGraw-Hill, USA (1997).

J. Pires, A. Carvalho, M. B. de Carvalho, "Adsorption of volatile organic compounds in Y zeolites and pillared clays" Microporous Mesoporous Mater. 43 (2001) 277-287.

P. Pre, F. Delage, P. Le Cloirec, "A Model to Predict the Adsorber Thermal Behavior during Treatment of Volatile Organic Compounds onto Wet Activated Carbon" Environ. Sci. Technol. 36 (2002) 4681-4688.

S. Qi, K. J. Hay, M. P. Cal, "Predicting humidity effect on adsorption capacity of activated carbon for water-immiscible organic vapors" Advances in Environmental Research 4 (2000) 357-362.

S. Z. Qiao, S. K. Bhatia, D. Nicholson, "Study of hexane adsorption in nanoporous MCM-41 silica" Langmuir 20, (2004) 389-395.

N. K. Raman, M. T. Anderson, C. J. Brinker, "Template-based approaches to the preparation of amorphous, nanoporous silicas" Chem. Mater. 8, 8 (1996) 1682-1701.

D. Redalieu "Handbook of Air Pollution Control Engineering and Technology" Chapter 2, J. C. Mycock, J. D. McKenna, L. Theodore, Editors, CRC Press, USA (1995).

C. R. Reid, K. M. Thomas, J. Phys. Chem. B, "Adsorption kinetics and size exclusion properties of probe molecules for the selective porosity in a carbon molecular sieve used for air separation" 105 (2001) 10619-10629.

M. M. L. Ribeiro Carrot, A. J. E. Candeias, P. J. M. Carrot, P. I. Ravikovitch, A. V. Neimark, A. D. Sequeira, "Adsorption of nitrogen, neopentane, n-hexane, benzene and

methanol for the evaluation of pore sizes in silica grades of MCM-41" Microporous Mesoporous Mater. 47 (2001) 323-337.

L. G. Roberts, A. C. Bevans, C. H. Schreiner, "Developmental and reproductive toxicity evaluation of toluene vapor in the rat: I. Reproductive toxicity" Reproductive Toxicology, 17, 6 (2003) 649-658.

E. N. Ruddy, L. N. Carrol, "Select the best VOC control strategy" Chem. Eng. Prog, 89, 7 (1993) 28.

D. M. Ruthven, R. Kumar, "An experimental study of single-component and binary adsorption equilibria by a chromatographic method" Ind. Eng. Chem. Fundam. 19 (1980) 27-32.

M. D. Ruthven "Principles of Adsorption and Adsorption Processes", John Wiley and Sons, U. S. A. (1984).

F de Santis, A. Fino, S. Menichelli, C. Vazzana, I. Allegrini, "Monitoring the air quality around an oil refinery through the use of diffusive sampling" Anal. Bioanal. Chem. 378 (2004) 782-788.

A. Sayari, P. Liu, M. Kruk, M. Jaroniec, "Characterization of large-pore MCM-41 molecular sieves obtained via hydrothermal restructuring" Chem. Mater. 9 (1997) 2499-2506.

A. Sayari, M. Kruk, M. Jaroniec, I. L. Moudrakovski, "New approaches to pore size engineering of mesoporous silicates' Adv. Mater. 10, 16 (1998) 1376-1379.

A. Sayari, Y. Yang, M. Kruk, M. Jaroniec, "Expanding the pore size of MCM-41 silicas: use of amines as expanders in direct Síntesis and postsynthesis procedures" J. Phys. Chem. B. 103 (1999) 3651-3658.

A. Sayari, S. Hamoudi, Y. Yang, I. L. Moudrakovski, J. R. Ripmeester, "New insights into the synthesis, morphology, and growth of periodic mesoporous organosilicas" Chem. Mater. 12 (2000a) 3857-3863.

A. Sayari, Y. Yang, "Highly ordered MCM-41 silica prepared in the presence of decyltrimethylammonium bromide" J. Phys. Chem. B 104 (2000b) 4835-4839.

A. Sayari, S. Hamoudi, "Periodic mesoporous silica-based organic-inorganic nanocomposite materials" Chem. Mater. 13 (2001) 3151-3168.

A. Sayari, S. Hamoudi, Y. Yang, "Applications of pore-expanded mesoporous silica. 1. Removal of heavy metal cations and organic pollutants from wastewater" Chem. Mater. 17, (2005) 212.

P. Schneider, J. M. Smith, "Adsorption Rate Constants from Chromatography" AIChE J. 14, 5 (1968) 762-771.

P. Selvam, S. K. Bhatia, C. G. Sonwane, "Recent advances in processing and characterization of periodic mesoporous MCM-41 silicate molecular sieves" Ind. Eng. Chem. Res. 40 (2001) 3237-3261.

D. P. Serrano, G. Calleja, J. A. Botas, F. J. Gutierrez, "Adsorption and hydrophobic properties of mesostructured MCM-41 and SBA-15 materials for volatile organic compound removal" Ind. Eng. Chem. Res. 43 (2004) 7010-7018.

N. Sonoyama, K. Ezaki, T. Sakata, "Continuous electrochemical decomposition of dichloromethane in aqueous solution using various column electrodes" Adv. Env. Res. 6 (2001) 1-8.

A. Stein, B. J. Melde, R. C. Schroden, "Hybrid inorganic-organic mesoporous silicates – nanoscopic reactors coming of age" Adv. Mater. 12, 19 (2000) 1403-1418.

P. T. Tanev, T. J. Pinnavaia, "Mesoporous silica molecular sieves prepared by ionic and neutral surfactant templating: A comparison of physical properties" Chem. Mater. 8, 8 (1996) 2068-2079.

G. Theyel, "Management practices for environmental innovation and performance", Int. J. Operations Product. Manag. 20, 2 (2000) 249-266.

J. M. Thomas, W. J. Thomas, "Principles and Practice of Heterogeneous Catalysis" VCH, Germany (1997).

W. J. Thomas, B. Chrittenden, "Adsorption Technology and Design" Butterworth-Heinemann, Great Britain (1998).

USEPA, "Clean Air Act Amendments of 1990, Detailed Summary of Titles", U. S. Environmental Protection Agency, USA (1990).

USEPA "Clean Air Act 1990" Electronic Resource available at www.epa.gov/oar/caa, (1990).

N. Uzun, Y. Kendirli, "Clinical, socio-demographic, neurophysiological and neuropsychiatric evaluation of children with volatile substance addiction" Child: Care Health and Development 31, 4 (2005) 425-432.

J. C. Vartuli, A. Malek, W. J. Roth, C. T. Kresge, S. B. McCullen, "The sorption properties of as-synthesized and calcined MCM-41 and MCM-48" Microporous Mesoporous Mater. 44-45 (2001) 691-695.

L. Wei, T. Tang, B. Huang, "Novel acidic porous clay heterostrucure with highly ordered organic-inorganic hybrid structure: one-pot snthesis of mesoporous organosilica in the galleries of clay" Microporous Mesoporous Mater. 67 (2004) 175-179.

B. A. Wofford, M. W. Jackson, C. Hartz, J. W. Bevan, "Surface wave plasma abatement of CHF_3 and CF_4 containing semiconductor process" Environ. Sci. Technol. 33 (1999) 1892-1897.

J. Wu, M. M. Abu-Omar, S. H. Tolbert, "Fluorescent probes of the molecular environment within mesostructured silica/surfactant composites under high pressure" Nano Lett. 1 (2001) 27-31.

D. Yaron-Marcovich, S. Nir, Y. Chen, "Fluoridone adsorption-desorption on organo-clays" Appl. Clay Sci. 24 (2004) 167-175.

C. L. Yaws, "Chemical Properties Handbook", McGraw-Hill, USA (1999).

P. E. Yu-Chin Chiang, P. E. Pen-Chi Chiang, E. E. Chang, "Effects of surface characteristics of activated carbons on VOC adsorption" J. Env. Eng. 127, 1 (2001) 54-62.

J. H. Yun, D. K. Choi, S. H. Kim, "Adsorption of organic solvent vapors on hydrophobic Y-type zeolie" AIChE J. 44, (1998) 1344-1350.

J. H. Yun, D. K. Choi, S. H. Kim, "Equilibria and dynamics for mixed vapors of BTX in an activated carbon bed" AIChE J. 45 (1999) 751-760.

J. H. Yun, J. Chem. Eng. Data, "Equilibrium isotherms of dichloromethane, trichloroethylene and 1, 1, 1-trichloroethane on activated carbon fiber" 46 (2001) 156-159.

H. Zhao, K. L. Nagy, J. S. Waples, G. F. Vance "Surfactant-Templated Mesoporous Slicate Materials as Sorbents for Organic Pollutants in Water" Environ. Sci. Technol. 34 (2000) 4822-4827.

H. Zhao, K. L. Nagy, "Dodecyl sulfate-hydrotalcite nanocomposites for trapping chlorinated organic pollutants in water" J. Colloid. Int. Sci. 274 (2004) 613-624.

X. S. Zhao, Q. Ma, G. Q. Lu, "VOC removal: comparison of MCM-41 with hydrophobic zeolites and activated Carbon" Energy Fuels, 12 (1998) 1051-1054.

X. S. Zhao, G. Q. Lu, X. Hu, "Organophilicity of MCM-41 adsorbents studied by adsorption and temperature-programmed desorption" Colloid. Surf. A 179 (2001) 261-269.

J. Zhu, R. Newhook, L. Marro, C. C. Chan, "Selected volatile organic compounds in residential air in the City of Ottawa, Canada" Environ. Sci. Technol. 39, 11 (2005) 3964-3971.

Appendix A. Nitrogen adsorption characterization results

MCM-41

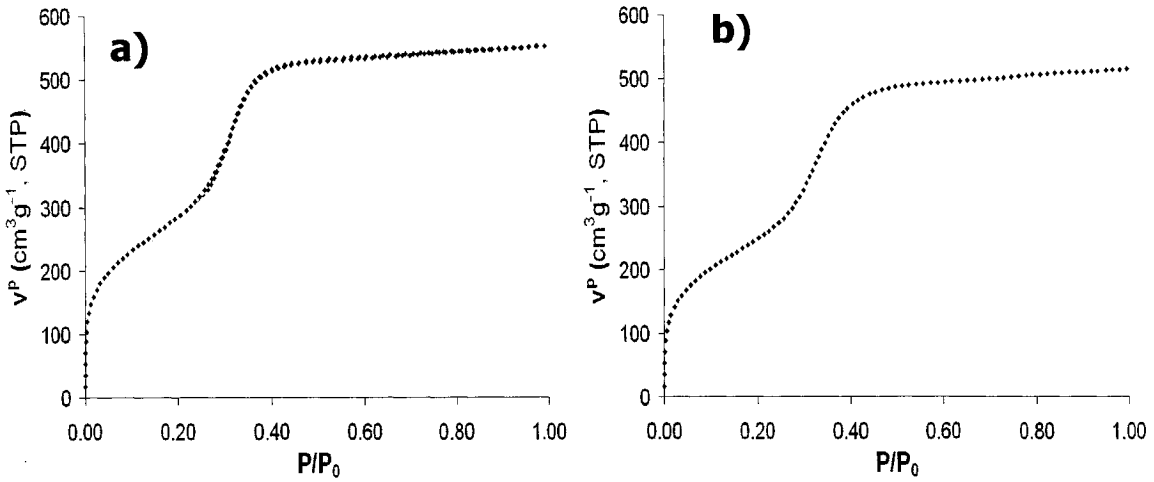

Nitrogen adsorption-desorption isotherms of MCM-41 a) before and b) after pelletization

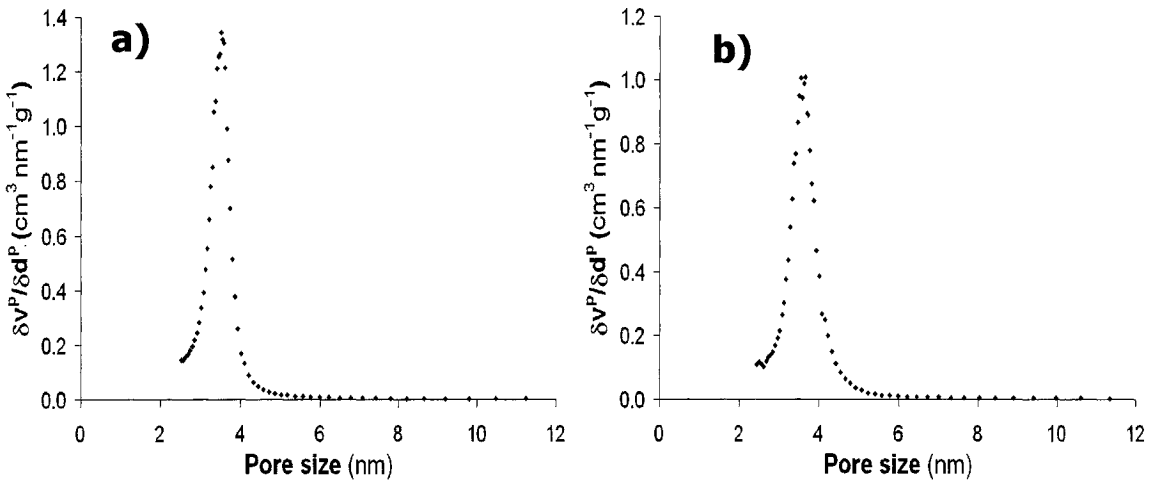

Pore size distribution of MCM-41 as a) powder and b) pellets

	a) Powder	b) Pellets
Surface area ($m^2\,g^{-1}$)	1086	940
Pore volume ($cm^3\,g^{-1}$)	0.86	0.81
Mean pore size (nm)	3.53	3.62

MCM-EC

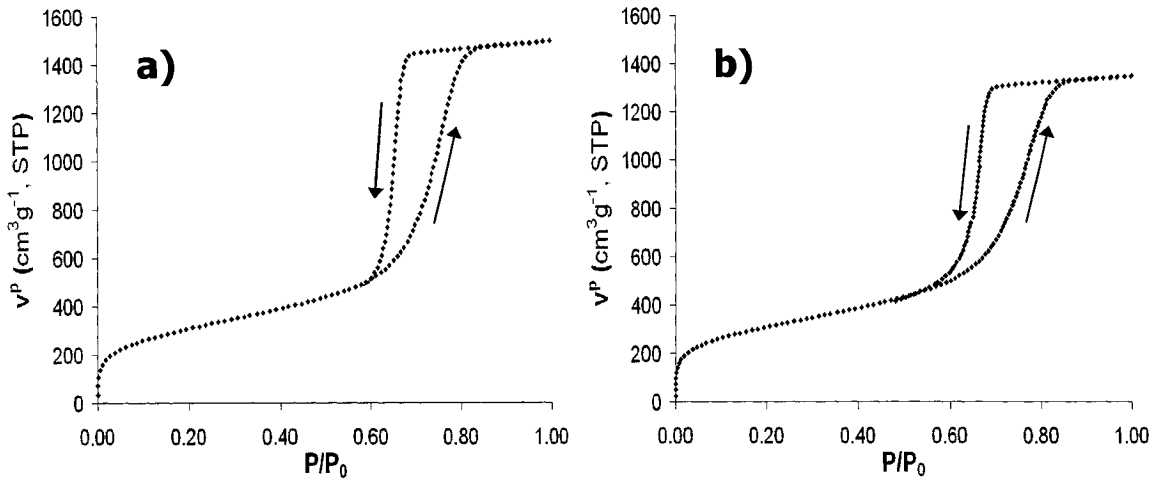

Nitrogen adsorption-desorption isotherms of MCM-EC a) before and b) after pelletization

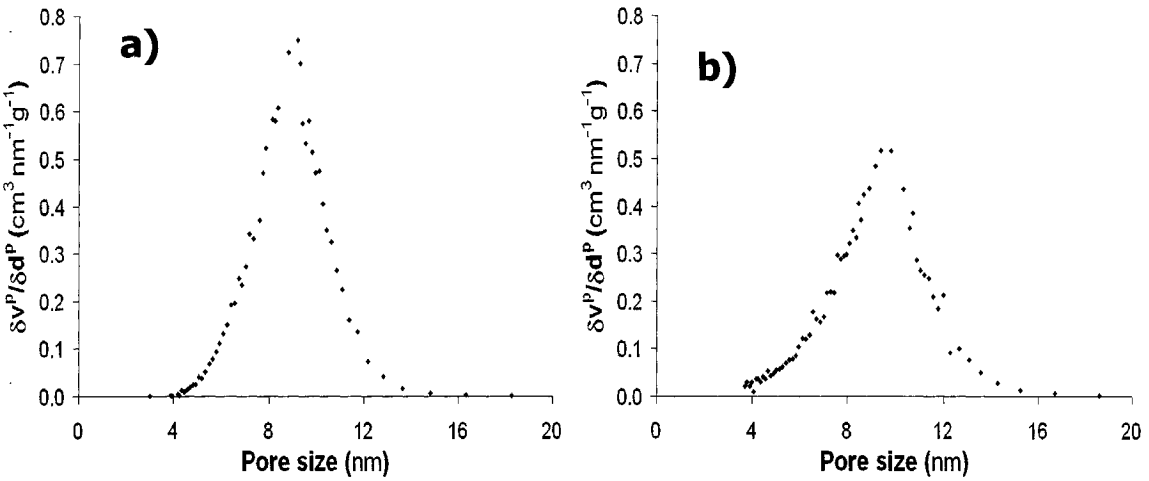

Pore size distribution of MCM-EC as a) powder and b) pellets

	a) Powder	b) Pellets
Surface area ($m^2 g^{-1}$)	1119	1129
Pore volume ($cm^3 g^{-1}$)	2.35	2.11
Mean pore size (nm)	9.18	9.62

MCM-EE

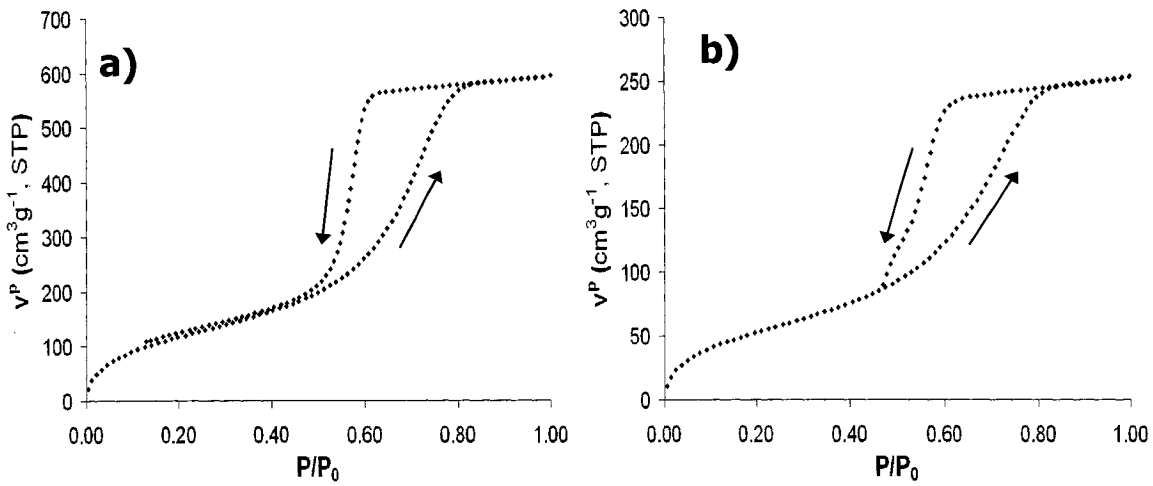

Nitrogen adsorption-desorption isotherms of MCM-EE a) before and b) after pelletization

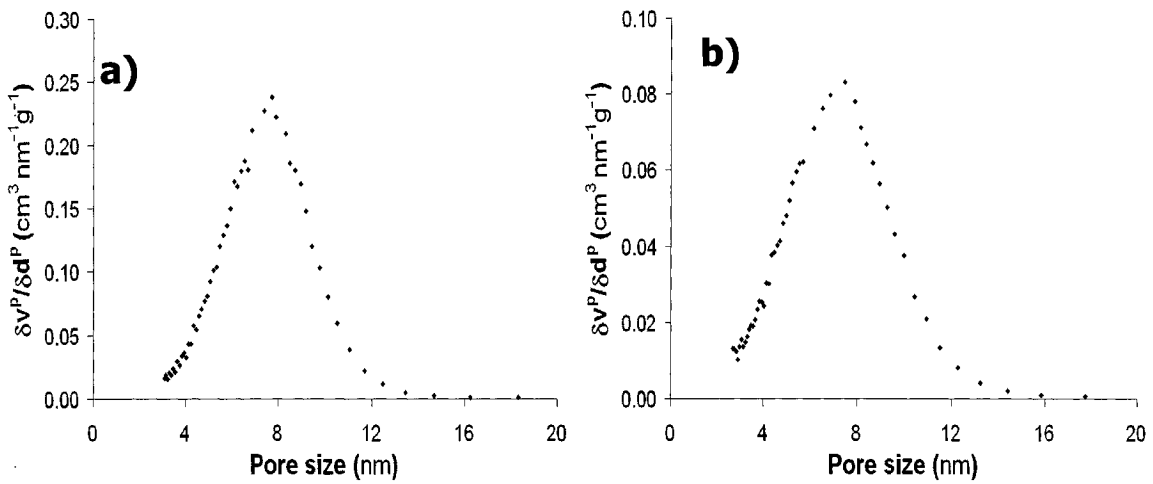

Pore size distribution of MCM-EE as a) powder and b) pellets

	a) Powder	b) Pellets
Surface area (m^2 g^{-1})	379	208
Pore volume (cm^3 g^{-1})	0.83	0.40
Mean pore size (nm)	7.74	7.10

Appendix B. Concentration profiles obtained from pulse chromatographic experiments

Dichloromethane

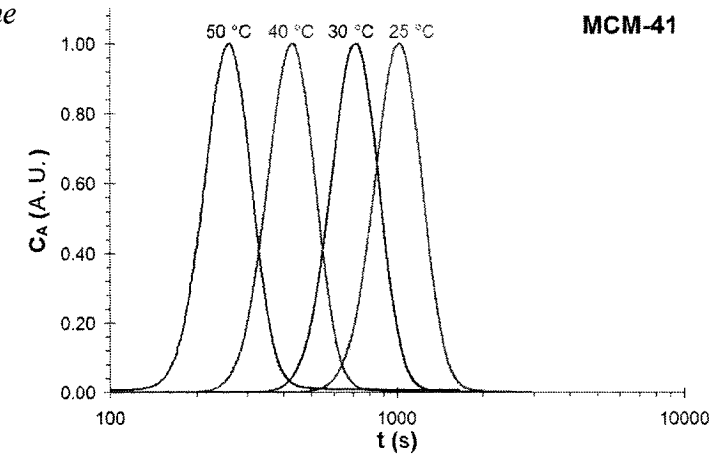

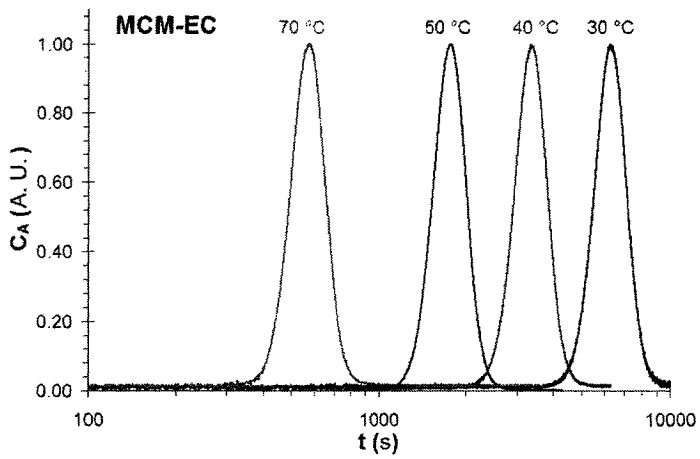

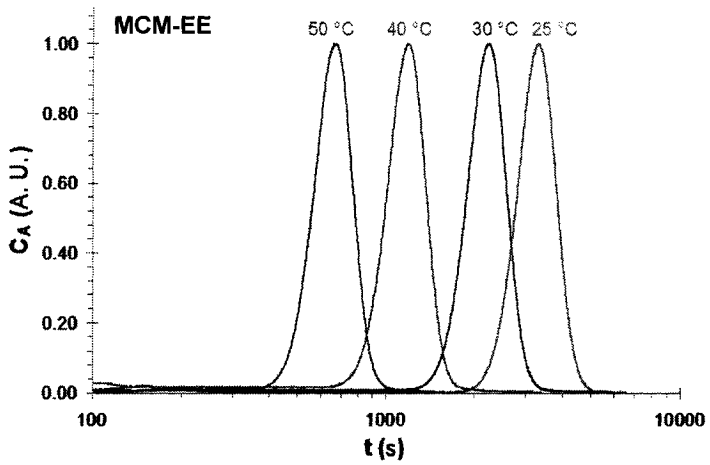

Chloroform

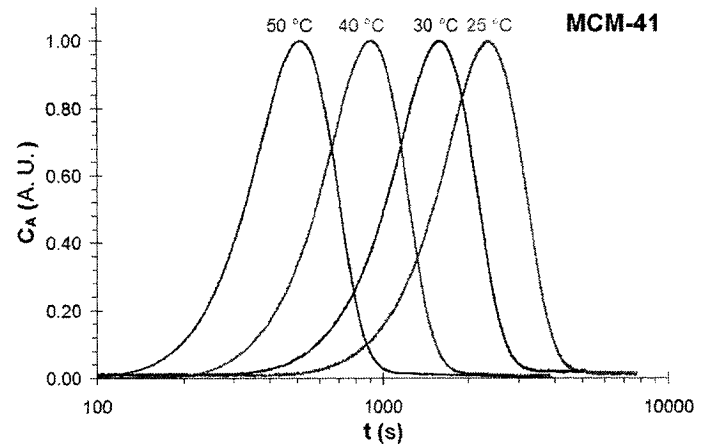
MCM-41
50 °C
40 °C
30 °C
25 °C
1.00
0.80
0.60
0.40
0.20
0.00
C_A (A. U.)
100
1000
10000
t (s)

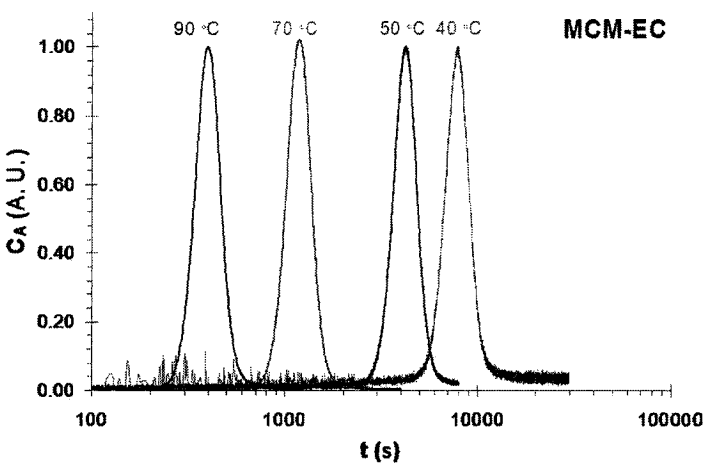
MCM-EC
90 °C
70 °C
50 °C
40 °C
1.00
0.80
0.60
0.40
0.20
0.00
C_A (A. U.)
100
1000
10000
100000
t (s)

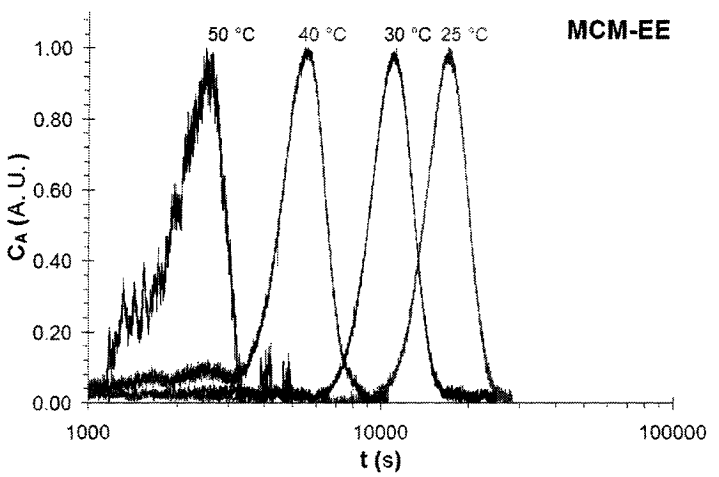
MCM-EE
50 °C
40 °C
30 °C
25 °C
1.00
0.80
0.60
0.40
0.20
0.00
C_A (A. U.)
1000
10000
100000
t (s)

Benzene

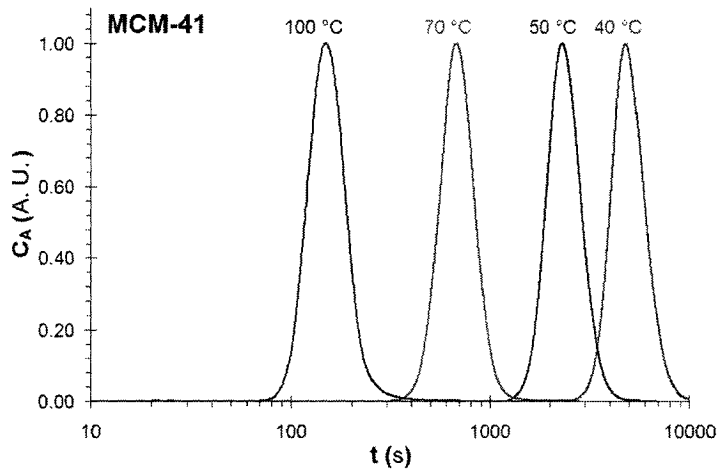
MCM-41
100 °C
70 °C
50 °C
40 °C
1.00
0.80
0.60
0.40
0.20
0.00
C_A (A.U.)
10
100
1000
10000
t (s)

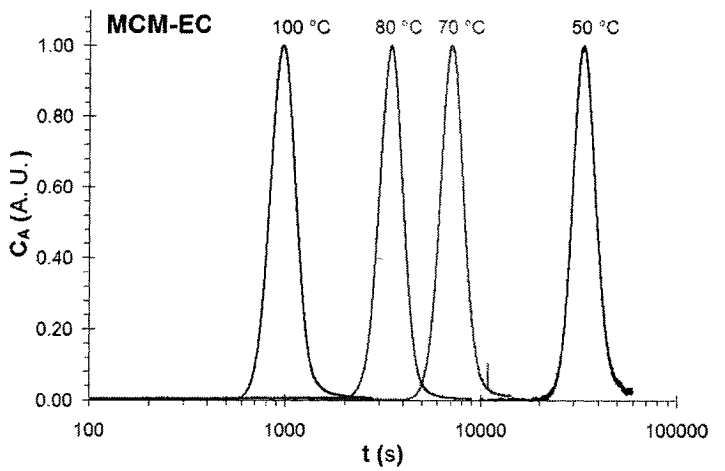
MCM-EC
100 °C
80 °C
70 °C
50 °C
1.00
0.80
0.60
0.40
0.20
0.00
C_A (A.U.)
100
1000
10000
100000
t (s)

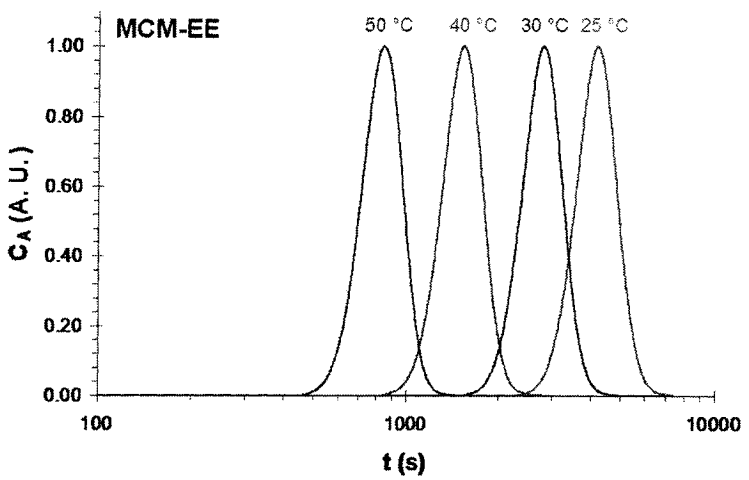
MCM-EE
50 °C
40 °C
30 °C
25 °C
1.00
0.80
0.60
0.40
0.20
0.00
C_A (A.U.)
100
1000
10000
t (s)

Toluene

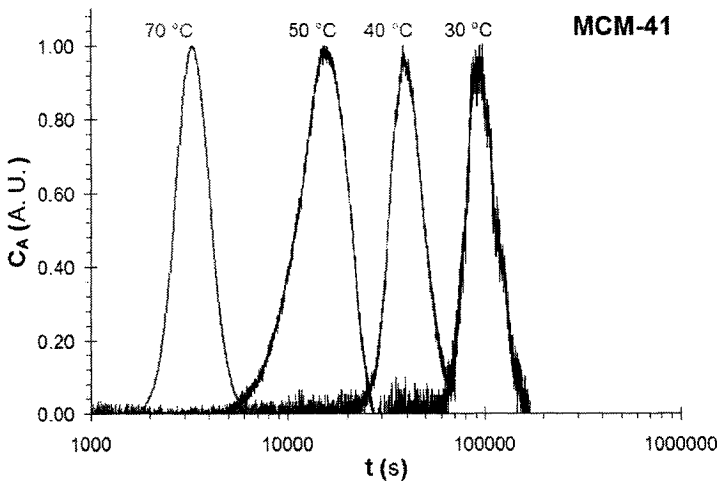
MCM-41
70 °C
50 °C
40 °C
30 °C
1.00
0.80
0.60
0.40
0.20
0.00
C_A (A. U.)
1000
10000
100000
1000000
t (s)

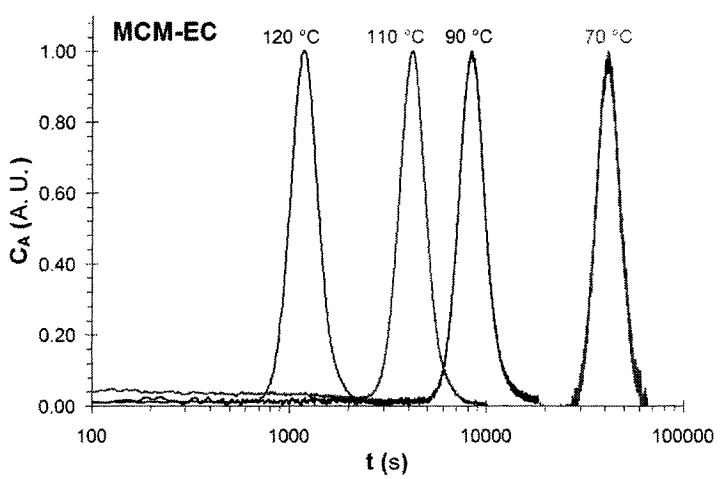
MCM-EC
120 °C
110 °C
90 °C
70 °C
1.00
0.80
0.60
0.40
0.20
0.00
C_A (A. U.)
100
1000
10000
100000
t (s)

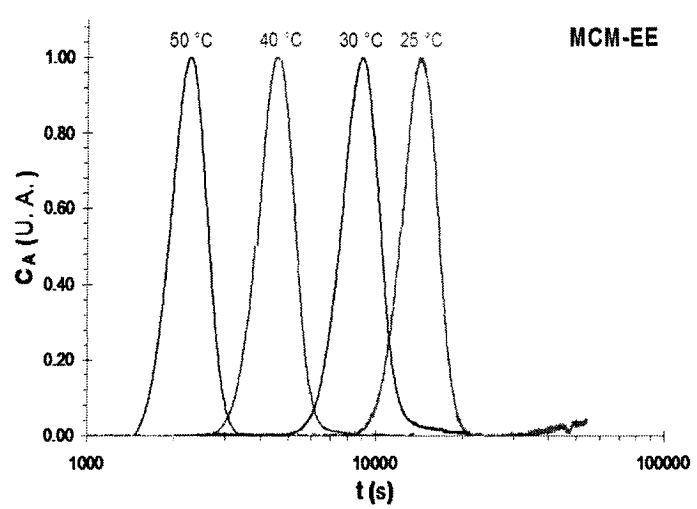
MCM-EE
50 °C
40 °C
30 °C
25 °C
1.00
0.80
0.60
0.40
0.20
0.00
C_A (U. A.)
1000
10000
100000
t (s)

Cyclohexane

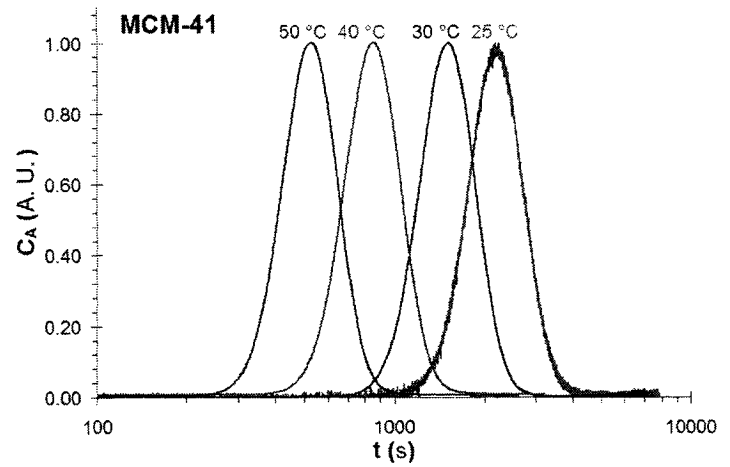

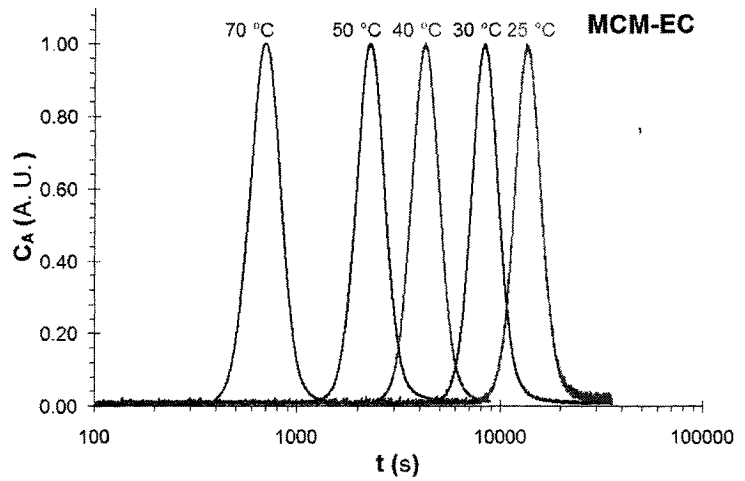

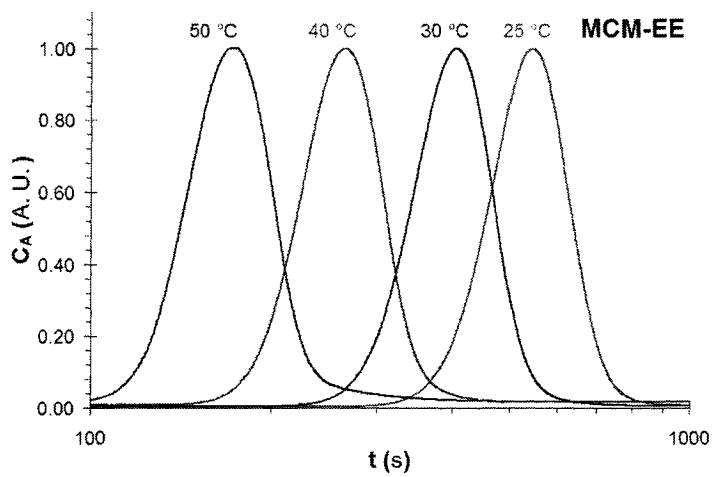

Appendix C. Vapor pressure of Organic Compounds as a Function of Temperature

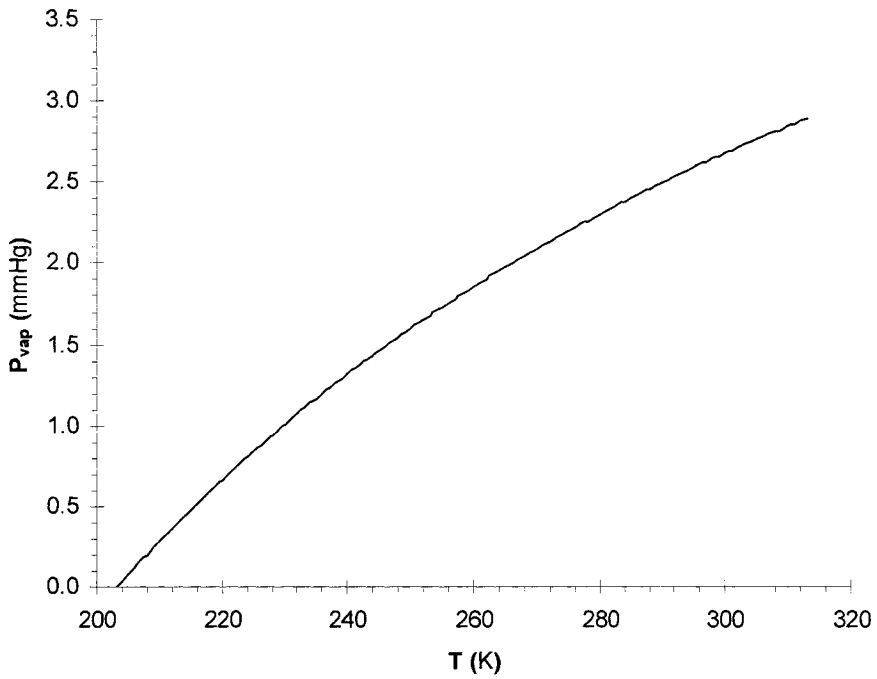

Vapor pressure of dichloromethane as a function of temperature

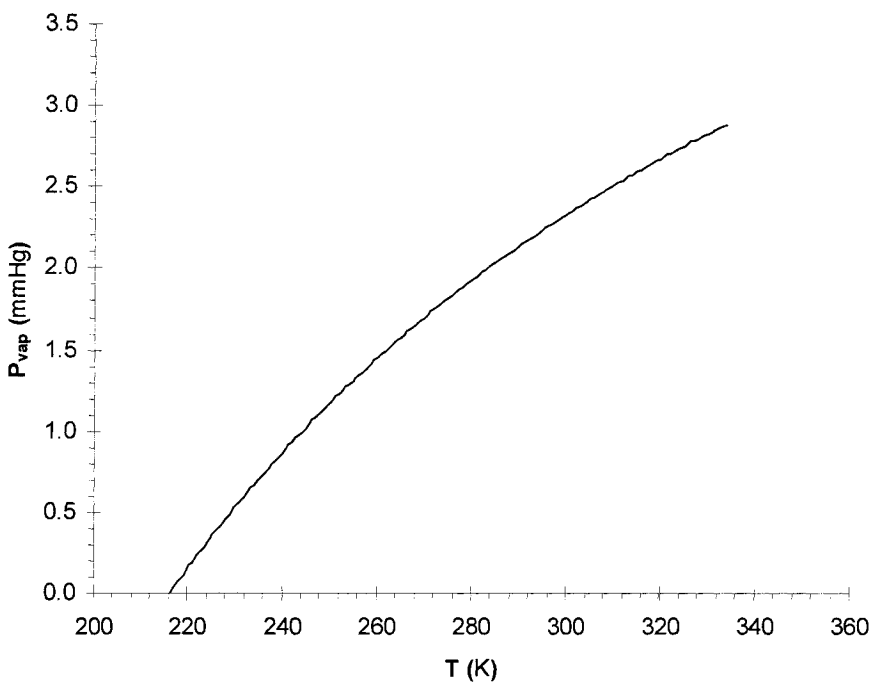

Vapor pressure of chloroform as a function of temperature

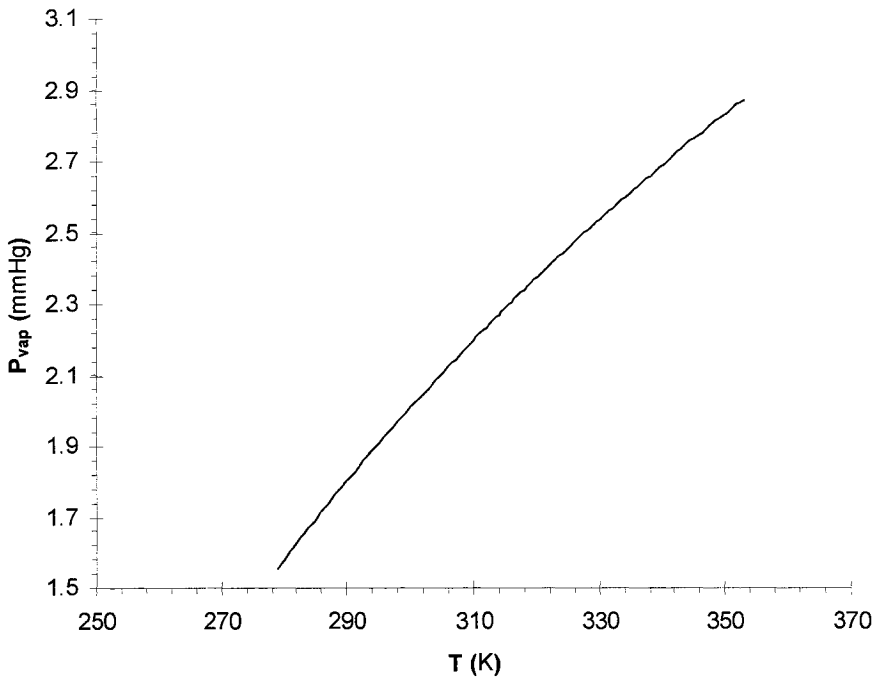

Vapor pressure of benzene as a function of temperature

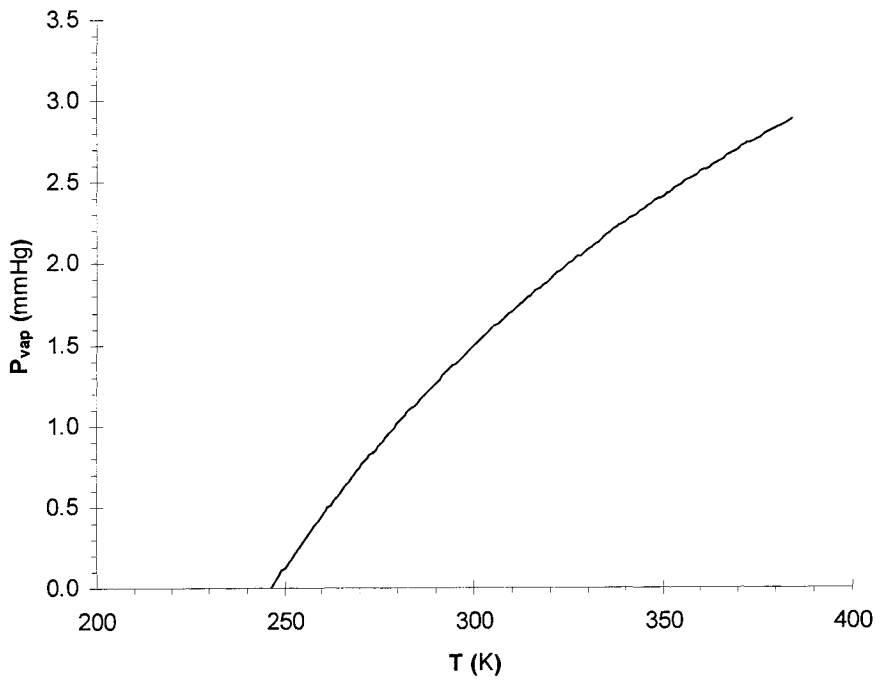

Vapor pressure of toluene as a function of temperature

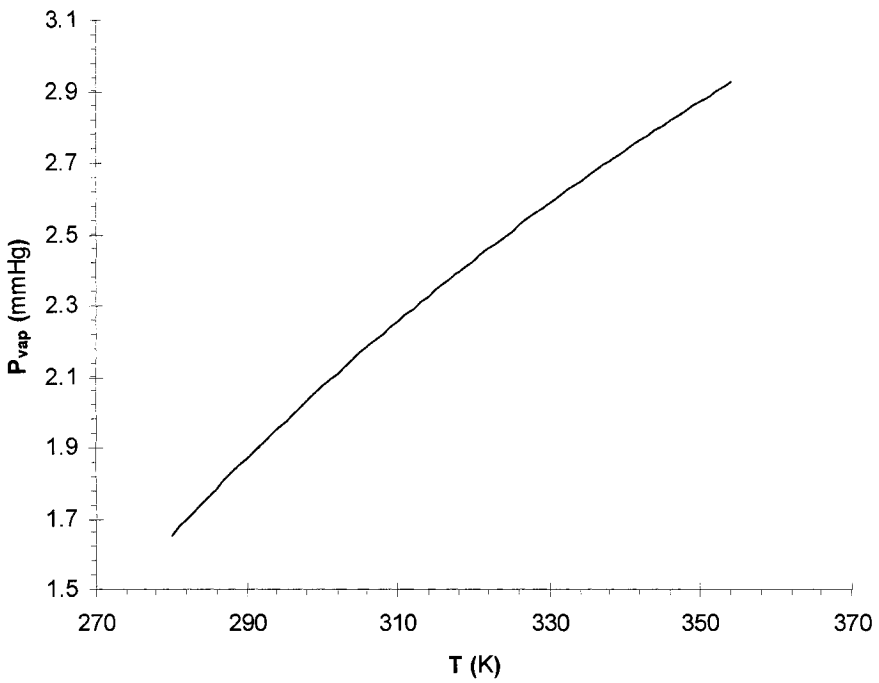

Vapor pressure of cyclohexane as a function of temperature